

Distributed detection and estimation in wireless sensor networks

Sergio Barbarossa, *Fellow, IEEE*, Stefania Sardellitti, *Member, IEEE*,
and Paolo Di Lorenzo, *Member, IEEE*

Department of Information, Electronics, and Telecommunications

“Sapienza” University of Rome, Via Eudossiana 18, 00184 Rome, Italy.

e-mail: sergio@infocom.uniroma1.it, Stefania.Sardellitti@uniroma1.it,
dilorenzo@infocom.uniroma1.it

I. INTRODUCTION

Wireless sensor networks (WSN) are receiving a lot of attention from both the theoretical and application sides, in view of the many applications spanning from environmental monitoring, as a tool to control physical parameters such as temperature, vibration, pressure, or pollutant concentration, to the monitoring of civil infrastructures, such as roads, bridges, buildings, etc. [1]. Some new areas of applications are emerging rapidly and have great potentials. A field that is gaining more and more interest is the use of WSN's as a support for *smart grids*. In such a case, a WSN is useful to: i) monitor and predict energy production from renewable sources of energy such as wind or solar energy, ii) monitor energy consumption; iii) detect anomalies in the network. A further area of increasing interest is *vehicular sensor networks*. In such a case, the vehicles are nodes of an ad hoc network. The sensors onboard the vehicle can measure speed and position of the vehicle and forward this information to nearby vehicles or to the road side units (RSU). This information enables the construction of dynamic spatial traffic maps, which can be exploited to reroute traffic in case of accidents or to minimize energy consumption. A relatively recent and interesting application of WSNs is *cognitive radio (CR)*. In such a case, opportunistic (or secondary) users are allowed to access temporally unoccupied spectrum holes, under the constraint of not interfering with licensed (primary) users, and to release the channels as soon as they are requested by licensed users. The basic step enabling this dynamic access is sensing. The problem is that if sensing

This work has been supported by TROPIC Project, Nr. 318784. To appear in E-Reference Signal Processing, R. Chellapa and S. Theodoridis, Eds., Elsevier, 2013.

is carried out at a single location, it might be severely degraded by shadowing phenomena: If the sensor is in shadowed area, it might miss the presence of a primary user and then transmit by mistake over occupied slots, thus generating an undue interference. To overcome shadowing, it is useful to resort to a WSN whose nodes sense the channels and exchange information with each other in order to mitigate the effect of local shadowing phenomena. The goal of the WSN in such an application is to build a spatial *map* of channel occupancy. An opportunistic user willing to access radio resources within a confined region could then interrogate the closest sensor of a WSN and get a reliable information about which channels are temporarily available and when this utilization has to be stopped.

The plethora of applications raises a series of challenging technical issues, which may be seen as sources of opportunities for engineers. Probably the first most important question concerns *energy supply*. In many applications, in fact, the sensors are battery-operated and it may be difficult or costly to recharge the batteries or to substitute them. As a consequence, energy consumption is a basic constraint that should be properly taken into account. A second major concern is *reliability* of the whole system. In many cases, to allow for an economy of scale, the single sensors are devices with limited accuracy and computational capabilities. Nevertheless, the decision taken by the network as a whole must be very reliable, because it might affect crucial issues like security, safety, etc. The question is then how to build a reliable system out of the combination of many potentially unreliable nodes. Nature exhibits many examples of such systems. Human beings are capable of solving very sophisticated tasks and yet they are essentially built around basic unreliable chemical reactions occurring within cells whose lifetime is typically much smaller than the lifetime of a human being. Clearly, engineering is still far away from approaching the skills of living systems, but important inspirations can be gained by observing biological systems. Two particular features possessed by biological systems are self-organization and self-healing capabilities. Introducing these capabilities within a sensor network is the way to tackle the problem of building a reliable system out of the cooperation of many potentially unreliable units. In particular, self-organization is a key tool to enable the network to reconfigure itself, in terms of acquisition and transfer of information from the sensing nodes to the control centers, responsible for taking decisions, launching alarms or activating actuators aimed to counteract adverse phenomena. The network architecture plays a fundamental role in terms of reliability of the whole system. In conventional WSNs, there is typically one or a few sink nodes that collect the observations taken by the sensor nodes and process them, in a centralized fashion, to produce the desired decision about the observed phenomenon. This architecture arises a number of critical issues, such as: a) potential congestion around the sink nodes; b) vulnerability of the whole network to attacks or failure of sink nodes; c) efficiency of the communication links established to send

data from the sensor nodes to the sink. For all these reasons, a desirable characteristic of a WSN is to be designed in such a way that decisions are taken in a decentralized manner. Ideally, every node should be able, in principle, to achieve the final decision, thanks to the exchange of information with the other nodes, either directly or through multiple hops. In this way, vulnerability would be strongly reduced and the system would satisfy a scalability property. In practice, it is not necessary to make every single node to be able to take decisions as reliably as in a centralized system. But what is important to emphasize is that proper interaction among the nodes may help to improve reliability of single nodes, reduce vulnerability and congestion events, and make a better usage of radio resource capabilities. This last issue points indeed to one of the distinctive features of decentralized decision systems, namely the fact that *sensing and communicating are strictly intertwined* with each other and a proper system design must consider them jointly. The first important constraint inducing a strict link between sensing and communicating is that the transmission of the measurements collected by the nodes to the decision points occurs over realistic channels, utilizing standard communication protocols. For example, adopting common digital communication systems, the data gathered by the sensors need to be quantized and encoded before transmission. In principle, the number of bits used in each sensor should depend on the accuracy of the data acquisition on that sensor. At the same time, the number of bits transmitted per each channel use is upper bounded by the channel capacity, which depends on the transmit power and on the channel between sensor and sink node. This suggests that the number of bits to be used in each node for data quantization should be made dependent on both sensor accuracy and transmission channel. A further important consequence of the network architecture and of the resulting flow of information from peripheral sensing nodes to central decision nodes is the latency with which a global decision can be taken. In a centralized decision system, the flow of information proceeds from the sensing nodes to the central control nodes, usually through multiple hops. The control node collects all the data, it carries out the computations, and takes a decision. Conversely, in a decentralized decision system, there is typically an iterated exchange of data among the nodes. This determines an increase of the time necessary to reach a decision. Furthermore, an iterated exchange of data implies an iterated energy consumption. Since in WSN's energy consumption is a fundamental concern, all the means to minimize the overall energy consumption necessary to reach a decision within a maximum latency are welcome. At a very fundamental level, we will see how an efficient design of the network requires a global cross layer design where the physical and the routing layers take explicitly into account the specific application for which the network has been built.

This article is organized as follows. In Section II, we provide a general framework aimed to show

how an efficient design of a sensor network requires a joint organization of in-network processing and communication. We show how the organization of the flow of information from the sensing nodes to the decision centers should depend not only on the WSN topology, but also on the statistical model of the observation. Finally, we briefly recall some fundamental information theoretical issues showing how in a multi-terminal decision network source and channel coding are strictly related to each other. In Section III we introduce the graph model as the formal tool to describe the interaction among the nodes. Then, we illustrate the so called consensus algorithm as a basic tool to reach globally optimal decisions through a decentralized approach. Since the interaction among the nodes occurs through a wireless channel, we also consider the impact of realistic channel models on consensus algorithm and show how consensus algorithms can be made robust against channel impairments. In Section IV we address the distributed estimation problem. We show first an entirely decentralized approach, where observations and estimations are performed without the intervention of a fusion center. In such a case, we show how to achieve a globally optimal estimation through the local exchange of information among nearby nodes. Then, we consider the case where the estimation is performed at a decision center. In such a case, we show how to allocate quantization bits and transmit powers in the links between the sensing nodes and the fusion center, in order to accommodate the requirement on the maximum estimation variance, under a constraint on the global transmit power. In Section V we extend the approach to the detection problem. Also in this case, we consider the entirely distributed approach, where every node is enabled to achieve a globally optimal decision, and the case where the decision is taken at a central control node. In such a case, we show how to allocate coding bits and transmit power in order to maximize the detection probability, under constraints on the false alarm rate and the global transmit power. Then, in Section VI, we generalize consensus algorithms illustrating a distributed procedure that does not force all the nodes to reach a common value, as in consensus algorithms, but rather to converge to the projection of the overall observation vector onto a signal subspace. This algorithm is especially useful, for example, when it is required to smooth out the effect of noise, but without destroying valuable information present in the spatial variation of the useful signal. In wireless sensor networks, a special concern is energy consumption. We address this issue in Section VII, where we show how to optimize the network topology in order to minimize the energy necessary to achieve a global consensus. We show how to convert this, in principle, combinatorial problem, into a convex problem with minimal performance losses. Finally, in Section VIII we address the problem of matching the topology of the observation network to the graph describing the statistical dependencies among the observed variables. Finally, in Section IX we draw some conclusions and we try to highlight some open problems and possible future developments.

II. GENERAL FRAMEWORK

The distinguishing feature of a decentralized detection or estimation system is that the measurements are gathered by a multiplicity of sensors dispersed over space, while the decision about what is being sensed is taken at one or a few fusion centers or sink nodes. The information gathered by the sensors has then to propagate from the peripheral nodes to the central control nodes. The challenge coming from this set-up is that in a WSN, information propagates through wireless channels, which are inherently broadcast, affected by fading and prone to interference. Installing a WSN requires then to set up a proper medium access control protocol (MAC) able to handle the communications among the nodes, in order to avoid interference and to ensure that the information reaches the final destination in a reliable manner. But what is decidedly specific of a WSN is that the sensing and communication aspects are strictly related to each other. In designing the MAC of a WSN, there are some fundamental aspects that distinguish a WSN from a typical telecommunication (TLC) network. The main difference stems from the analysis of goal and constraints of these two kinds of networks. A TLC network must make sure that every source packet reaches the final destination, perhaps through retransmission in case of errors or packet drop, irrespective of the packet content. In a WSN, what is really important is that the decision about what is being sensed be taken in the most reliable way, without necessarily implying the successful delivery of all source packets. Moreover, one of the major constraints in WSN's is energy consumption, because the nodes are typically battery operated and recharging the batteries is sometimes troublesome, especially when the nodes are installed in hard to reach places. Conversely, in a TLC network, energy provision is of course important, but it is not the central issue. At the same time, the trend in TLC networks is to support higher and higher data rates to accommodate for ever more demanding applications, while the data rates typically required in most WSN's are not so high. These considerations suggest that an efficient design of a WSN should take into account the application layer directly. This means, for example, that it is not really necessary that every packet sent by a sensor node reaches the final destination. What is important is only that the correct decision is taken in a reliable manner, possibly with low latency and low energy consumption. This enables data aggregation or in-network processing to avoid unnecessary data transmissions. It is then important to formulate this change of perspective in a formal way to envisage ad hoc information transmission and processing techniques.

A. *Computing while communicating*

In a very general setting, taking a decision based on the data collected by the sensors can be interpreted as computing a function of these data. Let us denote by x_i , with $i = 1, \dots, N$, the measurements

collected by the i -th node of the network, and by $f(\mathbf{x}) = f(x_1, \dots, x_N)$ the function to be computed. The straightforward approach for computing this function consists in sending all the measurements x_i to a fusion center through a proper communication network and then implement the computation of $f(\mathbf{x})$ at the fusion center. However, if $f(\mathbf{x})$ possesses a structure, it may be possible to take advantage of such a structure to better organize the flow of data from the sensing nodes to the fusion center. The idea of mingling computations and communications to make an efficient use of the radio resources, depending on the properties that the function $f(\mathbf{x})$ might possess, was proposed in [3]. Here, we will first recall the main results of [3]. Then, we will show how the interplay between computation and communication will be further affected by the structure of the probabilistic model underlying the observations.

To exploit the structure of the function $f(x_1, \dots, x_N)$ to be computed, it is necessary to define some relevant structural properties. One important property is *divisibility*. Let \mathcal{C} be a subset of $\{1, 2, \dots, N\}$ and let $\pi := \{C_1, \dots, C_s\}$ be a partition of \mathcal{C} . We denote by \mathbf{x}_{C_i} the vector composed by the set of measurements collected by the nodes whose indices belong to C_i . A function $f(x_1, \dots, x_N)$ is said to be divisible if, for any $\mathcal{C} \subset \{1, 2, \dots, N\}$ and any partition π , there exists a function $g^{(\pi)}$ such that

$$f(\mathbf{x}_{\mathcal{C}}) = g^{(\pi)}(f(\mathbf{x}_{C_1}), f(\mathbf{x}_{C_2}), \dots, f(\mathbf{x}_{C_s})). \quad (1)$$

In words, (1) represents a sort of “divide and conquer” property: A function $f(\mathbf{x})$ is divisible if it is possible to split its computation into partial computations over subsets of data and then recombine the partial results to yield the desired outcome.

Let us suppose now that the N sensing nodes are randomly distributed over a circle of radius R . We assume a simple propagation model, such that two nodes are able to send information to each other in a reliable way if their distance is less than a coverage radius $r_0(N)$. At the same time, the interference between two links is considered negligible if the interfering transmitter is at a distance greater than $\alpha r_0(N)$ from the receiver, where α is chosen according to the propagation model. For any random deployment of the nodes, the choice of $r_0(N)$ induces a network topology, such that there is a link between two nodes if their distance is less than $r_0(N)$. The resulting graph having the nodes as vertices and the edges as links, is a random graph, because the positions of the nodes are random. This kind of graph is known as a *Random Geometric Graph* (RGG)¹. To make an efficient use of the radio resources, it is useful to take $r_0(N)$ as small as possible, to save local transmit power and make possible the reuse of radio resources, either frequency or time slots. However, $r_0(N)$ should not be too small to loose connectivity. In other

¹A basic review of graph properties is reported in Appendix A.

words, we do not want the network to split in subnetworks that do not interact with each other. Since the node location is random, network connectivity can only be guaranteed in probability. It has been proved in [4] that, if $r_0(N)$ is chosen as follows

$$r_0(N) = R\sqrt{\frac{\log N + c(N)}{\pi N}} \quad (2)$$

with $c(N)$ going to infinity, as N goes to infinity, the resulting RGG is asymptotically connected with high probability, as N goes to infinity. For instance, if we take $c(N) = (\pi - 1) \log N$, the coverage radius can be expressed simply as

$$r_0(N) = R\sqrt{\frac{\log N}{N}}. \quad (3)$$

A further property of a node is the number of neighbors of that node. For an undirected graph, the number of neighbors of a node is known as the degree of the node. Denoting by $d(N)$ the degree of an RGG with N nodes, it was proved in [2] that, choosing the coverage radius as in (2), $d(N)$ is (asymptotically) upper bounded by a function that behaves as $\log N$. More specifically,

$$\lim_{N \rightarrow \infty} \mathbb{P}\{d(N) \leq c \log N\} = 1 \quad (4)$$

In [2] it was established an interesting link between the properties of the function $f(\mathbf{x})$ to be computed by the network and the topology of the communication network. In particular, assuming as usual that the measurements are quantized in order to produce a value belonging to a finite alphabet, let us denote by $\mathcal{R}(f, N)$ the range of $f(\mathbf{x})$ and by $|\mathcal{R}(f, N)|$ the cardinality of $\mathcal{R}(f, N)$. In [2], it was proved that, under the following assumptions:

A.1 $f(\mathbf{x})$ is divisible;

A.2 the network is connected;

A.3 the degree of each node is chosen as $d(N) \leq k_1 \log |\mathcal{R}(f, N)|$;

then, the rate for computing $f(\mathbf{x})$ scales with N as

$$R(N) \geq \frac{c_1}{\log |\mathcal{R}(f, N)|}. \quad (5)$$

This is an important result that has practical consequences. It states, in fact, that, whenever $\log |\mathcal{R}(f, N)|$ scales with a law that increases more slowly than N , we can have an increase of efficiency if we organize the local computation and the flow of partial results properly. For instance, if the sensors communicate to the sink node through a Time Division Multiplexing Access (TDMA) scheme, with a standard approach it is necessary to allocate N time slots to send all the data to the sink node. Conversely, Eqn. (5) suggests that, to compute the function $f(\mathbf{x})$, it is sufficient to allocate $\log |\mathcal{R}(f, N)|/c_1$ slots. The same result

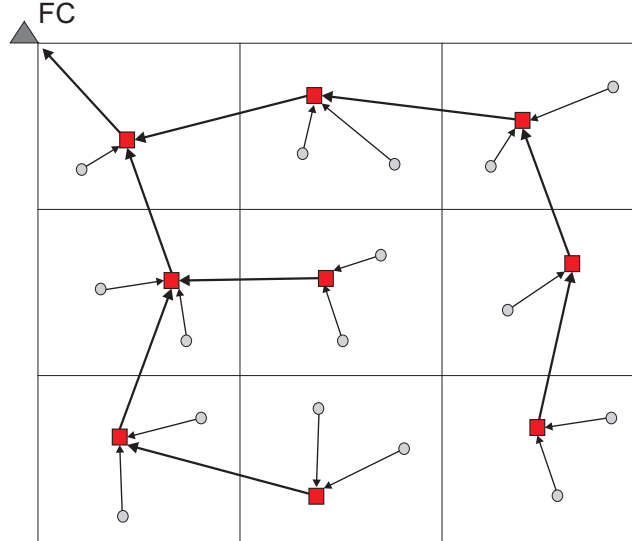


Fig. 1. Hierarchical organization of information flow from peripheral nodes to fusion center.

would apply in a Frequency Division Multiplexing Access (FDMA) scheme, simply reverting the role of time slots and frequency subchannels. This is indeed a paradigm shift, because it suggests that an efficient radio resource allocation in a WSN should depend on the cardinality of $\mathcal{R}(f, N)$. This implies a sort of cross-layer approach that involves physical, MAC and application layers jointly. The next question is how to devise an access protocol that enables such an efficient design. To this regard, the theorem proved in [2] contains a constructive proof, which suggests how to organize the flow of information from the sensing nodes to the control center. In particular, the strategy consists in making a tessellation of the area monitored by the sensor network, similarly to a cellular network, as pictorially described in Fig. 1. Furthermore, the information flows from the peripheral nodes to the fusion center through a tree-like graph, having the fusion center as its root. In each cell, the nodes (circles) identify a node as the relay node (square). The relay node collects data from the nodes within its own cell and from relay nodes of its leaves, performs local computations and communicates the result to the parent relay nodes, with the goal of propagating these partial results towards the root (sink node). To handle interference, a graph coloring scheme is used to avoid interference among adjacent cells. This allows spatial reuse of radio resources, e.g. frequency or time slots, which can be used in parallel without generating an appreciable interference. The communication structure is conceptually similar to a cellular network, with the important difference that now the flow of information is directly related to the computational task. A few examples are useful to better grasp the possibilities of this approach.

Data uploading: Suppose it is necessary to convey all the data to the sink node. If each observed vector belongs to an alphabet \mathcal{X} , with cardinality $|\mathcal{X}|$, the cardinality of the whole data set is $|\mathcal{R}(f, N)| = |\mathcal{X}|^N$. Hence, $\log |\mathcal{R}(f, N)| = N \log |\mathcal{X}|$. This means that, according to (5), the capacity of the network scales as $1/N$. This is a rather disappointing result, as it shows that there is no real benefit with respect to the simplest communication case one could envisage: The nodes have to split the available bandwidth into a number of sub-bands equal to the number of nodes, with a consequent rate reduction per node.

Decision based on the histogram of the measurements: Let us suppose now that the decision to be taken at the control node can be based on the histogram of the data collected by the nodes, with no information loss. In this case, the function $f(\mathbf{x})$ is the histogram. It can be verified that the histogram is a divisible function. Furthermore, the cardinality of the histogram is

$$|\mathcal{R}(f, N)| = \binom{N + |\mathcal{X}| - 1}{|\mathcal{X}| - 1}. \quad (6)$$

Furthermore, it can be shown that

$$(N/|\mathcal{X}|)^{|\mathcal{X}|} \leq \binom{N + |\mathcal{X}| - 1}{|\mathcal{X}| - 1} \leq (N + 1)^{|\mathcal{X}|}. \quad (7)$$

Hence, in this case $\log |\mathcal{R}(f, N)|$ behaves as $\log N$ and then the rate $R(N)$ in (5) scales as $1/\log N$. This is indeed an interesting result, showing that if the decision can be based on the histogram of the data, rather than on each single measurement, adopting the right communication scheme, the rate per node behaves as $1/\log N$, rather than $1/N$, with a rate gain $N/\log N$, which increases as the number of nodes increases.

Symmetric functions: Let us consider now the case where $f(\mathbf{x})$ is a symmetric function. We recall that a function $f(\mathbf{x})$ is symmetric if it is invariant to permutations of its arguments, i.e., $f(\mathbf{x}) = f(\Pi\mathbf{x})$ for any permutation matrix Π and any argument vector \mathbf{x} . This property reflects the so called *data-centric* view, where what is important is the measurement *per se*, and not which node has taken which measurement. Examples of symmetric functions include the mean, median, maximum/minimum, histogram, and so on. The key property of symmetric functions is that it can be shown that they depend on the argument \mathbf{x} only through the histogram of \mathbf{x} . Hence, the computation of symmetric functions is a particular case of the example examined before. Thus, the rate scales again as $1/\log N$.

B. Impact of observation model

Having recalled that the efficient design of a WSN requires an information flow that depends on the scope of the network, more specifically, on the structural properties of the function to be computed by the network, it is now time to be more specific on the decision tasks that are typical of WSN's, namely detection and estimation. Let us consider for example the simple hypothesis testing problem. In such a case, an ideal centralized detector having error-free access to the measurements collected by the nodes, should compute the likelihood ratio and compare it with a suitable threshold [67]. We denote with \mathcal{H}_0 and \mathcal{H}_1 the two alternative hypotheses, i.e. absence or presence of the event of interest, and with \mathbf{x}_i the set of measurements collected by node i . If we indicate with $p(\mathbf{x}_1, \dots, \mathbf{x}_N; \mathcal{H}_i)$ the joint probability density function of the whole set of observed data, under the hypothesis \mathcal{H}_i , with $i = 0, 1$, the likelihood ratio test amounts to comparing the likelihood ratio (LR) with a threshold γ , and decide for \mathcal{H}_1 if the threshold is exceeded or for \mathcal{H}_0 , otherwise. In formulas

$$\Lambda(\mathbf{x}) := \Lambda(\mathbf{x}_1, \dots, \mathbf{x}_N) = \frac{p(\mathbf{x}_1, \dots, \mathbf{x}_N; \mathcal{H}_1)}{p(\mathbf{x}_1, \dots, \mathbf{x}_N; \mathcal{H}_0)} \underset{\mathcal{H}_0}{\overset{\mathcal{H}_1}{\gtrless}} \gamma \quad (8)$$

The LR test (LRT) is optimal under a Bayes or a Neyman-Pearson criterion, the only difference being that the threshold γ assumes different values in the two cases [67]. In principle, to implement the LRT at the fusion center, every node should send its observation vector \mathbf{x}_i to the fusion center, through a proper MAC protocol. The fusion center, after having collected all the data, should then implement the LRT, as indicated in (8). However, the computation of the LR in (8) does not necessarily imply the transmission of the single vectors \mathbf{x}_i . Conversely, according to the theory recalled above, the transmission strategy should depend on the structural properties of the LR function, if any. Let us see how to exploit the structure of the LR function in two cases of practical interest.

1) *Statistically independent observations*: Let us start assuming that the observations taken by different sensors are statistically independent, conditioned to each hypothesis. This is an assumption valid in many cases. Under such an assumption, the LR can be factorized as follows

$$\Lambda(\mathbf{x}) := \frac{\prod_{n=1}^N p(\mathbf{x}_n; \mathcal{H}_1)}{\prod_{n=1}^N p(\mathbf{x}_n; \mathcal{H}_0)} := \prod_{n=1}^N \Lambda_n(\mathbf{x}_n) \underset{\mathcal{H}_0}{\overset{\mathcal{H}_1}{\gtrless}} \gamma \quad (9)$$

where $\Lambda_n(\mathbf{x}_n) = p(\mathbf{x}_n; \mathcal{H}_1)/p(\mathbf{x}_n; \mathcal{H}_0)$ denotes the local LR at the n th node. In this case, the global function $\Lambda(\mathbf{x})$ in (9) possesses a clear structure: It is factorizable in the product of the local LR functions. Then, since a factorizable function is divisible, it is possible to implement the efficient mechanisms described in the previous section to achieve an efficient design. The network nodes should cluster as in

Fig. 1. Every relay node should compute the local LR, multiply it to the data received from the relays pertaining to the lower clusters and send the partial result to the relay of the upper cluster, until the result reaches the fusion center. The efficiency comes from the fact that many transmissions can occur in parallel, exploiting spatial reuse of radio resources. This result suggests also that the proper source encoding to be implemented at each sensor node consists in the computation of the local LR.

2) *Markov observations*: The previous result is appealing, but it pertains to the simple situation where the observations are statistically independent, conditioned to the hypotheses. In some circumstances, however, this assumption is unjustified. This is the case, for example, when the sensors monitor a field of spatially correlated values, like a temperature or atmospheric pressure field. In such cases, nearby nodes sense correlated values and then the statistical independence assumption is no longer valid. It is then of interest, in such cases, to check whether the statistical properties of the observations can still induce a structure on the function to be computed that can be exploited to improve network efficiency.

There is indeed a broad class of observation models where the joint pdf cannot be factorized into the product of the individual pdf's pertaining to each node, but it can still be factorized into functions of subsets of variables. This is the case of Bayes networks or Markov random fields. Here we will recall the basic properties of these models, as relevant to our problem. The interested reader can refer to many excellent books, like, for example, [5] or [6].

In the Bayes network's case, the statistical dependency among the random variables is described by an acyclic directed graph, whose vertices represent the random variables, while the edges represent local conditional probabilities. In particular, given a node x_i , whose parent nodes are identified by the set of indices $\text{pa}(i)$, the joint probability density function (pdf) of a Bayes network can be written as

$$p(x_1, \dots, x_N) = \prod_{i=1}^N p(x_i / \mathbf{x}_{\text{pa}(i)}), \quad (10)$$

where $\mathbf{x}_{\text{pa}(i)}$ collects all the variables corresponding to the parents of node i . If a node in (10) does not have parents, the corresponding probability is unconditional.

Alternatively, a Markov random field is represented through an undirected graph. More specifically, a Markov network consists of:

- 1) An undirected graph $G = (V, E)$, where each vertex $v \in V$ represents a random variable and each edge $\{u, v\} \in E$ represents statistical dependency between the random variables u and v ;
- 2) A set of potential (or compatibility) functions $\psi_c(\mathbf{x}_c)$ (also called clique potentials), that associate

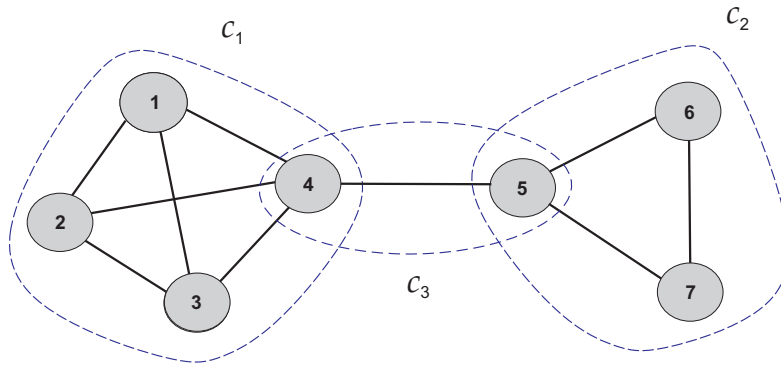


Fig. 2. Example of Markov graph.

a non-negative number to the cliques ² of G .

Let us denote by \mathcal{C} the set of all cliques present in the graph. The random vector \mathbf{x} is Markovian if its joint pdf admits the following factorization

$$p(\mathbf{x}) = \frac{1}{Z} \prod_{c \in \mathcal{C}} \psi_c(\mathbf{x}_c), \quad (11)$$

where \mathbf{x}_c denotes the vector of variables belonging to the clique c . The functions $\psi_c(\mathbf{x}_c)$ are called *compatibility functions*. The term Z is simply a normalization factor necessary to guarantee that $p(\mathbf{x})$ is a valid pdf. A node p is conditionally independent of another node q in the Markov network, given some set S of nodes, if every path from p to q passes through a node in S . Hence, representing a set of random variables by drawing the correspondent Markov graph is a meaningful pictorial way to identify the conditional dependencies occurring across the random variables. As an example, let us consider the graph reported in Fig. 2. The graph represents conditional independencies among seven random variables. The variables are grouped into 3 cliques. In this case, for example, we can say that nodes 1 to 4 are statistically independent of nodes 6 and 7, conditioned to the knowledge of node 5. In this example, the joint pdf can be written as follows

$$p(\mathbf{x}) = \frac{1}{Z} \psi_1(x_1, x_2, x_3, x_4) \psi_2(x_5, x_6, x_7) \psi_3(x_4, x_5). \quad (12)$$

If the product in (11) is strictly positive for any \mathbf{x} , we can introduce the functions

$$V_c(\mathbf{x}_c) = -\log \psi_c(\mathbf{x}_c) \quad (13)$$

²A clique is a subset of nodes which are fully connected and maximal, i.e. no additional node can be added to the subset so that the subset remains fully connected.

so that (11) can be rewritten in exponential form as

$$p(\mathbf{x}) = \frac{1}{Z} \exp \left(- \sum_{c \in \mathcal{C}} V_c(\mathbf{x}_c) \right). \quad (14)$$

This distribution is known, in physics, as the Gibbs (or Boltzman) distribution with interaction *potentials* $V_c(\mathbf{x}_c)$ and *energy* $\sum_{c \in \mathcal{C}} V_c(\mathbf{x}_c)$.

The independence graph conveys the key probabilistic information through absent edges: If nodes i and j are not neighbors, the random variables x_i and x_j are statistically independent, conditioned to the other variables. This is the so called *pairwise Markov property*. Given a subset $a \subset V$ of vertices, $p(\mathbf{x})$ factorizes as

$$p(\mathbf{x}) = \frac{1}{Z} \prod_{c: c \cap a \neq \emptyset} \psi_c(\mathbf{x}_c) \prod_{c: c \cap a = \emptyset} \psi_c(\mathbf{x}_c) \quad (15)$$

where the second factor does not depend on a . As a consequence, denoting by $S - a$ the set of all nodes except the nodes in a and by \mathcal{N}_a the set of neighbors of the nodes in a , $p(\mathbf{x}_a / \mathbf{x}_{S-a})$ reduces to $p(\mathbf{x}_a / \mathcal{N}_a)$. Furthermore,

$$p(\mathbf{x}_a / \mathcal{N}_a) = \frac{1}{Z_a} \prod_{c: c \cap a \neq \emptyset} \psi_c(\mathbf{x}_c) = \frac{1}{Z_a} \exp \left(- \sum_{c: c \cap a \neq \emptyset} V_c(\mathbf{x}_c) \right). \quad (16)$$

This property states that the joint pdf factorizes in terms that contain only variables whose vertices are neighbors.

An important example of jointly Markov random variables is the Gaussian Markov Random Field (GMRF), characterized by having a pdf expressed as in (14), with the additional property that the energy function is a quadratic function of the variables. In particular, a vector \mathbf{x} of random variables is a GMRF if its joint pdf can be written as

$$p(\mathbf{x}) = \frac{1}{\sqrt{(2\pi)^N |\mathbf{C}|}} e^{-\frac{1}{2}(\mathbf{x} - \boldsymbol{\mu})^T \mathbf{C}^{-1}(\mathbf{x} - \boldsymbol{\mu})} = \sqrt{\frac{|\mathbf{A}|}{(2\pi)^N}} e^{-\frac{1}{2}(\mathbf{x} - \boldsymbol{\mu})^T \mathbf{A}(\mathbf{x} - \boldsymbol{\mu})}, \quad (17)$$

where $\boldsymbol{\mu} = \mathbb{E}\{\mathbf{x}\}$ is the expected value of \mathbf{x} , $\mathbf{C} = \mathbb{E}\{(\mathbf{x} - \boldsymbol{\mu})(\mathbf{x} - \boldsymbol{\mu})^T\}$ is the covariance matrix of \mathbf{x} and $\mathbf{A} = \mathbf{C}^{-1}$ is the so called *precision* matrix. In this case, the *Markovianity* of \mathbf{x} manifests itself through the *sparsity* of the precision matrix. As a particular case of (16), the coefficient a_{ij} of \mathbf{A} is different from zero if and only if nodes i and j are neighbors.

Having recalled the main properties of GMRF's, let us now go back to the problem of organizing the flow of information in a WSN aimed at deciding between two alternative hypotheses of GMRF. Let us consider for example the decision about the two alternative hypotheses:

$$\mathcal{H}_0 : \mathbf{x} \sim p(\mathbf{x}; \mathcal{H}_0) = \frac{1}{Z_0} \prod_{c \in \mathcal{C}} \psi_c(\mathbf{x}_c; \mathcal{H}_0) \quad (18)$$

$$\mathcal{H}_1 : \mathbf{x} \sim p(\mathbf{x}; \mathcal{H}_1) = \frac{1}{Z_1} \prod_{c' \in \mathcal{C}'} \psi_{c'}(\mathbf{x}_{c'}; \mathcal{H}_1) \quad (19)$$

where the sets of cliques involved in the two cases are, in general, different. The factorizations in (18, 19) suggest how to implement the computation of the LRT:

- 1) Each cluster in the WSN should be composed of the nodes associated to the random variables pertaining to the same clique in the statistical dependency graph;
- 2) The observations gathered by the nodes pertaining to a clique c are locally encoded into the clique potential $\psi_c(\mathbf{x}_c; \mathcal{H}_i)$. This is the value that has to be transmitted by each cluster towards upper layers or to the FC;
- 3) As in Fig. 1, each relay in the lowest layer compute the local potentials and forward these results to the upper layers. The relays of the intermediate clusters receive the partial results from the lower clusters, multiply these values by the local potential and forward the results to the relay of the upper cluster, until reaching the FC.

In general, different grouping may occur depending on the hypothesis. This organization represents a generalization of the distributed computation observed in the conditionally independent case, where the groups are simply singletons, i.e. sets composed by exactly one element. In that case, the clustering among nodes is only instrumental to the communication purposes, i.e. to enable spatial reuse of radio resources. In the more general Markovian case, the organization of the communication network in clusters (cells) should take into account, *jointly*, the grouping suggested by the cliques of the underlying dependency graph and the spatial grouping of nodes to enable concurrent transmission over the same radio resources without incurring in undesired interference. To visualize this general perspective, it is useful to have in mind two superimposed graphs, as depicted in Fig. 3: the communication graph (top), whose vertices are the network nodes while the edges are the radio links; the dependency graph (bottom), whose vertices represent random variables, while the arcs represent statistical dependencies. Each communication cluster should incorporate at least one clique. Furthermore, in each cluster there is a relay node that is responsible for the exchange of data with nearby clusters. The whole communication network has a hierarchical tree-structure. Each node in the tree is a relay node belonging to a cluster. This node collects the measurements from the nodes belonging to its cluster, computes the potential (or the product of potentials if more cliques belong to the same cluster) and forwards this value to its relay parents. While we have depicted the two graphs as superimposed in Fig. 3, it is useful to clarify that the nodes of the communication network are located in space and their relative position is well defined in a metric space. Conversely, the nodes of the Markov graph represent random variables for which there is no well defined notion of distance

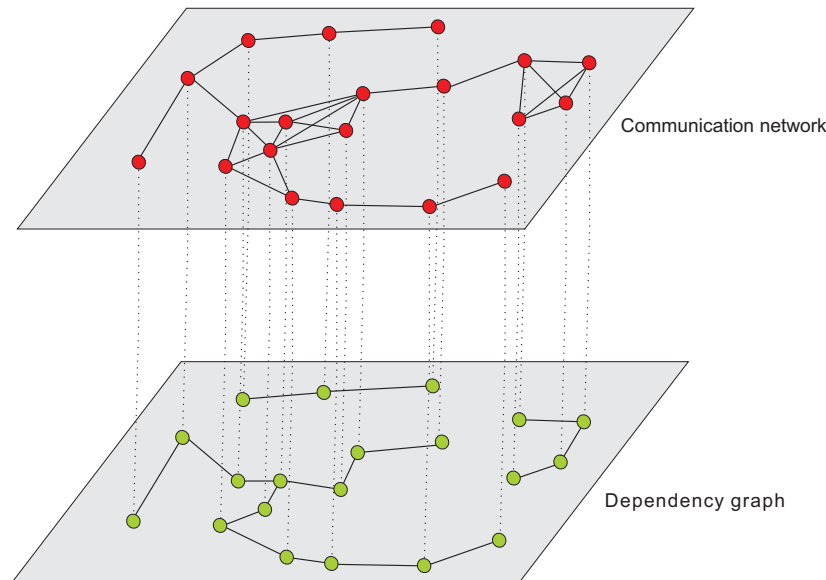


Fig. 3. Superposition of communication layer (top) over a Markov statistical dependency graph (bottom).

or, even if we define one, it is a notion that in general does not have a correspondence with distance in space. In other words, while the neighborhood of nodes in the top graph has to do with the concept of spatial distance among the nodes, the neighborhood of the nodes in the Markov graph has only to do with statistical dependencies. Nevertheless, it is also true that in the observation of physical entities like a temperature field, for example, it is reasonable to expect higher correlation among nearby (in the spatial sense) nodes (variables). An example of GMRF where the statistical dependencies incorporate the spatial distances was suggested in [7]. In summary, the previous considerations suggest that an efficient design of the communication network topology should keep into account the structure, if any, of dependency graph describing the observed variables. At the same time, the design of the network topology should keep into account physical constraints like the power consumption necessary to maintain the links with sufficient reliability (i.e., to insure the sufficient signal-to-noise ratio at the receiver). This is indeed an interesting line of research: How to match the network topology to the dependency graph, under physical constraints dictated by energy consumption, delay, etc. Some works have already addressed this issue. For example, in [8] the authors addressed the problem of implementing data fusion policies with minimal energy consumption, assuming a Markov random field observation model, and established the scaling laws for optimal and suboptimal fusion policies. An efficient message-passing algorithm taking into account the communication network constraints was recently proposed in [9].

C. Fundamental information-theoretical issues

In this section, we recall very briefly some of the fundamental information-theoretic limits of multi-terminal decision networks. We will not go into the details of this challenging fundamental problem. The interested reader can refer to [24] and the references therein. In a WSN, each sensor is observing a physical phenomenon, which can be regarded as a source of information, and the goal of the network is to take decisions about what is being sensed. In some cases, the decision is taken by a fusion center; in others, the decision is distributed across the nodes. In general, the data gathered by the nodes has to travel through realistic channels, prone to additive noise, channel fading and interference. This requires source and channel coding. In a point-to-point communication, when there is only one sensor transmitting data to the fusion center, the encoding of the data gathered by the sensor follows well known rules. In particular, the observation is first time-sampled and each sample is encoded in a finite number, let us say R , of bits per symbol. This converts an analog source of information into a digital source. In this analog-to-digital (AD) conversion, there is usually a distortion that can be properly quantified. More precisely, the source coding rate R depends on the constraint on the mean-square distortion level D . At the same time, given a constraint on the power budget (cost) P available at the transmit side, the maximum rate that can be transmitted with arbitrarily low error probability is the channel capacity $C(P)$, which depends on the transmit power constraint. A rate-distortion pair (D, P) is achievable if and only if

$$R(D) \leq C(P). \quad (20)$$

The source-channel coding separation theorem [11] states that the encoding operation necessary to transmit information through a noisy channel can be split, without loss of optimality, into the cascade of two successive *independent* operations: i) source coding, where each symbol emitted by the source is encoded in a finite number of bits per symbol; ii) channel coding, where a string of k bits are encoded into a codeword of length n bits, to make the codeword error probability arbitrarily low. This theorem has been a milestone in digital communications, as it allows system designers to concentrate, separately, on source coding and channel coding techniques, with no loss of optimality. However, when we move from the point-to-point link to the multipoint-to-multipoint case, there is no equivalent of the source-channel coding separation theorem. This means that in the multi-terminal setting, splitting coding into source and channel coding does not come without a cost, anymore. Rephrasing the source/channel coding theorem in the multi-terminal context, denoting by $\mathcal{R}(D)$ the *rate region*, comprising all the source codes that satisfy the distortion constraint D , and by $\mathcal{C}(P)$ the *capacity region*, containing all the transmission rates

satisfying the transmit power constraint P , a pair (D, P) is achievable if

$$\mathcal{R}(D) \cap \mathcal{C}(P) \neq \emptyset. \quad (21)$$

However, Equation (21) is no longer a necessary condition, meaning that there may exist a code that achieves the prescribed distortion D at a power cost P , which cannot be split into a source compression encoder *followed* by a channel encoder. In general, in the multiterminal case, a *joint* source/channel encoding is necessary. This suggests, from a fundamental theoretical perspective, that, again, in a distributed WSN local processing and communication have to be considered jointly.

D. Possible architectures

Alternative networks architectures may be envisaged depending on how the nodes take decision and exchange information with each other. A few examples are shown in Fig. 4 where there is a set of N nodes observing a given phenomenon, denoted as “nature” for simplicity. The measurements made by node i are collected into the vector \mathbf{y}_i , with $i = 1, \dots, N$. In Fig. 4 a), each node takes an individual decision, which is represented by the variable u_i : $u_i = 1$ if node i decides for the presence of the event, otherwise $u_i = 0$. More generally, u_i could also be the result of a local source encoder, whose aim is to reduce the redundancy present in the observed data. The simplest case is sketched in Fig. 4 a), where a set of nodes observes a state of nature and each node takes a decision. Even if this is certainly the simplest form of monitoring, if the local decisions are taken according to a global optimality criterion, even in the case of statistically independent observations, the local decisions are coupled in a non trivial form. The next step, in terms of complexity, is to combine all the observations collected by the sensing nodes in a centralized node, called fusion center or sink node. This strategy is depicted in the architecture of Fig. 4 b). In such a case, each node takes a local decision and sends this information to the fusion center, which combines the local decision according to a globally optimum criterion. What is important, in a practical setting, is that the limitations occurring in the transmission of information from the sensing nodes to the fusion center are properly taken into account. An alternative approach is reported in Fig. 4 c), where node 1 takes a local decision and it notifies node 2 about this decision. Node 2, on its turn, based on the decision of node 1 and on its own measurements as well, takes a second decision, and so on. A further generalization occurs in the example of Fig. 4 d), where the nodes take local decisions and exchange information with the other nodes. In such a case, there is no fusion center and the final decision can be taken, in principle, by every node.

Besides the architecture describing the flow of information through the network, a key aspect concerns the

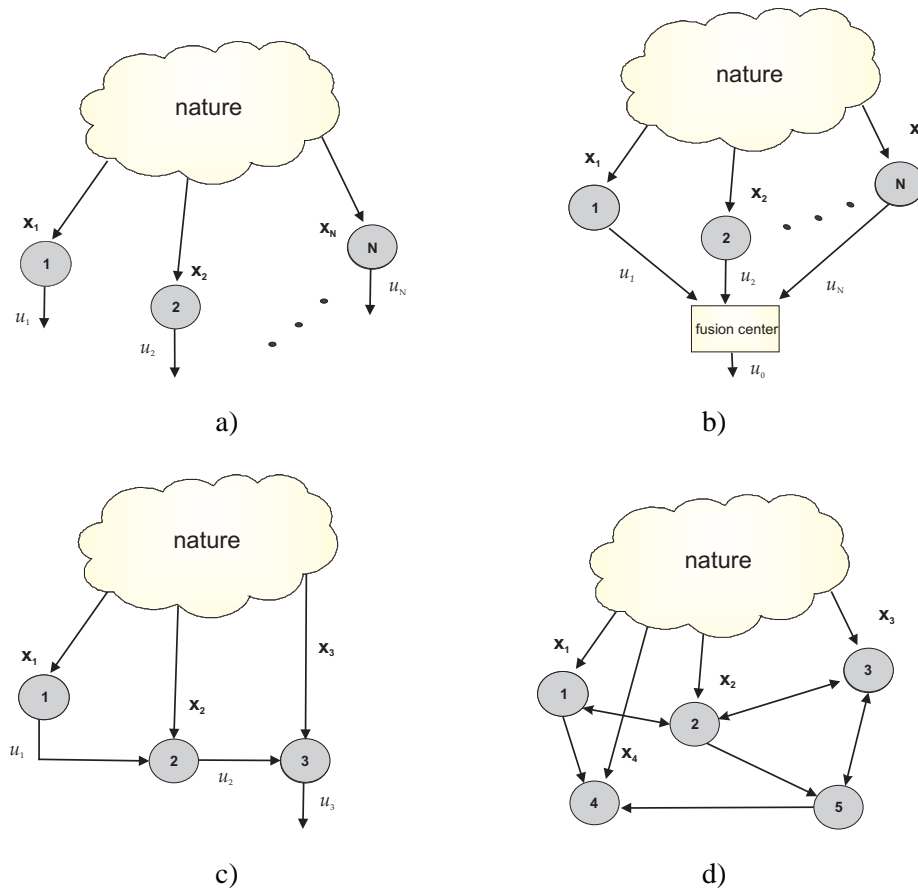


Fig. 4. Alternative communication architectures between peripheral nodes and fusion center.

constraint imposed by the communication links. Realistic channels are in fact affected by noise, fading, delays, and so on. Hence, a globally optimal design must incorporate the decision and communication aspects jointly in a common context. The first step in this global design passes through a formal description of the interaction among the nodes.

III. GRAPHICAL MODELS AND CONSENSUS ALGORITHM

The proper way to describe the interactions among the network nodes is to introduce the graph model of the network. Let us consider a network composed of N sensors. The flow of information across the sensing nodes implementing some form of distributed computation can be properly described by introducing a graph model whose vertices are the sensors and there is an edge between two nodes if they exchange information with each other³. Let us denote the graph as $\mathcal{G} = \{\mathcal{V}, \mathcal{E}\}$ where \mathcal{V} denotes the set

³ We refer the reader to Appendix A for a review of the basic notations and properties of graphs.

of N vertices (nodes) v_i and $\mathcal{E} \subseteq \mathcal{V} \times \mathcal{V}$ is the set of edges $e_{ij}(v_i, v_j)$. The most powerful tool to grasp the properties of a graph is *algebraic graph theory* [64], which is based on the description of the graph through appropriate matrices, whose definition we recall here below. Let $\mathbf{A} \in \mathbb{R}^{N \times N}$ be the *adjacency* matrix of the graph \mathcal{G} , whose elements a_{ij} represent the weights associated to each edge with $a_{ij} > 0$ if $e_{ij} \in \mathcal{E}$ and $a_{ij} = 0$ otherwise. According to this notation and assuming no self-loops, i.e., $a_{ii} = 0$, $\forall i = 1, \dots, N$, the out-degree of node v_i is defined as $\deg_{out}(v_i) = \sum_{j=1}^N a_{ji}$. Similarly, the in-degree of node v_i is $\deg_{in}(v_i) = \sum_{j=1}^N a_{ij}$. The *degree* matrix \mathbf{D} is defined as the diagonal matrix whose i -th diagonal entry is $d_{ii} = \deg(v_i)$. Let \mathcal{N}_i denote the set of neighbors of node i , so that $|\mathcal{N}_i| = \deg_{in}(v_i)$ ⁴. The *Laplacian* matrix $\mathbf{L} \in \mathbb{R}^{N \times N}$ of the graph \mathcal{G} is defined as $\mathbf{L} := \mathbf{D} - \mathbf{A}$. Some properties of the Laplacian will be used in the distributed algorithms to be presented later on, and then it is useful to recall them.

Properties of the Laplacian matrix

P.1: \mathbf{L} has, by construction, a null eigenvalue with associated eigenvector the vector $\mathbf{1}$ composed by all ones.

This property can be easily checked verifying that $\mathbf{L}\mathbf{1} = \mathbf{0}$ since by construction, $\sum_{j=1}^N a_{ij} = d_{ii}$.

P.2: The multiplicity of the null eigenvalue is equal to the number of connected components of the graph. Hence, the null eigenvalue is *simple* (it has multiplicity one) if and only if the graph is connected.

P.3: If we associate a state variable x_i to each node of the graph, if the graph is undirected, the disagreement between the values assumed by the variables is a quadratic form built on the Laplacian [64]:

$$J(\mathbf{x}) := \frac{1}{4} \sum_{i=1}^N \sum_{j \in \mathcal{N}_i} a_{ij} (x_i - x_j)^2 = \frac{1}{2} \mathbf{x}^T \mathbf{L} \mathbf{x}, \quad (22)$$

where $\mathbf{x} = [x_1, \dots, x_N]^T$ denotes the network state vector.

⁴By $|\cdot|$ we denote the cardinality of the set.

A. Consensus algorithm

Given a set of measurements $x_i(0)$, for $i = 1, \dots, N$, collected by the network nodes, the goal of consensus algorithm is to minimize the disagreement among the nodes. This can be useful, for example, when the nodes are measuring some common variable and their measurement is affected by error. The scope of the interaction among the nodes is to reduce the effect of local errors on the final estimate. In fact, consensus is one of fundamental tools to design distributed decision algorithms that satisfy a global optimality principle, as corroborated by many works on distributed optimization, see, e.g., [38], [39], [40], [41], [92], [42], [43]. We recall now the consensus algorithm as this will form the basis of the distributed estimation and detection algorithms developed in the ensuing sections.

Let us consider, for simplicity, the case where the nodes are measuring a temperature and the goal is to find the average temperature. In this case, reaching a consensus over the average temperature can be seen as the minimization of the disagreement, as defined in (22), between the states $x_i(0)$ associated to the nodes. The minimization of the disagreement can be obtained by using a simple gradient-descent algorithm. More specifically, using a continuous-time system, the minimum of (22) can be achieved by running the following dynamical system [41]

$$\dot{\mathbf{x}}(t) = -\mathbf{L} \mathbf{x}(t), \quad (23)$$

initialized with $\mathbf{x}(0) = \mathbf{x}_0$, where \mathbf{x}_0 is the vector containing all the initial measurements collected by the network nodes. This means that the state of each node evolves in time according to the first order differential equation

$$\dot{x}_i(t) = \sum_{j \in \mathcal{N}_i} a_{ij} (x_j(t) - x_i(t)) \quad (24)$$

where \mathcal{N}_i indicates the set of neighbors of node i . Hence, every node updates its own state only by interacting with its neighbors.

Equation (23) assumes the form of a diffusion equation. Let us consider for example the evolution of a diffusing physical quantity $\psi(z; t)$ as a function of the spatial variable z and of time t ($\psi(z; t)$ could represent, for instance, the heat distribution), the diffusion equation assumes the form

$$\frac{\partial \psi(z; t)}{\partial t} = D \frac{\partial^2 \psi(z; t)}{\partial z^2} \quad (25)$$

where D is the diffusion coefficient. If we discretize the space variable and approximate the second order derivative with a discrete-time second order difference, the diffusion equation (25) can be written as in (23), where the Laplacian matrix represents the discrete version of the Laplacian operator. This conceptual link between consensus equation and diffusion equation has been exploited in [63] to derive a

fast consensus algorithm, mimicking the effect of advection. The interesting result derived in [63] is that to speed up the consensus (diffusion) process, it is necessary to use a *directed* graph, with time-varying adjacency matrix coefficients a_{ij} .

The solution of (23) is given by

$$\mathbf{x}(t) = \exp(-\mathbf{L}t) \mathbf{x}(0). \quad (26)$$

In the case analyzed so far, since the consensus algorithm has been deduced from the minimization of the disagreement and the disagreement has been defined for undirected graphs, the matrix \mathbf{L} is symmetric. Hence, its eigenvalues are real. The convergence of (26) is guaranteed because all the eigenvalues of \mathbf{L} are non-negative, by construction. If the graph is connected, according to property *P.2*, the eigenvalue zero has multiplicity one. Furthermore, the eigenvector associated to the zero eigenvalue is the vector $\mathbf{1}$. Hence, the system (23) converges to the consensus state:

$$\lim_{t \rightarrow \infty} \mathbf{x}(t) = \frac{1}{N} \mathbf{1} \mathbf{1}^T \mathbf{x}(0). \quad (27)$$

This means that every node converges to the average value of the measurements collected by the whole network, i.e.,

$$\lim_{t \rightarrow \infty} x_i(t) = \frac{1}{N} \sum_{i=1}^N x_i(0) = x^*. \quad (28)$$

The convergence rate of system (24) is lower bounded by the slowest decaying mode of the dynamical system (23), i.e. by the second smallest eigenvalue of \mathbf{L} , $\lambda_2(\mathbf{L})$, also known as the *algebraic connectivity* of the graph [65]. More specifically, if the graph is connected or, equivalently, if $\lambda_2(\mathbf{L}) > 0$, then the dynamical system (23) converges to consensus exponentially [41], i.e. $\|\mathbf{x}(t) - x^* \mathbf{1}\| \leq \|\mathbf{x}(0) - x^* \mathbf{1}\| O(e^{-rt})$ with $r = \lambda_2(\mathbf{L})$.

In some applications, the nodes are required to converge to a *weighted* consensus, rather than average consensus. This can be achieved with a slight modification of the consensus algorithm. If we premultiply the left side of (24) by a positive coefficient c_i , the resulting equation

$$c_i \dot{x}_i(t) = \sum_{j \in \mathcal{N}_i} a_{ij} (x_j(t) - x_i(t)) \quad (29)$$

converges to the weighted average

$$\lim_{t \rightarrow \infty} x_i(t) = \frac{\sum_{i=1}^N c_i x_i(0)}{\sum_{i=1}^N c_i}. \quad (30)$$

This property will be used in deriving distributed estimation mechanisms in the next section.

Alternatively, the minimization of (22) can be achieved in discrete-time through the following iterative algorithm

$$\mathbf{x}[k+1] = \mathbf{x}[k] - \epsilon \mathbf{L} \mathbf{x}[k] := \mathbf{W} \mathbf{x}[k], \quad (31)$$

where we have introduced the so called *transition* matrix $\mathbf{W} = \mathbf{I} - \epsilon \mathbf{L}$. Also in this case, the discrete time equation is initialized with the measurements taken by the sensor nodes at time 0, i.e., $\mathbf{x}[0] := \mathbf{x}_0$. This time, to guarantee convergence of the system (31), we need to choose the coefficient ϵ properly. More specifically, the discrete time equation (31) converges if the eigenvalues of \mathbf{W} are bounded between -1 and 1 . This can be seen very easily considering that reiterating (31) k times, we get

$$\mathbf{x}[k] = \mathbf{W}^k \mathbf{x}[0]. \quad (32)$$

Let us denote by \mathbf{u}_k the eigenvectors of \mathbf{W} associated to the eigenvalues $\lambda_k(\mathbf{W})$, with $k = 1, \dots, N$. The eigenvalues of \mathbf{W} are real and we consider them ordered in increasing sense, so that $\lambda_N(\mathbf{W}) \geq \lambda_{N-1}(\mathbf{W}) \geq \dots \geq \lambda_1(\mathbf{W})$. Hence, the evolution of system (32) can be written as

$$\mathbf{x}[k] = \sum_{n=1}^N \lambda_n^k(\mathbf{W}) \mathbf{u}_n \mathbf{u}_n^T \mathbf{x}[0]. \quad (33)$$

The matrix \mathbf{W} has an eigenvector equal to $\mathbf{1}/\sqrt{N}$, associated to the eigenvalue 1 by construction. In fact, $\mathbf{W} \mathbf{1}/\sqrt{N} = \mathbf{1}/\sqrt{N} - \epsilon \mathbf{L} \mathbf{1}/\sqrt{N} = \mathbf{1}/\sqrt{N}$. If the graph is connected, the eigenvalue 1 of \mathbf{W} has multiplicity one. Furthermore, if ϵ is chosen such that $\epsilon(\mathbf{L}) < 2/\lambda_N(\mathbf{L})$, all other eigenvalues are less than 1 . Hence, for a connected graph, the system (33) converges to

$$\lim_{k \rightarrow \infty} \mathbf{x}[k] = \frac{1}{N} \mathbf{1} \mathbf{1}^T \mathbf{x}[0]. \quad (34)$$

Again, this corresponds to having every node converging to the average consensus.

The consensus algorithm can be extended to the case of directed graphs. This case is indeed much richer of possibilities than the undirected case, because the consensus value ends up to depend more strictly on the graph topology. In the directed case, in fact, \mathbf{L} is an asymmetric matrix. The most important difference is that the graph connectivity turns out to depend on the orientation of the edges. Furthermore, each eigenvalue of \mathbf{L} gives rise to a pair of left and right eigenvectors which do not coincide with each other. These differences affect the final consensus state and induce different forms of consensus, as shown below.

The convergence of the system in (31) can be proved by exploiting the properties of non-negative matrices. A nonnegative matrix is row (or column) stochastic if all its row (or column) sums are equal to one. Furthermore if the graph associated to the network is strongly connected, i.e. the zero eigenvalue

associated to \mathbf{L} has multiplicity one (see Appendix A), \mathbf{W} is called an *irreducible* matrix. An irreducible stochastic matrix is primitive if it has only one eigenvalue with maximum modulus. Primitive nonnegative matrices, often named *Perron matrices*, satisfy the Perron-Frobenius theorem [81].

Theorem 1: Let γ_l and γ_r , respectively, the left and right eigenvectors associated to the unit eigenvalue of the primitive nonnegative matrix \mathbf{W} , i.e. $\mathbf{W}\gamma_r = \gamma_r$ and $\gamma_l^T \mathbf{W} = \gamma_l^T$ with $\gamma_r^T \gamma_l = 1$, then $\lim_{k \rightarrow \infty} \mathbf{W}^k = \gamma_r \gamma_l^T$.

Let us now apply to a sensor network modeled by the graph \mathcal{G} with adjacency matrix \mathbf{A} the distributed consensus algorithm

$$x_i[k+1] = x_i[k] - \epsilon \sum_{j \in \mathcal{N}_i} a_{ij} (x_i[k] - x_j[k]) \quad (35)$$

with $0 < \epsilon < 1/d_{max}$.

Interestingly, different forms of consensus can be achieved in a directed graph, depending on the graph connectivity properties [43]:

- a) *If the graph is strongly connected, the dynamical system in (35) converges to a weighted consensus, for any initial state vector $\mathbf{x}[0]$, i.e.,*

$$\lim_{k \rightarrow \infty} \mathbf{W}^k \mathbf{x}[0] = \mathbf{x}^* = \mathbf{1} \gamma_l^T \mathbf{x}[0] \quad (36)$$

where $\gamma_l(i) > 0, \forall i$, and $\sum_{i=1}^N \gamma_l(i) = 1$. In this case, since the graph is strongly connected, \mathbf{W} is an irreducible matrix. Then, applying Gershgorin theorem [81], it can be deduced that there exists a single eigenvalue $\mu_1(\mathbf{W}) = 1$ with maximum modulus. Then \mathbf{W} is a primitive nonnegative matrix and from Theorem 1 the convergence in (36) is straightforward. In this case, every node contributes to the final consensus value. Furthermore, the consensus value is a weighted combination of the initial observations, where the weights are the entries of the left eigenvector associated to the null eigenvalue of \mathbf{L} (or the unit eigenvalue of \mathbf{W}).

- b) *If the digraph is strongly connected and balanced, i.e. $\mathbf{1}^T \mathbf{L} = \mathbf{0}$ and $\mathbf{L} \mathbf{1} = \mathbf{0}$, the systems achieves an average consensus or $\mathbf{x}^* = \frac{\mathbf{1} \mathbf{1}^T}{N} \mathbf{x}[0]$. In fact, for balanced graphs, \mathbf{W} is a double stochastic matrix with $\gamma_l = \gamma_r = \mathbf{1}/\sqrt{N}$;*
- c) *If the digraph \mathcal{G} is weakly connected (WC), but not strongly connected, and it contains a forest with K strongly connected root components, the graph splits in K disjoint clusters $\mathcal{C}_1, \dots, \mathcal{C}_K \subseteq \{1, \dots, N\}$,⁵ and all the nodes pertaining to each cluster converge to the consensus values*

$$x_q^* = \frac{\sum_{i \in \mathcal{C}_k} \gamma_i x_i[0]}{\sum_{i \in \mathcal{C}_k} \gamma_i}, \quad \forall q \in \mathcal{C}_k, \quad k = 1, \dots, K. \quad (37)$$

⁵In general, the clusters $\mathcal{C}_1, \dots, \mathcal{C}_K$ are not a partition of the set of nodes $\{1, \dots, N\}$.

In words, there is no single consensus, in this case, but there is a local consensus within each cluster. Different clusters typically converge to different consensus values.

- d) *If the digraph \mathcal{G} is composed of a single spanning tree, every node converges to the value assumed by the root node.*

As far as the convergence rate, instead, in [41] it has been shown for undirected connected graphs that the dynamical system in (31) converges exponentially to the average consensus with a rate at least equal to $\mu_2(\mathbf{W}) = 1 - \epsilon\lambda_2(\mathbf{L})$ where $\mu_2(\mathbf{W})$ is the second largest eigenvalue of the Perron matrix \mathbf{W} . In fact by defining the disagreement vector $\boldsymbol{\delta} = \mathbf{x} - \mathbf{x}^*$, it can be easily verified [41] that $\boldsymbol{\delta}$ evolves according to the disagreement dynamic given by $\boldsymbol{\delta}[k+1] = \mathbf{W}\boldsymbol{\delta}[k]$. Hence $\psi[k] := \boldsymbol{\delta}[k]^T \boldsymbol{\delta}[k]$ represents a candidate Lyapunov function for the disagreement dynamics so that

$$\psi[k+1] = \boldsymbol{\delta}[k+1]^T \boldsymbol{\delta}[k+1] = \|\mathbf{W}\boldsymbol{\delta}[k]\|^2 \leq \mu_2(\mathbf{W})^2 \|\boldsymbol{\delta}[k]\|^2 = \mu_2(\mathbf{W})^2 \psi[k] \quad (38)$$

with $0 < \mu_2(\mathbf{W}) < 1$ since \mathbf{W} is a symmetric and primitive matrix. As a consequence the algorithm converges exponentially to consensus with a rate at least equal to $\mu_2(\mathbf{W})$.

B. Consensus algorithms over realistic channels

So far, we have recalled the basic properties of consensus algorithm assuming that the exchange of information across the nodes occurs with no errors. In this section we study what happens to consensus algorithms when the communications among the nodes are affected by quantization errors, noise, packet drops, etc. The problem of consensus protocols affected by stochastic disturbance has been considered in a series of previous papers [45]-[50]. In [45], the authors use a decreasing sequence of weights to prove the convergence of consensus protocols to an agreement space in the presence of additive noise under a fixed network topology. The works in [46]-[47] consider consensus algorithms in the presence of link failures, which are modeled as i.i.d. Laplacian matrices of a directed graph. The papers present necessary and sufficient conditions for consensus exploiting the ergodicity of products of stochastic matrices. A distributed consensus algorithm in which the nodes utilize probabilistically quantized information to communicate with each other was proposed in [48]. As a result, the expected value of the consensus is equal to the average of the original sensor data. A stochastic approximation approach was followed in [49], which considered a stochastic consensus problem in a strongly connected directed graph where each agent has noisy measurements of its neighboring states. Finally, the study of a consensus protocol that is affected by both additive channel noise and a random topology was considered in [50]. The resulting algorithm

relates to controlled Markov processes and the convergence analysis relies on stochastic approximation techniques.

In the study of consensus mechanisms over realistic channels, we consider the following sources of randomness:

1) *Node positions*: The first randomness is related to the spatial positions of the nodes, which are in general unknown. We model the spatial distribution of nodes as a random geometric graph composed of N nodes. In graph theory, a random geometric graph (RGG) is a random undirected graph drawn on a bounded region, eg. the unit disk, generated by:

- 1) Placing vertices at random uniformly and independently on the region,
- 2) Connecting two vertices, u, v if and only if the distance between them is inside a threshold radius r_0 , i.e. $d(u, v) \leq r_0$.

Several probabilistic results are known about RGG's. In particular, as shown in [4], if N nodes are placed in a disc of unit area in \mathbb{R}^2 and each node transmits with a power scaling with N as in (2), the resulting network is asymptotically connected with probability one, as $N \rightarrow \infty$.

2) *Random link failures model*: In a realistic communication scenario, the packets exchanged among sensors may be received with errors, because of channel fading or noise. The retransmission of erroneous packets can be incorporated into the system, but packet retransmission introduces a nontrivial additional complexity in decentralized implementations and, most important, it introduces an unknown delay and delay jitter. It is then of interest to examine simple protocols where erroneous packets are simply dropped. Random packet dropping can be taken into account by modeling the coefficient a_{ij} describing the network topology as random variables that assume the value 1 or 0, if the packet is correctly delivered or not, respectively. In this case, the Laplacian varies with time as a sequence of i.i.d. matrices $\{\mathbf{L}[k]\}$, which can be written, without any loss of generality, as

$$\mathbf{L}[k] = \bar{\mathbf{L}} + \tilde{\mathbf{L}}[k] \quad (39)$$

where $\bar{\mathbf{L}}$ denotes the mean matrix and $\tilde{\mathbf{L}}[k]$ are i.i.d. perturbations around the mean. We do not make any assumptions about the link failure model. Although the link failures and the Laplacians are independent over time, during the same iteration, the link failures can still be spatially correlated. It is important to remark that we do not require the random instantiations $G[k]$ of the graph be connected for all k . We only require the graph to be connected on average. This condition is captured by requiring $\lambda_2(\bar{\mathbf{L}}) > 0$.

3) *Dithered quantization* : We assume that each node encodes the message to be exchanged with the other nodes using a uniform quantizer, with a finite number of bits n_b , defined by the following vector mapping, $\mathbf{q}(\cdot) : \mathbb{R}^L \rightarrow Q^L$,

$$\mathbf{q}(\mathbf{y}) = [b_1\Delta, \dots, b_L\Delta]^T = \mathbf{y} + \mathbf{e}_q(\mathbf{y}), \quad (40)$$

where the entries of the vector \mathbf{y} , the quantization step $\Delta > 0$, and the error \mathbf{e}_q satisfy

$$(b_m - 1/2)\Delta \leq y_m \leq (b_m + 1/2)\Delta, \quad 1 \leq m \leq L, \quad (41)$$

$$-\Delta/2 \mathbf{1}_L \leq \mathbf{e}_q(\mathbf{y}) \leq \Delta/2 \mathbf{1}_L, \quad \text{for all } \mathbf{y}. \quad (42)$$

The quantization alphabet is

$$Q^L = \{[b_1\Delta, \dots, b_L\Delta]^T | b_m \in \mathbb{Z}, \forall m\}. \quad (43)$$

Conditioned on the input, the quantization error $\mathbf{e}_q(\mathbf{y})$ is deterministic. This induces a correlation among the quantization errors resulting at different nodes and different times, which may affect the convergence properties of the distributed algorithm. To avoid undesired error correlations, we introduce dithering, as in [51], [52]. In particular, the dither added to randomize the quantization effects satisfies a special condition, namely the Schuchman conditions, as in subtractively dithered systems, [53]. Then, at every time instant k , adding to each component $y_m[k]$ a dither sequence $\{d_m[k]\}_{k \geq 0}$ of i.i.d. uniformly distributed random variables on $[-\Delta/2, \Delta/2)$ independent of the input sequence, the resultant error sequence $\{e_m[k]\}_{k \geq 0}$ becomes

$$e_m[k] = q(y_m[k] + d_m[k]) - (y_m[k] + d_m[k]). \quad (44)$$

The sequence $\{e_m[k]\}_{k \geq 0}$ is now an i.i.d. sequence of uniformly distributed random variables on $[-\Delta/2, \Delta/2)$, which is independent of the input sequence.

The convergence of consensus algorithm in the presence of random disturbance can be proved by exploiting results from supermartingale theory [90]. In an ideal communication case, by selecting the step-size of the algorithm to be sufficiently small (smaller than $2/\lambda_N(\mathbf{L})$, where $\lambda_N(\mathbf{L})$ is the maximum eigenvalue of the Laplacian matrix of the graph), the discrete-time consensus algorithm will asymptotically converge to the agreement subspace. However, in a realistic communication scenario, the links among the sensors may fail randomly and the exchanged data is corrupted by quantization noise. Under these nonideal conditions, the consensus algorithm needs to be properly adjusted to guarantee convergence. A

discrete time consensus algorithm that accounts for random link failures and dithered quantization noise can be written as:

$$\mathbf{x}_i[k+1] = \mathbf{x}_i[k] + \alpha[k] \sum_{j=1}^N a_{ij}[k] (\mathbf{q}(\mathbf{x}_j[k] + \mathbf{d}_{ij}[k]) - \mathbf{x}_i[k]), \quad i = 1, \dots, N,$$

where $\alpha[k]$ is a positive iteration dependent step-size, and $\mathbf{d}_{ij}[k]$ is the dithered quantization vector. Now, exploiting the feature of subtractively dithered systems in (44), the previous expression can be recast as:

$$\mathbf{x}_i[k+1] = \mathbf{x}_i[k] + \alpha[k] \sum_{j=1}^N a_{ij}[k] (\mathbf{x}_j[k] - \mathbf{x}_i[k] + \mathbf{d}_{ij}[k] + \mathbf{e}_{ij}[k]), \quad i = 1, \dots, N.$$

Starting from some initial value, $\mathbf{x}_i[0] \in \mathbb{R}^L$, each node generates via (45) a sequence of state variables, $\{\mathbf{x}_i[k]\}_{k \geq 0}$. The value $\mathbf{x}_i[k+1]$ at the i -th node at time $k+1$ is a function of: its previous state $\mathbf{x}_i[k]$ and the quantized states correctly received at time k by the neighboring sensors. As described previously, the data are subtractively dithered-quantized, so that the quantized data received by the i -th sensor from the j -th sensor at time k is $\mathbf{q}(\mathbf{x}_j[k] + \mathbf{d}_{ij}[k])$. It then follows that the quantization error $\mathbf{e}_{ij}[k]$ is a random vector, whose components are i.i.d., uniformly distributed on $[-\Delta/2, \Delta/2)$, and independent of $\mathbf{x}_j[k]$.

One way to guarantee convergence of the previous system is to use a positive iteration-dependent step size $\alpha[k]$ satisfying [45], [50]

$$\lim_{k \rightarrow \infty} \alpha[k] = 0, \quad \sum_{k=0}^{\infty} \alpha[k] = \infty, \quad \sum_{k=0}^{\infty} \alpha^2[k] < \infty. \quad (45)$$

Exploiting results from stochastic approximation theory, this choice drives the noise variance to zero while guaranteeing the convergence to the consensus subspace.

A numerical example is useful to show the robustness of consensus algorithm in the presence of link failures and quantization noise. We consider a connected network composed of 20 nodes as depicted on the left side of Fig. 5. The initial value of the state variable at each node is randomly chosen in the interval $[0, 1)$. At the k -th iteration of the updating rule (45), each node communicates to its neighbors its current state, i.e., a scalar $x_i[k]$. Because of fading and additive noise, a communication link among two neighbors has a certain probability p to be established correctly. The values to be exchanged are (dither) quantized with 6 bits. The iteration-dependent step size is chosen as $\alpha[k] = \alpha_0/k$, with $\alpha_0 = 1.5/\lambda_N(\mathbf{L})$, in order to satisfy (45). The right side of Fig. 5 shows the average behavior of the disagreement among the sensors in the network, versus the iteration index, for different values of the probability p to establish a communication link correctly. The result is averaged over 100 independent realizations. The ideal case corresponds to $p = 1$ and it is shown as a benchmark. As we can notice from the right side of Fig. 5, even in the presence of random disturbances, an agreement is always reached by the network for any

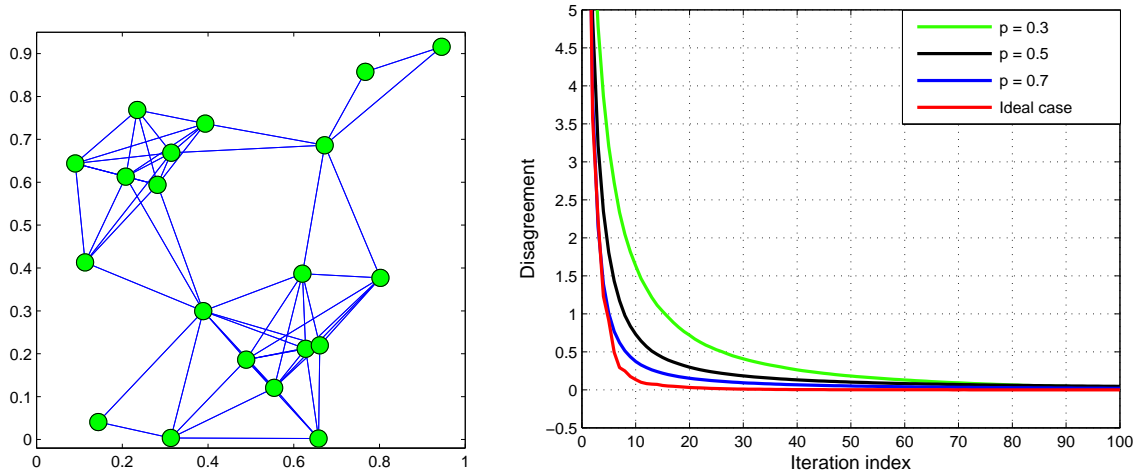


Fig. 5. Network (left). Disagreement vs. time index (right), for different probabilities of correct packet reception.

value of p . The only effect of the random link failures is to slow down the convergence process, without altering the final value of the global potential function. This proves the robustness of the algorithm.

IV. DISTRIBUTED ESTIMATION

Having introduced all the tools necessary to study distributed estimation and detection mechanisms, let us now start with the estimation problem. This problem has been the subject of an extensive literature, see, e.g. [25], [26], [27], [28], [29], [30], [31], [32], [33]. Most of the algorithms proposed in these works propose a mix of local estimation and consensus among neighbor nodes to improve upon the performance of the local estimators. In a first class of methods, like [26], [27] for example, the nodes collect all the data first, perform local estimation and then interact iteratively with their neighbors. In alternative methods, the nodes keep interacting with each other while collecting new measurements or, in general, receiving new information, like in [28], [29], [33]. These two classes of methods can be seen as assigning different time scales to the local estimation and consensus steps. Indeed, it can be proved that a proper combination of local estimation and consensus can bring the whole network to a globally optimal estimate, provided that the graph describing the interaction among the nodes is connected. This approach was pursued, for example in [26], where the so called bridge nodes fulfilled the scope of enforcing local consensus. In the following, we will show how alternative formulations of the globally optimal estimation problem naturally lead to a different mix of the local estimation and the consensus steps, without the need to introduce any node having a special role nor enforcing different time scales a priori.

Let us denote with $\theta \in \mathbb{R}^M$ the parameter vector to be estimated. In some cases, there is no prior

information about θ . In other cases, θ is known to belong to a given set \mathcal{C} : For instance, its entries are known to be positive or to belong to a finite interval of known limits, and so on. In some applications, θ may be the outcome of a random variable described by a known pdf $p_{\Theta}(\theta)$. Let us denote by \mathbf{x}_i the measurement vector collected by node i and by $\mathbf{x} := [\mathbf{x}_1^T, \dots, \mathbf{x}_N^T]^T$ the whole set of data collected by all the nodes. In the two cases of interest, the estimation can be obtained as the solution of the following problems:

Arbitrary case

$$\max_{\theta} p_{X;\Theta}(\mathbf{x}; \theta) \quad (46)$$

$$\text{s.t. } \theta \in \mathcal{C} \quad (47)$$

where $p_{X;\Theta}(\mathbf{x}; \theta)$ is the joint pdf of vector \mathbf{x} , for a given arbitrary vector θ , or

Random case

$$\max_{\theta} p_{X/\Theta}(\mathbf{x}/\theta) p_{\Theta}(\theta) \quad (48)$$

where $p_{\Theta}(\theta)$ is (known) prior pdf of the parameter vector and $p_{X/\Theta}(\mathbf{x}/\theta)$ is the pdf of \mathbf{x} conditioned to θ .

In general, it is not necessary to reconstruct the whole joint pdf $p_{X;\Theta}(\mathbf{x}; \theta)$ (or $p_{X/\Theta}(\mathbf{x}/\theta)$) to obtain the optimal estimate. Let us consider, for example, the case where the pdf can be factorized as

$$p_{X;\Theta}(\mathbf{x}; \theta) = g[\mathbf{T}(\mathbf{x}), \theta] h(\mathbf{x}), \quad (49)$$

where $g(\cdot, \cdot)$ depends on \mathbf{x} only through $\mathbf{T}(\mathbf{x})$, whereas $h(\cdot)$ does not depend on θ . The function $\mathbf{T}(\mathbf{x})$ is called a *sufficient statistic* for θ [66]. In general, the sufficient statistic $\mathbf{T}(\mathbf{x})$ is a vector, as it may be constituted by a set of functions. If (49) holds true, all is necessary to estimate θ is not really $p_{X;\Theta}(\mathbf{x}; \theta)$, but only $g[\mathbf{T}(\mathbf{x}), \theta]$. This means that any sensor able to evaluate $\mathbf{T}(\mathbf{x})$ through an interaction with the other sensors is able to find out the optimal parameter vector θ as the vector that maximizes $g[\mathbf{T}(\mathbf{x}), \theta]$.

A simple (yet common) example is given by the so called *exponential family* of pdf

$$p(\mathbf{x}; \theta) = \exp [A(\theta)B(\mathbf{x}) + C(\mathbf{x}) + D(\theta)]. \quad (50)$$

Examples of random variables described by this class include the Gaussian, Rayleigh, and exponential pdf's. Hence, this is a rather common model. Let us assume now that the observations \mathbf{x}_i collected by different nodes are statistically independent and identically distributed (i.i.d.), according to (50). It is

easy to check, simply applying the definition in (49), that a sufficient statistic in such a case is the scalar function:

$$T(\mathbf{x}) = \sum_{i=1}^N B(\mathbf{x}_i). \quad (51)$$

This structure suggests that a simple distributed way to enable every node in the network to estimate the vector θ locally, without loss of optimality with respect to the centralized approach, is to run a consensus algorithm, where the initial state of every node is set equal to $B(\mathbf{x}_i)$. At convergence, if the network is connected, every node has a state equal to the consensus value, i.e., $T(\mathbf{x})/N$. This enables every node to implement the optimal estimation by simply interacting with its neighbors to achieve a consensus. The only necessary condition for this simple method to work properly is that the network be connected. This is indeed a very simple example illustrating how consensus can be a fundamental step in deriving an optimal estimation through a purely decentralized approach relying only upon the exchange of data among neighbors.

In the next two sections, we will analyze in more details the purely distributed case (with no fusion center) where the global estimation can be carried out in any node and the centralized case, where the final estimation is taken at the fusion center.

A. Decentralized observations with decentralized estimation

In the following we analyze different observation models and illustrate alternative distributed estimation algorithms. We will start with the conditionally independent case and then we will generalize the approach to a conditionally dependent model.

1) *Conditionally independent observations:* A case amenable for finding distributed solutions is given by the situations where the observations collected by different sensors are conditionally independent. In such a case, the joint pdf $p_{X;\Theta}(\mathbf{x}; \theta)$ can be factorized as follows

$$p_{X;\Theta}(\mathbf{x}; \theta) = \prod_{i=1}^N p_{X_i;\Theta}(\mathbf{x}_i; \theta) \quad (52)$$

where $p_{X_i;\Theta}(\mathbf{x}_i; \theta)$ is the pdf of the vector \mathbf{x}_i observed by node i . Taking the log of this expression, the optimization problem can be cast, equivalently, as

$$\max_{\theta} \sum_{i=1}^N \log p_{X_i;\Theta}(\mathbf{x}_i; \theta). \quad (53)$$

Even if the objective function to be maximized is written as a sum of functions depending each on a local observation vector, the solution of the previous problem still requires a centralized approach because the vector $\boldsymbol{\theta}$ to be estimated is common to all the terms. A possible way to find a distributed solution to the problem in (53) consists in introducing an instrumental common variable \mathbf{z} and rewriting the previous problem in the following form

$$\begin{aligned} \min_{\boldsymbol{\theta}_i} & - \sum_{i=1}^N \log p_{X_i; \Theta}(\mathbf{x}_i; \boldsymbol{\theta}_i) \\ \text{s.t.} & \quad \boldsymbol{\theta}_i = \mathbf{z}, \quad i = 1, 2, \dots, N. \end{aligned} \quad (54)$$

This is a constrained problem, whose Lagrangian is

$$L(\boldsymbol{\theta}, \boldsymbol{\lambda}, \mathbf{z}) := \sum_{i=1}^N \left[-\log p_{X_i; \Theta}(\mathbf{x}_i; \boldsymbol{\theta}_i) + \boldsymbol{\lambda}_i^T (\boldsymbol{\theta}_i - \mathbf{z}) \right], \quad (55)$$

where $\boldsymbol{\lambda}_i$ are the vectors whose entries are the Lagrange multipliers associated to the equality constraints in (54). In many cases, it is useful to introduce the so called *augmented* Lagrangian [36]:

$$L_\rho(\boldsymbol{\theta}, \boldsymbol{\lambda}, \mathbf{z}) := \sum_{i=1}^N \left[-\log p_{X_i; \Theta}(\mathbf{x}_i; \boldsymbol{\theta}_i) + \boldsymbol{\lambda}_i^T (\boldsymbol{\theta}_i - \mathbf{z}) + \frac{\rho}{2} \|\boldsymbol{\theta}_i - \mathbf{z}\|_2^2 \right], \quad (56)$$

where ρ is a *penalty* parameter. Minimizing the augmented Lagrangian leads to the same solution as minimizing the original Lagrangian because any feasible vector satisfying the linear constraint yields a zero penalty. Nevertheless, there are some benefits in working with the augmented Lagrangian, namely: i) the objective function is differentiable under milder conditions than with the original Lagrangian; ii) convergence can be achieved without requiring strict convexity of the objective function (see [36] for more insight into the augmented Lagrangian method).

If the pdf's involved in (56) are log-concave functions of $\boldsymbol{\theta}$, the problem in (56) is strongly convex and then it admits a unique solution and there are efficient algorithms to compute the solution. Here, we are interested in deriving decentralized solutions.

A possible method to find a distributed solution of the problem in (56) is the *alternating direction method of multipliers (ADMM)* [36]. An excellent recent review of ADMM and its applications is [37]. The application of ADMM to distributed estimation problems was proposed in [26]. The method used in [26] relied on the introduction of the so called *bridge* nodes. Here, we will describe methods that do not require the introduction of any special class of nodes (in principle, every node has the same functionality as any other node). This is useful to simplify the estimation method as well as network design and

management.

The ADMM algorithm applied to solve (56) works through the following steps:

$$\begin{aligned}\boldsymbol{\theta}_i[k+1] &= \arg \min_{\boldsymbol{\theta}_i} \left\{ -\log p_{X_i; \Theta}(\mathbf{x}_i; \boldsymbol{\theta}_i) + \boldsymbol{\lambda}_i^T[k](\boldsymbol{\theta}_i - \mathbf{z}[k]) + \frac{\rho}{2} \|\boldsymbol{\theta}_i - \mathbf{z}[k]\|_2^2 \right\}, \\ \mathbf{z}[k+1] &= \arg \min_{\mathbf{z}} \sum_{i=1}^N \left\{ \boldsymbol{\lambda}_i^T[k](\boldsymbol{\theta}_i[k+1] - \mathbf{z}) + \frac{\rho}{2} \|\boldsymbol{\theta}_i[k+1] - \mathbf{z}\|_2^2 \right\}, \\ \boldsymbol{\lambda}_i[k+1] &= \boldsymbol{\lambda}_i[k] + \rho(\boldsymbol{\theta}_i[k+1] - \mathbf{z}[k+1]).\end{aligned}\tag{57}$$

The first and second steps aim at minimizing the primal function (i.e., the augmented Lagrangian) over the unknown variables $\boldsymbol{\theta}$ and \mathbf{z} , for a given value of the Lagrange multipliers' vectors $\boldsymbol{\lambda}_i$, as computed in the previous iteration.

The third step is a dual variable update, whose goal is to maximize the dual function, as in the dual ascent method. We recall that, in our case, the dual function is defined as

$$g(\boldsymbol{\lambda}) = \inf_{\boldsymbol{\theta}, \mathbf{z}} L_{\rho}(\boldsymbol{\theta}, \boldsymbol{\lambda}, \mathbf{z}).\tag{58}$$

In ADMM, the dual ascent step uses a gradient ascent approach to update $\boldsymbol{\lambda}$ in order to maximize $g(\boldsymbol{\lambda})$, for a given value of vectors $\boldsymbol{\theta}_i$ and \mathbf{z} , with the important difference that the step size used to compute the update is exactly the penalty coefficient ρ .

In our case, the second step can be computed in closed form as follows

$$\boldsymbol{\theta}_i[k+1] = \arg \min_{\boldsymbol{\theta}_i} \left\{ -\log p_{X_i; \Theta}(\mathbf{x}_i; \boldsymbol{\theta}_i) + \boldsymbol{\lambda}_i^T[k](\boldsymbol{\theta}_i - \mathbf{z}[k]) + \frac{\rho}{2} \|\boldsymbol{\theta}_i - \mathbf{z}[k]\|_2^2 \right\},\tag{59}$$

$$\mathbf{z}[k+1] = \frac{1}{N} \sum_{i=1}^N \left(\boldsymbol{\theta}_i[k+1] + \frac{1}{\rho} \boldsymbol{\lambda}_i[k] \right),\tag{60}$$

$$\boldsymbol{\lambda}_i[k+1] = \boldsymbol{\lambda}_i[k] + \rho(\boldsymbol{\theta}_i[k+1] - \mathbf{z}[k+1]).\tag{61}$$

From this formulation, we can see that the first and third steps can be run in parallel, over each node. The only step that requires an exchange of values among the nodes is the second step that requires the computation of an average value. But, as we know from previous section, the average value can be computed through a distributed consensus algorithm. The only condition for the convergence of consensus algorithm to the average value is that the graph representing the links among the nodes is connected.

The step in (60) can be further simplified as follows. Let us denote with \bar{x} the averaging operation across the nodes, i.e.

$$\bar{x} := \frac{1}{N} \sum_{i=1}^N x_i.\tag{62}$$

Using this notation, the z -update can be written as

$$z[k+1] = \overline{\boldsymbol{\theta}[k+1]} + \frac{1}{\rho} \overline{\boldsymbol{\lambda}[k]}. \quad (63)$$

Similarly, averaging over the $\boldsymbol{\lambda}$ -update yields

$$\overline{\boldsymbol{\lambda}[k+1]} = \overline{\boldsymbol{\lambda}[k]} + \rho \left(\overline{\boldsymbol{\theta}[k+1]} - z[k+1] \right). \quad (64)$$

Substituting (63) in (64), it is easy to check that, after the first iteration, $\overline{\boldsymbol{\lambda}[k+1]} = 0$. Hence, using $z[k] = \overline{\boldsymbol{\theta}[k]}$, the overall algorithm proceeds as indicated in Table I.

A.1	
STEP 1: Set $k = 0$, ϵ equal to a small positive value and initialize $\boldsymbol{\theta}_i[0]$, $\boldsymbol{\lambda}_i[0]$, $\forall i$, and \boldsymbol{z} randomly;	
STEP 2: Compute $\boldsymbol{\theta}_i[1]$, $\forall i$ using (59);	
STEP 3: Run consensus over $\boldsymbol{\theta}_i[1]$ and $\boldsymbol{\lambda}_i[0]$ to get $\overline{\boldsymbol{\theta}[1]}$ and $\overline{\boldsymbol{\lambda}[0]}$;	
STEP 4: Set $z[1] = \overline{\boldsymbol{\theta}[1]} + \frac{1}{\rho} \overline{\boldsymbol{\lambda}[0]}$;	
STEP 5: Compute $\boldsymbol{\lambda}_i[1]$, $\forall i$, using (61);	
STEP 6: Set $k = 1$;	
STEP 7: Repeat until convergence	
$\boldsymbol{\theta}_i[k+1] = \arg \min_{\boldsymbol{\theta}_i} \left\{ -\log p_{X_i; \Theta}(\boldsymbol{x}_i; \boldsymbol{\theta}_i) + \boldsymbol{\lambda}_i^T[k](\boldsymbol{\theta}_i - \overline{\boldsymbol{\theta}[k]}) + \frac{\rho}{2} \ \boldsymbol{\theta}_i - \overline{\boldsymbol{\theta}[k]}\ _2^2 \right\} \quad (65)$	
Run consensus over $\boldsymbol{\theta}_i[k+1]$ until convergence;	
$\boldsymbol{\lambda}_i[k+1] = \boldsymbol{\lambda}_i[k] + \rho \left(\boldsymbol{\theta}_i[k+1] - \overline{\boldsymbol{\theta}[k+1]} \right) \quad (66)$	
Set $k = k + 1$, if convergence criterion is satisfied stop, otherwise go to step 7.	

TABLE I
ALGORITHM A.1

The convergence criterion used in the steps of the algorithm is based on the relative absolute difference at two successive iterations: Given a sequence $\boldsymbol{y}[k]$, the algorithm stops when $\|\boldsymbol{y}[k+1] - \boldsymbol{y}[k]\| / \|\boldsymbol{y}[k]\| \leq \epsilon$,

with ϵ a small positive value.

Equations (65)-(66) give rise to an interesting interpretation: the primal update (first equation) aims at implementing a local optimization, with a penalty related to the disagreement between the local solution and the global one; the dual update (second equation) aims at driving all the local solutions to converge to a common (consensus) value, which coincides with the globally optimal solution.

The straightforward implementation of (65)-(66) requires running, at each step k of the ADMM algorithm, a consensus algorithm. A possible alternative approach can be envisaged by reformulating the optimization problem as follows:

$$\begin{aligned} \min_{\boldsymbol{\theta}_i} \quad & \left\{ -\sum_{i=1}^N \log p_{X_i; \Theta}(\mathbf{x}_i; \boldsymbol{\theta}_i) + \sum_{i=1}^N \sum_{j \in \mathcal{N}_i} \lambda_{ij}^T (\boldsymbol{\theta}_j - \boldsymbol{\theta}_i) + \frac{\rho}{2} \sum_{i=1}^N \sum_{j \in \mathcal{N}_i} \|\boldsymbol{\theta}_j - \boldsymbol{\theta}_i\|^2 \right\} \quad (67) \\ \text{s.t.} \quad & \boldsymbol{\theta}_j = \boldsymbol{\theta}_i; \forall j \in \mathcal{N}_i; \quad i = 1, 2, \dots, N, \end{aligned}$$

where \mathcal{N}_i denotes the set of node i 's neighbors. To make more clear the interaction among the nodes, it is useful to introduce the graph notation, as in previous section. Using the adjacency matrix \mathbf{A} , the previous problem can be rewritten as follows:

$$\begin{aligned} \min_{\boldsymbol{\theta}_i} \quad & \left\{ -\sum_{i=1}^N \log p_{X_i; \Theta}(\mathbf{x}_i; \boldsymbol{\theta}_i) + \sum_{i=1}^N \sum_{j=1}^N a_{ij} \lambda_{ij}^T (\boldsymbol{\theta}_j - \boldsymbol{\theta}_i) + \frac{\rho}{2} \sum_{i=1}^N \sum_{j=1}^N a_{ij} \|\boldsymbol{\theta}_j - \boldsymbol{\theta}_i\|^2 \right\} \quad (68) \\ \text{s.t.} \quad & \boldsymbol{\theta}_j = \boldsymbol{\theta}_i; \forall j \in \mathcal{N}_i; \quad i = 1, 2, \dots, N. \end{aligned}$$

This formulation does not require the introduction of the instrumental variable z . We keep enforcing the constraint that all the local estimates $\boldsymbol{\theta}_i$ converge to the same value. However, the penalty is now formulated as the disagreement between the local estimates. From consensus algorithm, we know that nulling the disagreement is equivalent to forcing all the vectors $\boldsymbol{\theta}_i$ to reach the same value if the graph describing the interactions among the nodes is connected. Hence, if the network is connected, at convergence, the disagreement goes to zero and there is no bias resulting from the introduction of the disagreement penalty.

The formulation in (68) is more amenable for an implementation that does not require, at any step of the algorithm, the convergence of consensus algorithms. In fact, applying ADMM to the solution of (68) yields the algorithm described in Table II.

A.2
STEP 1: Set $k = 0$, and initialize $\boldsymbol{\theta}_i[0]$, $\boldsymbol{\lambda}_{ij}[0]$, $\forall i, j \in \mathcal{N}_i$;
STEP 2: Repeat until convergence
$\boldsymbol{\theta}_i[k+1] = \arg \min_{\boldsymbol{\theta}_i} \left\{ -\sum_{i=1}^N \log p_{X_i; \Theta}(\mathbf{x}_i; \boldsymbol{\theta}_i) + \sum_{i=1}^N \sum_{j=1}^N a_{ij} \boldsymbol{\lambda}_{ij}^T[k] (\boldsymbol{\theta}_j[k] - \boldsymbol{\theta}_i) + \frac{\rho}{2} \sum_{i=1}^N \sum_{j=1}^N a_{ij} \ \boldsymbol{\theta}_j[k] - \boldsymbol{\theta}_i\ ^2 \right\}$ <div style="text-align: right;">(69)</div>
$\boldsymbol{\lambda}_{ij}[k+1] = \boldsymbol{\lambda}_{ij}[k] + \rho a_{ij} (\boldsymbol{\theta}_j[k+1] - \boldsymbol{\theta}_i[k+1])$ <div style="text-align: right;">(70)</div>
Set $k = k + 1$, if convergence criterion is satisfied stop, otherwise go to step 2.

TABLE II
ALGORITHM A.2

Some examples of applications are useful to grasp the main features of these algorithms.

2) *Distributed ML estimation under Gaussian noise*: Let us consider the common situation where the measured vector $\mathbf{x}_i \in \mathbb{R}^Q$ is related to the parameter vector $\boldsymbol{\theta} \in \mathbb{R}^M$, with $Q \geq M$, through a linear observation model, as:

$$\mathbf{x}_i = \mathbf{A}_i \boldsymbol{\theta} + \mathbf{v}_i, \quad i = 1, \dots, N \quad (71)$$

where $\mathbf{A}_i \in \mathbb{R}^{Q \times M}$ and \mathbf{v}_i is a vector of jointly Gaussian random variables with zero mean and covariance matrix \mathbf{C}_i , i.e. $\mathbf{v}_i \sim \mathcal{N}(\mathbf{0}, \mathbf{C}_i)$.

In such a case, algorithm **A.1** in (65) simplifies as the first step of (65) can be expressed in closed form

$$\begin{aligned} \boldsymbol{\theta}_i[k+1] &= (\mathbf{A}_i^T \mathbf{C}_i^{-1} \mathbf{A}_i + \rho \mathbf{I})^{-1} \left(\mathbf{A}_i^T \mathbf{C}_i^{-1} \mathbf{x}_i - \boldsymbol{\lambda}_i[k] + \overline{\rho \boldsymbol{\theta}[k]} \right), \\ \boldsymbol{\lambda}_i[k+1] &= \boldsymbol{\lambda}_i[k] + \rho \left(\boldsymbol{\theta}_i[k+1] - \overline{\boldsymbol{\theta}[k+1]} \right). \end{aligned} \quad (72)$$

The two updates can be computed in parallel by all the nodes, after having computed the average values through the consensus algorithm.

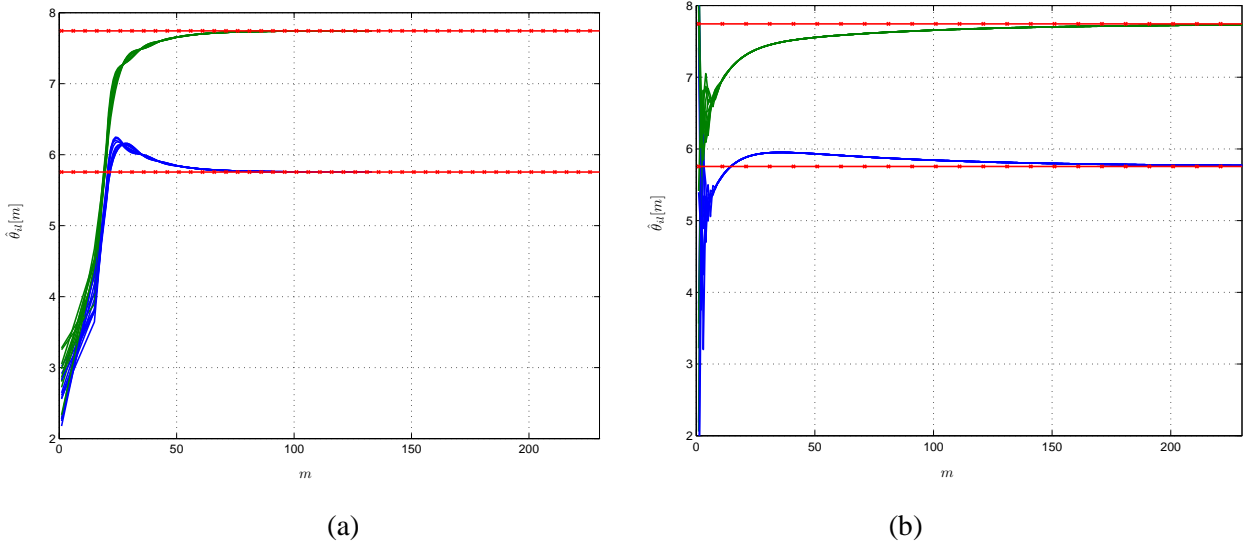


Fig. 6. Per node parameter estimation versus the iteration index m using algorithms **A.1** (left) and **A.2** (right).

Alternatively, algorithm **A.2** becomes

$$\boldsymbol{\theta}_i[k+1] = \left(\mathbf{A}_i^T \mathbf{C}_i^{-1} \mathbf{A}_i + 2\rho \sum_{j=1}^N a_{ij} \mathbf{I} \right)^{-1} \left(\mathbf{A}_i^T \mathbf{C}_i^{-1} \mathbf{x}_i + \sum_{j=1}^N a_{ij} (\boldsymbol{\lambda}_{ij}[k] - \boldsymbol{\lambda}_{ji}[k]) + 2\rho \sum_{j=1}^N a_{ij} \boldsymbol{\theta}_j[k] \right),$$

$$\boldsymbol{\lambda}_{ij}[k+1] = \boldsymbol{\lambda}_{ij}[k] + \rho a_{ij} (\boldsymbol{\theta}_j[k+1] - \boldsymbol{\theta}_i[k+1]). \quad (73)$$

In this case, there is no need of running the consensus algorithm for every iteration. Some numerical results are useful to compare the methods. As an example, we considered a connected network composed of $N = 10$ sensors. We set $\rho = 30$ and assumed an observation vector of size $Q = 30$. In Fig. 6 we report the estimates $\hat{\theta}_{i,l}$, for $l = 1, 2$, versus the iteration index m , for the two algorithms **A.1** (left plot) and **A.2** (right plot). The iteration index m includes also the iterations necessary for the consensus algorithm to converge within a prescribed accuracy (in this case, we stopped the consensus algorithm as soon as the absolute difference between two consecutive updates is below of 10^{-2} for all the nodes). In both figures, we report, as a benchmark, the maximum likelihood estimate (red line) achievable by a centralized node that knows all the observation vectors and all the model parameters, i.e. $\mathbf{A}_i, \mathbf{C}_i, \forall i$. From Fig.6, we can see that the estimates obtained with both methods converge to the optimal ML estimates.

In the specific case where the observation model is as in (71), with additive Gaussian noise, and the noise vectors pertaining to different sensors are mutually uncorrelated, the globally optimal ML estimate

is

$$\hat{\boldsymbol{\theta}}_{ML} = \left(\sum_{i=1}^N \mathbf{A}_i^T \mathbf{C}_i^{-1} \mathbf{A}_i \right)^{-1} \left(\sum_{i=1}^N \mathbf{A}_i^T \mathbf{C}_i^{-1} \mathbf{x}_i \right). \quad (74)$$

This formula is a vector weighted sum of the observations. Recalling that consensus algorithms, if properly initialized, can be made to converge to a weighted sum of the initial states, we can use the consensus algorithm directly to compute the globally optimal ML estimate through a totally distributed mechanism. In particular, in this case, the consensus algorithm proceeds as in Table III.

A.3
STEP 1: Set $k = 0$, and initialize $\boldsymbol{\theta}_i[0] = (\mathbf{A}_i^T \mathbf{C}_i^{-1} \mathbf{A}_i)^{-1} (\mathbf{A}_i^T \mathbf{C}_i^{-1} \mathbf{x}_i)$;
STEP 2: Repeat until convergence
$\boldsymbol{\theta}_i[k+1] = \boldsymbol{\theta}_i[k] + \epsilon \left(\mathbf{A}_i^T \mathbf{C}_i^{-1} \mathbf{A}_i \right)^{-1} \sum_{j=1}^N a_{ij} (\boldsymbol{\theta}_j[k] - \boldsymbol{\theta}_i[k]) \quad (75)$
Set $k = k + 1$, if convergence criterion is satisfied stop, otherwise go to step 2.

TABLE III
ALGORITHM A.3

Using again the basic properties of consensus algorithm, if the graph is connected and the step size ϵ is sufficiently small, the iterations in (75) converge to the globally optimal estimate (74).

3) *Distributed Bayesian estimation under Gaussian noise and Laplacian prior*: Let us consider now the case where the parameter vector is a random vector with known prior probability density function. Following a Bayesian approach, as in (48), the practical difference is that in such a case the objective function must include a term depending on the prior probability. Let us consider, for instance, the interesting case where the observation is Gaussian, as in the previous example, and the prior pdf is Laplacian, i.e.

$$p_{\Theta}(\boldsymbol{\theta}) = \mu \exp(-\mu \|\boldsymbol{\theta}\|_1) \quad (76)$$

with $\mu > 0$, where $\|\mathbf{x}\|_1$ denotes the l_1 norm of vector \mathbf{x} . In this case, the problem to be solved is the following

$$\min_{\boldsymbol{\theta}} \left\{ \sum_{i=1}^N \|\mathbf{x}_i - \mathbf{A}_i \boldsymbol{\theta}\|_{C_i^{-1}}^2 + \mu \|\boldsymbol{\theta}\|_1 \right\}, \quad (77)$$

where $\|\mathbf{x}\|_A^2$ denotes the weighted l_2 norm of \mathbf{x} , i.e. $\|\mathbf{x}\|_A^2 := \frac{\mathbf{x}^T \mathbf{A} \mathbf{x}}{2}$.

Interestingly, this formulation coincides with the formulation resulting from having no prior pdf, but incorporating an l_1 norm in order to drive the solution towards a sparse vector. This is the so called *least-absolute shrinkage and selection operator (lasso)* method [57]. A distributed algorithm to solve a linear regression problem with sparsity constraint was proposed in [35]. Here we provide a similar approach, with the important difference that, in each iteration, the update is computed in closed form. A decentralized solution can be found by reformulating the problem as follows

$$\begin{aligned} \min_{\boldsymbol{\theta}_i} \quad & \left\{ \sum_{i=1}^N \|\mathbf{x}_i - \mathbf{A}_i \boldsymbol{\theta}_i\|_{C_i^{-1}}^2 + \frac{\rho}{2} \sum_{i=1}^N \|\boldsymbol{\theta}_i - \mathbf{z}\|^2 + \mu \|\mathbf{z}\|_1 \right\}, \\ \text{s.t.} \quad & \boldsymbol{\theta}_i = \mathbf{z}, \quad i = 1, \dots, N. \end{aligned} \quad (78)$$

Using the ADMM approach, the algorithm proceeds through the following updates

$$\begin{aligned} \boldsymbol{\theta}_i[k+1] &= (\mathbf{A}_i^T C_i^{-1} \mathbf{A}_i + \rho \mathbf{I})^{-1} (\mathbf{A}_i^T C_i^{-1} \mathbf{x}_i - \boldsymbol{\lambda}_i[k] + \rho \mathbf{z}[k]), \\ \mathbf{z}[k+1] &= \arg \min_{\mathbf{z}} \left\{ \mu \|\mathbf{z}\|_1 + \frac{\rho}{2} \sum_{i=1}^N \|\boldsymbol{\theta}_i[k+1] - \mathbf{z}\|^2 + \sum_{i=1}^N \boldsymbol{\lambda}_i^T (\boldsymbol{\theta}_i[k+1] - \mathbf{z}) \right\} \\ \boldsymbol{\lambda}_i[k+1] &= \boldsymbol{\lambda}_i[k] + \rho (\boldsymbol{\theta}_i[k+1] - \bar{\mathbf{z}}[k+1]). \end{aligned} \quad (79)$$

The second equation can also be expressed in closed form. Moreover, defining the vector threshold function $\mathbf{t}_\mu(\mathbf{x})$ as the vector whose entries are obtained by applying the scalar thresholding function $t_\mu(x)$ to each element of vector \mathbf{x} , where

$$t_\mu(x) = \begin{cases} x - \mu, & x > \mu \\ 0, & -\mu \leq x \leq \mu \\ x + \mu, & x < -\mu \end{cases} \quad (80)$$

the overall algorithm is as in Table IV.

As a numerical example, in Fig. 7 we report the behavior of the estimated variable obtained using Algorithm A.4 versus the iteration index m , which includes the convergence times of two consensus algorithms in the equation (82). The example refers to a network of $N = 10$ nodes, using $\rho = \mu = 10$. The constant red line represents the centralized optimal solution. The parameter vector of this example

A.4

STEP 1: Set $k = 0$, and initialize $\theta_i[0]$, $\lambda_i[0]$, $\forall i$, and $z[0]$ randomly;

STEP 2: Repeat until convergence

$$\theta_i[k+1] = \left(A_i^T C_i^{-1} A_i + \rho I \right)^{-1} \left(A_i^T C_i^{-1} x_i - \lambda_i[k] + \rho z[k] \right) \quad (81)$$

Run consensus over $\theta_i[k+1]$ and $\lambda_i[k]$ to get $\overline{\theta}[k+1]$ and $\overline{\lambda}[k]$ until ϵ -convergence;

$$z[k+1] = \frac{1}{\rho N} t_\mu \left(N \overline{\lambda}[k] + \rho N \overline{\theta}[k+1] \right) \quad (82)$$

$$\lambda_i[k+1] = \lambda_i[k] + \rho (\theta_i[k+1] - \overline{z}[k+1]) \quad (83)$$

Set $k = k + 1$, if convergence criterion is satisfied stop, otherwise go to step 2.

TABLE IV
ALGORITHM A.4

has two components, one of which has been set to zero to test the capability to recover the sparsity. We can notice from Fig. 7 that, as expected, the algorithm converges to the globally optimal values.

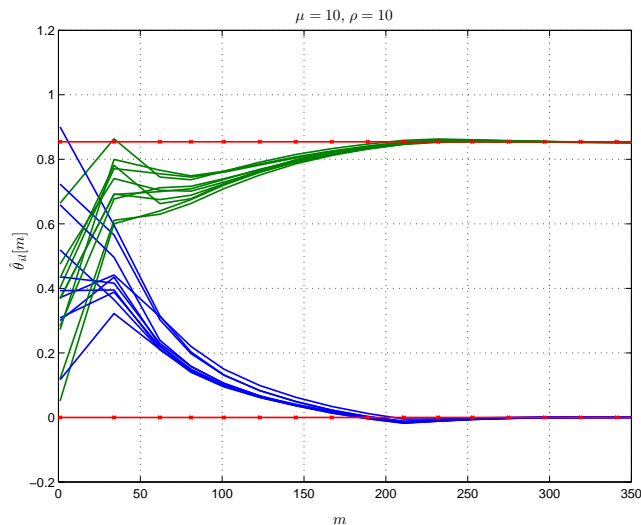


Fig. 7. Per node estimated variable versus the iteration index m for distributed Bayesian estimation using the ADMM approach.

To show the impact of the penalty coefficient μ on the sparsity of the estimated vector, in Fig. 8 we

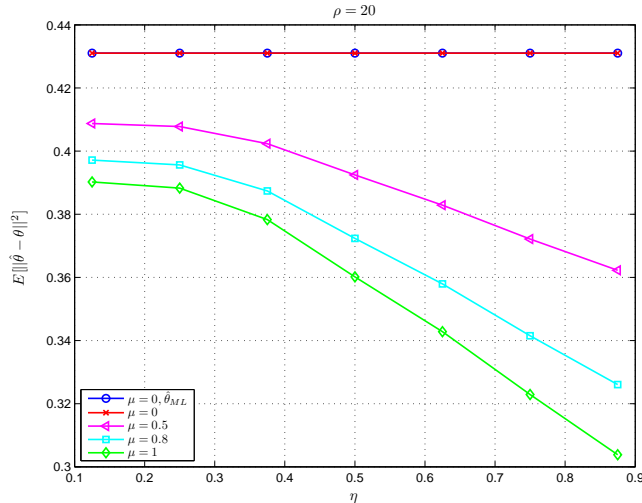


Fig. 8. Mean square estimation error versus the fraction η of null entries, for different μ values.

have reported the average mean square estimation error versus the coefficient η , defined as the fraction of zeros entries in the vector θ to be estimated, for different values of μ . It can be noted from Fig. 8 that for $\mu = 0$ the optimal solution is independent by η and it coincides with the optimal (centralized) ML solution. Furthermore, we can observe that, as μ and η increase, the average estimation error decreases thanks to the recovering sparsity property of the ADMM approach with the lasso constraint.

4) *Distributed recursive least square estimation with sparsity constraint:* In some applications, the parameters to be estimated may be changing over time. In these cases, it is more advisable to adopt recursive procedure rather than the batch approach followed until now. We show now how to obtain a distributed recursive least square (RLS) estimation incorporating a sparsity constraint.

Let us assume a linear observation model

$$\mathbf{x}_i(l) = \mathbf{A}_i(l)\boldsymbol{\theta} + \mathbf{v}_i(l), \quad (84)$$

where $\mathbf{x}_i(l)$ denotes the observation taken by node i at time l , $\mathbf{A}_i(l)$ is a known, possibly time-varying, mixing matrix and $\mathbf{v}_i(l)$ is the observation noise, supposed to have zero mean and covariance matrix $\mathbf{C}_i(l)$.

In RLS estimation with a sparsity constraint, the goal is to find the parameter vector $\boldsymbol{\theta}$, at each time

instant n , that minimizes the following objective function

$$\sum_{i=1}^N \sum_{l=1}^n \beta^{n-l} \|\mathbf{x}_i(l) - \mathbf{A}_i(l) \boldsymbol{\theta}\|_{C_i^{-1}(l)}^2 + \mu \|\boldsymbol{\theta}\|_1, \quad (85)$$

where $0 < \beta \leq 1$ is a forgetting factor used to weight more the most recent observations with respect to the older ones. The coefficient μ weights the importance of the sparsity constraint.

Proceeding as in the previous examples, a distributed solution can be found by formulating the problem, at each time n , as a constrained problem incorporating an instrumental variable \mathbf{z} to force all the nodes to converge to a common estimate. The problem can be made explicit as

$$\begin{aligned} \min_{\boldsymbol{\theta}_i} \quad & \sum_{i=1}^N \sum_{l=1}^n \beta^{n-l} \|\mathbf{x}_i(l) - \mathbf{A}_i(l) \boldsymbol{\theta}_i\|_{C_i^{-1}(l)}^2 + \frac{\rho}{2} \sum_{i=1}^N \|\boldsymbol{\theta}_i - \mathbf{z}\|^2 + \mu \|\mathbf{z}\|_1, \\ \text{s.t.} \quad & \boldsymbol{\theta}_i = \mathbf{z}, \quad i = 1, \dots, N. \end{aligned} \quad (86)$$

Again, the solution can be achieved by applying ADMM and the result is given by the algorithm described in Table V.

A.5
STEP 1: Set $n = 0$ and $k = 0$, and initialize $\boldsymbol{\theta}_i[0, 0]$, $\boldsymbol{\lambda}_i[0, 0]$, $\forall i$, and $\mathbf{z}[0, 0]$ randomly;
STEP 2: Repeat until convergence over index k
$\boldsymbol{\theta}_i[k+1, n] = \left(\sum_{l=1}^n \beta^{n-l} \mathbf{A}_i^T(l) \mathbf{C}_i^{-1}(l) \mathbf{A}_i(l) + \rho \mathbf{I} \right)^{-1} \left(\sum_{l=1}^n \beta^{n-l} \mathbf{A}_i^T(l) \mathbf{C}_i^{-1}(l) \mathbf{x}_i(l) - \boldsymbol{\lambda}_i[k, n] + \rho \mathbf{z}[k, n] \right)$
Run consensus over $\boldsymbol{\theta}_i[k+1, n]$ and $\boldsymbol{\lambda}_i[k, n]$ to get $\overline{\boldsymbol{\theta}}[k+1, n]$ and $\overline{\boldsymbol{\lambda}}[k, n]$ until convergence;
$\mathbf{z}[k+1, n] = \frac{1}{\rho N} t_\mu \left(N \overline{\boldsymbol{\lambda}}[k, n] + \rho N \overline{\boldsymbol{\theta}}[k+1, n] \right) \quad (87)$
$\boldsymbol{\lambda}_i[k+1, n] = \boldsymbol{\lambda}_i[k, n] + \rho (\boldsymbol{\theta}_i[k+1, n] - \overline{\boldsymbol{\theta}}[k+1, n])$
Set $k = k + 1$, if convergence criterion is satisfied set $n = n + 1$ and go to step 2, otherwise go to step 2.

TABLE V
ALGORITHM A.5

As before, the only step requiring the interaction among the nodes is a consensus algorithm to be run to compute the averages appearing in (87).

To test the convergence of Algorithm **A.5**, we considered a possible application to cooperative sensing for cognitive radio. We assumed the presence of a macro base station transmitting using a multicarrier scheme. We considered for simplicity of representation four channels, but the method can be easily extended to a larger number of channels. The sensing nodes aim to recover the activity of the macro transmitter, represented by a vector θ composed of four entries, one for each channel. To improve the accuracy of the local estimation, the sensors cooperate with each other by running Algorithm **A.5**. At some time, the activity level switches from on to off or viceversa. As an example, in Fig. 9 we report the four parameters to be estimated, indicated by the red lines. At time $n = 50$, the parameters switch to test the tracking capability of the proposed method.

In Fig. 9 we draw also the estimated parameters $\hat{\theta}_l$ for $l = 1, \dots, 4$ versus the current observation index n . We used $\beta = 0.6$, $\rho = 40$ and two values of the sparsity coefficient: $\mu = 0$ and $\mu = 40$. We can notice from Fig. 9 that the method is able to track the true parameters. It is also interesting to see that, as the penalty coefficient μ increases, the zero coefficients are estimated with greater accuracy. Conversely, the positive coefficients are recovered with a slightly larger bias.

To evaluate the impact of the forgetting factor β on the accuracy and tracking capability of the distributed RLS method, in Fig. 10 we reported the estimated parameters using $\beta = 0.6$ and $\beta = 0.9$, having set $\rho = \mu = 40$. It can be noted that, as β increases, the larger memory of the filter yields more accurate estimates. At the same time, having a larger memory implies slower time to reaction to the parameter switch, as evidenced in Fig. 10.

For any given forgetting factor β , the only possibility to improve the estimation accuracy is to have more nodes sensing a common macro base station. As an example, in Fig. 11 we report the behavior of the estimates obtained with different number of nodes, for a forgetting factor $\beta = 0.6$. We can notice that, as expected, increasing the number of nodes, the estimation accuracy increases as well. This reveals a trade-off between forgetting factor (time memory) and number of nodes involved in cooperative sensing.

5) *Distributed parameter estimation in spatially correlated observations*: So far, we have analyzed the case of conditionally independent observations. Let us consider now the case where the observation noise is spatially correlated. More specifically, we assume here the following observation model, for each sensor

$$x_i = \theta + v_i, \quad i = 1, \dots, N, \quad (88)$$

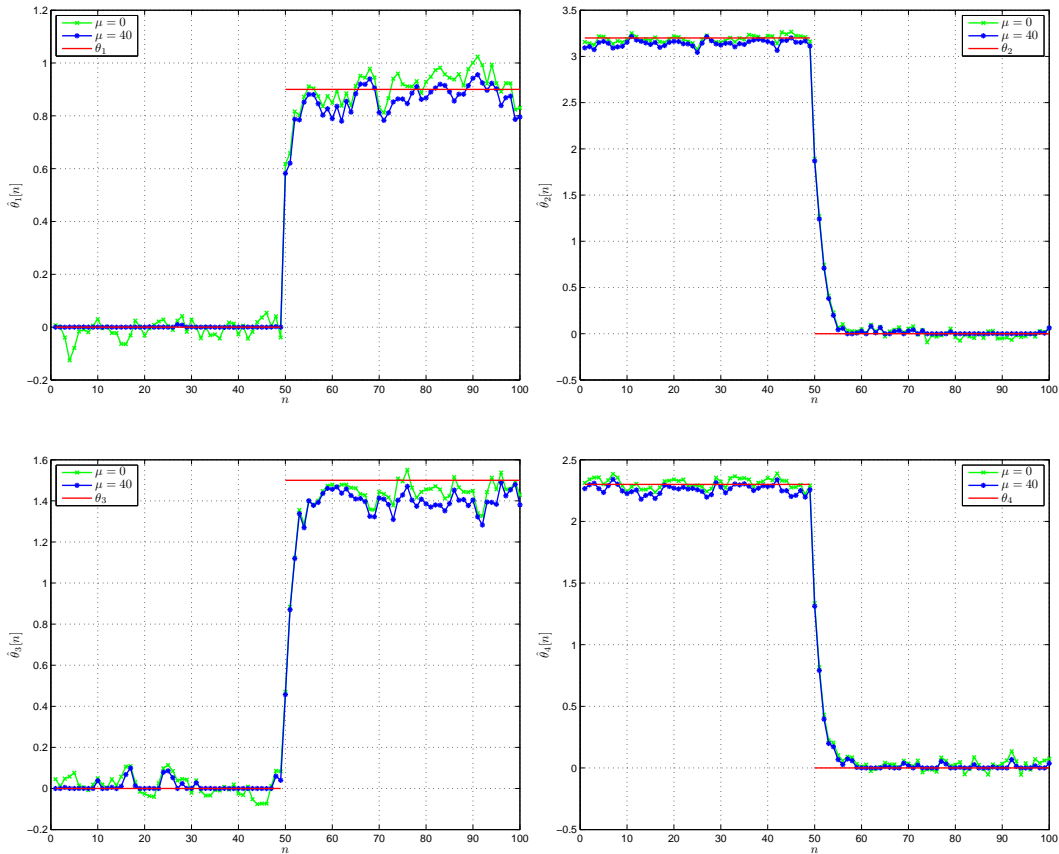


Fig. 9. Estimated parameters versus the number of current observations n for the RLS algorithm assuming $N = 10$, $\beta = 0.6$ and $\rho = 40$.

where the noise variables v_i are jointly Gaussian with zero mean and covariance matrix \mathbf{C} , or precision matrix $\mathbf{A} = \mathbf{C}^{-1}$. Furthermore, we assume that \mathbf{v} is a Gaussian Markov random field, so that the precision matrix is typically a sparse matrix. The joint pdf of the observation vector can then be written as in (17), i.e.,

$$p(\mathbf{x}; \theta) = \sqrt{\frac{|\mathbf{A}|}{(2\pi)^N}} \exp \left[-\frac{1}{2} (\mathbf{x} - \theta \mathbf{1})^T \mathbf{A} (\mathbf{x} - \theta \mathbf{1}) \right] := \sqrt{\frac{|\mathbf{A}|}{(2\pi)^N}} \exp [-V(\mathbf{x})] \quad (89)$$

where $V(\mathbf{x})$ can be rewritten as follows

$$V(\mathbf{x}) = \sum_{i=1}^N \phi_i(\mathbf{x}_i; \theta) \quad (90)$$

with $\mathbf{x}_i = [x_i, \{x_j\}_{j \in \mathcal{N}_i, j > i}]^T$, and

$$\phi_i(\mathbf{x}_i; \theta) := \frac{1}{2} a_{ii} (x_i - \theta)^2 + \sum_{j \in \mathcal{N}_i, j > i} a_{ij} (x_j - \theta) (x_i - \theta). \quad (91)$$

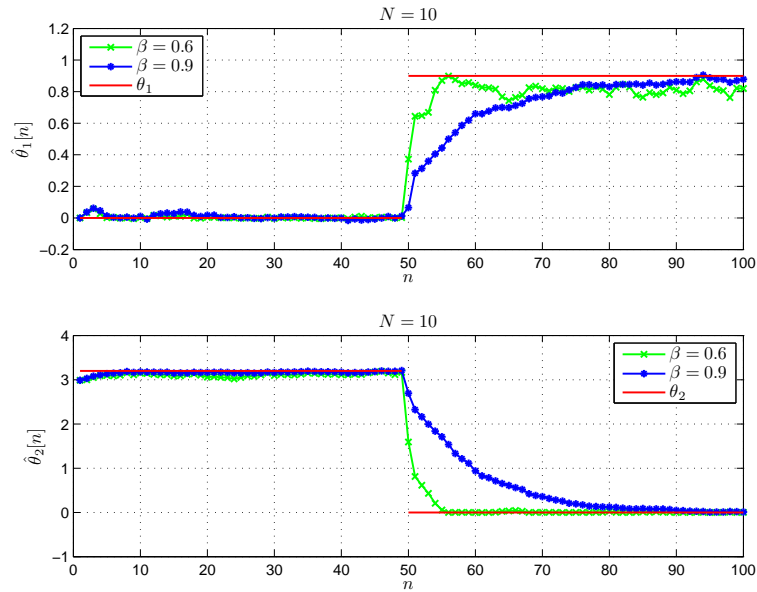


Fig. 10. Parameter estimation versus the number of observations n of the recursive least square estimation using the ADMM approach, considering $N = 10$ and two different values of β .

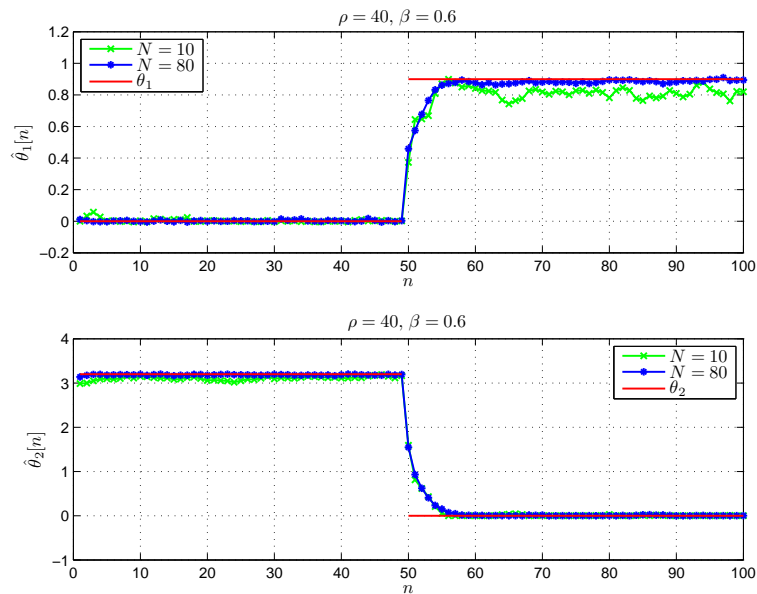


Fig. 11. Parameter estimation versus the number of observations n of the recursive least square estimation using the ADMM approach, considering $\beta = 0.6$, $\mu = 40$ and two different values of N .

As in the previous cases, also here a decentralized solution can be reached by formulating the problem as the minimization of the augmented Lagrangian

$$L_\rho(\boldsymbol{\theta}, \boldsymbol{\lambda}, z) := \sum_{i=1}^N \left\{ \phi_i(\mathbf{x}_i; \theta) + \lambda_i(\theta_i - z) + \frac{\rho}{2}(\theta_i - z)^2 \right\}, \quad (92)$$

subject to $\theta_i = z$. Applying the ADMM algorithm to this case, we get the following algorithm

$$\begin{aligned} \theta_i[k+1] &= \arg \min_{\theta} \left[\phi_i(\mathbf{x}_i; \theta) + \lambda_i(\theta_i - z) + \frac{\rho}{2}(\theta_i - z)^2 \right], \\ z[k+1] &= \frac{1}{N} \sum_{i=1}^N \left(\theta_i[k+1] + \frac{1}{\rho} \lambda_i[k] \right), \\ \lambda_i[k+1] &= \lambda_i[k] + \rho (\theta_i[k+1] - z[k+1]). \end{aligned} \quad (93)$$

It is important to notice that, in this case, even if the global problem concerning the minimization of the augmented Lagrangian in (92) is certainly convex, the local problem in (93) is not necessarily convex because there is no guarantee that the term $\phi_i(\mathbf{x}_i; \theta)$ is a positive definite function. Nevertheless, the quadratic penalty present in (93) can make every local problem in (93) convex. At the same time, at convergence the penalty goes to zero and thus it does not induce any undesired bias on the final result.

The first step in (93) can be made explicit, so that the algorithm assumes the form described in Table VI.

As an example, in Fig. 12 we report the estimation versus the cumulative iteration index m that includes the consensus steps and the iterations over k . The results refer to a connected network with $N = 5$ nodes; ρ has been chosen equal to 10 to guarantee that every local problem is convex. It can be noticed from Fig. 12 that the distributed solution converges to the optimal centralized solution (red line).

B. Decentralized observations with centralized estimation

In many cases, the observations are gathered in distributed form, through sensors deployed over a certain area, but the decision (either estimation or detection) is carried out in a central fusion center. In this section, we review some of the problems related to distributed estimation, with centralized decision. In such a case, the measurements gathered by the sensors are sent to a fusion center through rate-constrained physical channels. The question is how to design the quantization step in each sensor in order to optimize some performance metric related to the estimation of the parameter of interest. Let us start with an example, to introduce the basic issues.

A.6	
STEP 1: Set $k = 0$, and initialize $\theta_i[0]$, $\lambda_i[0]$, $\forall i$, and $z[0]$ randomly;	
STEP 2: Repeat until convergence	
$\theta_i[k+1] = \frac{1}{a_{ii} + \rho + 2 \sum_{j \in \mathcal{N}_i, j > i} a_{ij}} \left(\rho z[k] - \lambda_i[k] + a_{ii} x_i + \sum_{j \in \mathcal{N}_i, j > i} a_{ij} (x_i + x_j) \right) \quad (94)$	
Run consensus over $\theta_i[k+1]$ and $\lambda_i[k]$ to get $\overline{\theta[k+1]}$ and $\overline{\lambda[k]}$ until ϵ -convergence;	
$z[k+1] = \overline{\theta[k+1]} + \frac{1}{\rho} \overline{\lambda[k]} \quad (95)$	
$\lambda_i[k+1] = \lambda_i[k] + \rho (\theta_i[k+1] - z[k+1]) \quad (96)$	
Set $k = k + 1$, if convergence criterion is satisfied stop, otherwise go to step 2.	

TABLE VI
ALGORITHM A.6

Let us consider a network of N sensors, each observing a value x_k containing a deterministic parameter θ , corrupted by additive noise v_k , i.e.

$$x_k = \theta + v_k, \quad k = 1, \dots, N. \quad (97)$$

The noise variables v_k are supposed to be zero mean spatially uncorrelated random variables with variance σ_k^2 . Suppose that the sensors transmit their observations via some orthogonal multiple access scheme to a control center which wishes to estimate the unknown signal θ by minimizing the estimation mean square error (MSE) $E[(\hat{\theta} - \theta)^2]$. In the ideal case, where the observations are unquantized and received by the control center without distortion, the best linear unbiased estimator (BLUE) can be performed by the control center and the estimate $\hat{\theta}$ is given by

$$\hat{\theta} = \left(\sum_{k=1}^N \frac{1}{\sigma_k^2} \right)^{-1} \sum_{k=1}^N \frac{x_k}{\sigma_k^2} \quad (98)$$

with MSE given by $E[(\hat{\theta} - \theta)^2] = \left(\sum_{k=1}^N \frac{1}{\sigma_k^2} \right)^{-1}$. This estimator coincides with the maximum likelihood estimator when the noise variables are jointly Gaussian and uncorrelated.

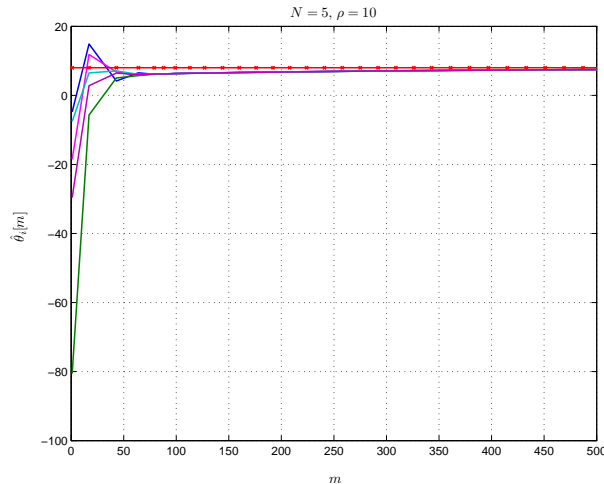


Fig. 12. Per node parameter estimation versus the iteration index m for spatially correlated observations using the ADMM approach.

Let us consider now the realistic case, where each sensor quantizes the observation x_k to generate a discrete message m_k of n_k bits. Assuming an error-free transmission, the fusion center must then provide an estimate $\hat{\theta}$ of the true parameter, based on the messages m_k transmitted by all the nodes. More specifically, assuming a uniform quantizer which generates unbiased message functions, the estimator at the control center performs a linear combination of the received messages. Let us suppose that the unknown signal to be estimated belongs to the range $[-A, A]$ and each sensor uniformly divides the range $[-A, A]$ into 2^{n_k} intervals of length $W_k = 2A/2^{n_k}$ rounding x_k to the midpoint of these intervals. In this case, the quantized value m_k at the k -th sensor can be written as $m_k = \theta + v_k + w_k$, where the quantization noise w_k is independent of v_k . It can be proved that m_k is an unbiased estimator of θ with

$$\text{Var}\{m_k\} \leq \delta_k^2 + \sigma_k^2 \quad (99)$$

where δ_k^2 denotes an upper bound on the quantization noise variance and is given by

$$\delta_k^2 = \frac{W_k^2}{12} = \frac{A^2}{3 \cdot 2^{2n_k}}. \quad (100)$$

A linear unbiased estimator of θ is [21]

$$\hat{\theta} = \left(\sum_{k=1}^N \frac{1}{\sigma_k^2 + \delta_k^2} \right)^{-1} \sum_{k=1}^N \frac{m_k}{\sigma_k^2 + \delta_k^2}. \quad (101)$$

This estimate yields an MSE upper bound

$$E[(\hat{\theta} - \theta)^2] \leq \left(\sum_{k=1}^N \frac{1}{\sigma_k^2 + \delta_k^2} \right)^{-1}. \quad (102)$$

As mentioned before, the previous strategy assumes that there are no transmission errors. This property can be made as close as possible to reality by enforcing the transmission rate of sensor k to be strictly less than the channel capacity from sensor k to the fusion center. If we denote by p_k the transmit power of sensor k , h_k the channel coefficient between sensor k and control node and N_0 is the noise variance at the control node receiver, the bound on transmit rate guaranteeing an arbitrarily small error probability is

$$n_k \leq \frac{1}{2} \log \left(1 + \frac{p_k h_k^2}{N_0} \right). \quad (103)$$

The problem is then how to allocate power and bits over each channel in order to fulfil some optimality criterion dictated by the estimation problem. This problem was tackled in [21] where it was proposed the minimization of the Euclidean norm of the transmit power vector under the constraint that the estimation variance is upper bounded by a given quantity and that the number of bits per symbol is less than the channel capacity. Here we formulate the problem as the minimization of the total transmit power under the constraint that the final MSE be upper bounded by a given quantity $\epsilon > 0$. From (103), defining $a_k = \frac{h_k^2}{N_0}$, we can derive the number of quantization level as a function of the transmit power,⁶

$$2^{2n_k} = (1 + p_k a_k). \quad (104)$$

Our aim is to minimize the sum of powers transmitted by all the sensors under the constraint

$$\left(\sum_{k=1}^N \frac{1}{\sigma_k^2 + \delta_k^2} \right)^{-1} \leq \epsilon. \quad (105)$$

Denoting with $\mathbf{p} = [p_1, \dots, p_N]$ the power vector, the optimization problem can be formulated as

$$\begin{aligned} \min_{\mathbf{p}} \quad & \sum_{k=1}^N p_k \\ \text{s.t.} \quad & \sum_{k=1}^N \frac{1}{\sigma_k^2 + \frac{A^2}{3 \cdot 2^{2n_k}}} \geq \frac{1}{\epsilon} \\ & \mathbf{p} \geq \mathbf{0} \end{aligned} \quad (106)$$

where n_k is a function of p_k , as in (103). In practice, the values n_k are integer. However, searching for the optimal integer values n_k leads to an integer programming problem. To relax the problem, we assume that the variables n_k are real. Then, by using (104), the optimization problem in (106) can be formulated

⁶We neglect here the discretization of n_k , to simplify the problem and arrive at closed form expressions.

as

$$\begin{aligned}
& \min_{\mathbf{p}} \quad \sum_{k=1}^N p_k \\
& \text{s.t.} \quad \sum_{k=1}^N \frac{1}{\sigma_k^2 + \frac{A^2}{3(1+p_k a_k)}} \geq \frac{1}{\epsilon} \quad (\mathcal{P}). \\
& \mathbf{p} \geq \mathbf{0}
\end{aligned} \tag{107}$$

Problem (\mathcal{P}) is indeed a convex optimization problem and it is feasible if $\sum_{k=1}^N \frac{1}{\sigma_k^2} > \frac{1}{\epsilon}$.

The optimal solution of the convex problem (\mathcal{P}) can be found by imposing the KKT conditions of (\mathcal{P}) , i.e.,

$$\begin{aligned}
1 - \mu_k - \lambda \frac{3A^2 a_k}{[3\sigma_k^2(1+p_k a_k) + A^2]^2} &= 0 \quad \forall k = 1, \dots, N \\
0 \leq \lambda \perp \sum_{k=1}^N \frac{3(1+p_k a_k)}{3\sigma_k^2(1+p_k a_k) + A^2} - \frac{1}{\epsilon} &\geq 0 \\
0 \leq \mu_k \perp p_k \geq 0 \quad \forall k = 1, \dots, N
\end{aligned} \tag{108}$$

where λ and μ_k denote the Lagrangian multipliers associated to the $N + 1$ constraints. The solution for the optimal powers turns out to be

$$p_k^* = \left[\frac{1}{\sigma_k^2} \sqrt{\frac{\lambda A^2}{3a_k}} - \frac{1}{a_k} - \frac{A^2}{3a_k \sigma_k^2} \right]^+ \tag{109}$$

where $(x)^+ = \max(0, x)$ and $\lambda > 0$ is found by imposing the MSE constraint to be valid with equality.

It is now useful to present some numerical results. To guarantee the existence of a solution, we set the bound $\epsilon = \beta \epsilon_{min}$ with $\beta > 1$ and $\epsilon_{min} = \left(\sum_{k=1}^N \frac{1}{\sigma_k^2} \right)^{-1}$. In Fig. 13 we report the sum of the optimal transmit powers vs. β , for different SNR values. The number of sensors is $N = 20$. We can notice that the minimum transmit power increases for smaller values of β , i.e. when we require the realistic system to perform closer and closer to the ideal communication case.

In the bottom subplot of Fig. 14 we report an example of optimal power allocation obtained by solving the optimization problem (\mathcal{P}) , corresponding to the channel realization shown in the top subplot, assuming a constant observation noise variance $\sigma_k^2 = 0.01$. We can observe that the solution is that only the nodes with the best channels coefficients are allowed to transmit. Finally, in Fig. 15 we plot the sum of the optimal transmit powers versus the number of sensors N , for different values of β . We can see that, as N increases, a lower power is necessary to achieve the desired estimation variance, as expected.

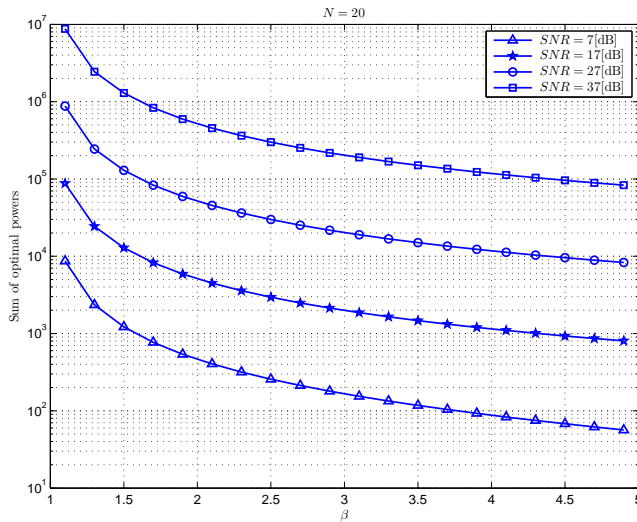


Fig. 13. Sum of the optimal powers for problem (\mathcal{P}) versus β for several values of σ_k^2 .

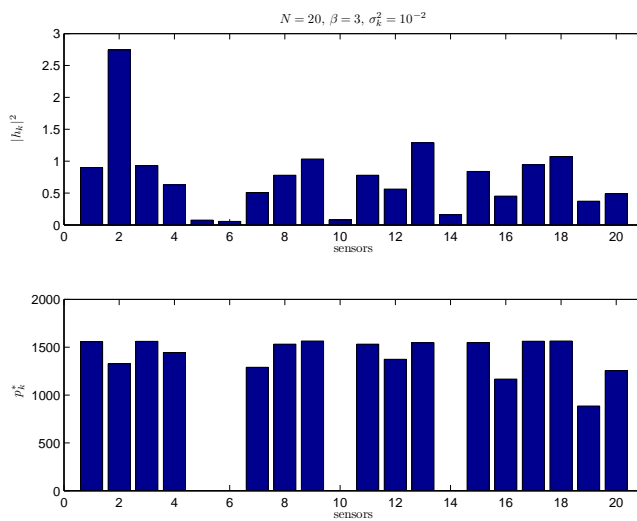


Fig. 14. Optimal power allocation of the sensors for problem (\mathcal{P}) , fixing the per-node observation noise variance.

V. DISTRIBUTED DETECTION

The distributed detection problem is in general more difficult to handle than the estimation problem. There is an extensive literature on distributed detection problem, but there is still a number of open problems. According to decision theory, an ideal centralized detector having error-free access to all the measurements collected by a set of nodes, should form the likelihood ratio and compare it with a suitable threshold [67]. Denoting with \mathcal{H}_0 and \mathcal{H}_1 the two alternative hypotheses, i.e. absence or presence of the

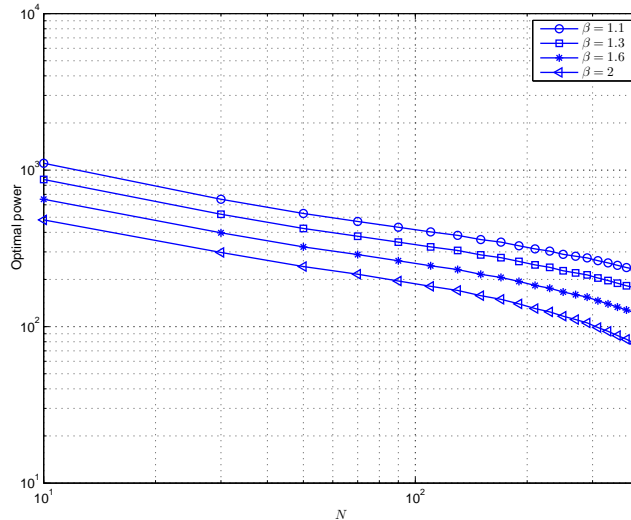


Fig. 15. Sum of optimal powers versus N for several values of β .

event of interest, and with $p(\mathbf{x}_1, \dots, \mathbf{x}_N; \mathcal{H}_i)$ the joint probability density function of the whole set of observed data, under the hypothesis \mathcal{H}_i , many decision tests can be cast as threshold strategies where the likelihood ratio (LR) is compared with a threshold γ , which depends on the decision criterion. This is true, for example, for two important formulations leading to the Bayes approach and to the Neyman-Pearson criterion, the only difference between the two's being the values assumed by the threshold γ . The detection rule decides for \mathcal{H}_1 if the threshold is exceeded or for \mathcal{H}_0 , otherwise. In formulas,

$$\Lambda(\mathbf{x}) := \Lambda(\mathbf{x}_1, \dots, \mathbf{x}_N) = \frac{p(\mathbf{x}_1, \dots, \mathbf{x}_N; \mathcal{H}_1)}{p(\mathbf{x}_1, \dots, \mathbf{x}_N; \mathcal{H}_0)} \underset{\mathcal{H}_0}{\overset{\mathcal{H}_1}{\gtrless}} \gamma. \quad (110)$$

Ideally, with no communication constraints, every node should then send its observation vector \mathbf{x}_i , with $i = 1, \dots, N$ to the fusion center, which should then use all the received vectors to implement the LR test, as in (110). In reality, there are intrinsic limitations due to, namely: a) the finite number of bits with which every sensor has to encode the measurements before transmission; b) the maximum latency with which the decision has to be taken; c) the finite capacity of the channel between sensors and fusion center. The challenging problem is then how to devise an optimum decentralized detection strategy taking into account the limitations imposed by the communication over realistic channels. The global problem, in the most general setting, is still an open problem, but there are many works in the literature addressing some specific cases. The interested reader may check the book [12] or the excellent tutorial reviews given in [13], [14], [15]. The situation becomes more complicated when we take explicitly into account the capacity bound imposed by the communication channel and we look for the number of

bits to be used to quantize the local observations before transmitting to the fusion center. This problem was addressed in [18], [19], where it was shown that binary quantization is optimal for the problem of detecting deterministic signals in Gaussian noise and for detecting signals in Gaussian noise using a square-law detector. The interesting indication, in these contexts, is that the gain offered by having more sensor nodes outperforms the benefits of getting more detailed (nonbinary) information from each sensor. A general framework to cast the problem of decentralized detection is the one where the topology describing the exchange of information among sensing nodes is not simply a tree, with all nodes sending data to a fusion center, but it is a graph. Each node is assumed to transmit a finite-alphabet symbol to its neighbors and the problem is how to find out the encoding (quantization) rule on each node. A class of problems admitting a message passing algorithm with provable convergence properties was proposed in [9]. The solution is a sort of distributed fusion protocol, taking explicitly into account the limits on the communication resources. An interesting and well motivated observation model is a correlated random field, as in many applications the observations concern physical quantities, like temperature or pressure, for example, which, being subject to diffusion processes, are going to be spatially and temporally correlated. One of the first works addressing the detection of a known signal embedded in a correlated Gaussian noise was [22]. Using large deviations theory, the authors of [20] study the impact of node density, assuming that observations become increasingly correlated as sensors are in closer proximity of each other. More recently, the detection of a Gauss-Markov Random field (GMRF) with nearest-neighbor dependency was studied in [7]. Scaling laws for the energy consumption of optimal and sub-optimal fusion policies were then presented in [8]. The problem of energy-efficient routing of sensor observations from a Markov random field was analyzed in [10].

A classification of the various detection algorithms depends on the adopted criterion. A first important classification is the following:

- 1) Global decision is taken at the fusion center
 - a) Nodes send data to FC; FC takes global decision
 - b) Nodes send local decisions to FC; FC fuses local decisions
- 2) Every node is able to take a global decision
 - a) Nodes exchange data with their neighbors
 - b) Nodes exchange local decisions with their neighbors

In the first case, the observation is distributed across the nodes, but the decision is centralized. This case

has received most of the attention. The interested reader may check, for example, the book [12] or the tutorial reviews given in [13], [14], [15]. In the second case, also the decision is decentralized. This case has been considered only relatively recently. Some references are, for example, [68], [69], [70], [71], [72], [73], [74].

An alternative classification is between

- 1) Batch algorithms
- 2) Sequential algorithms

In the first case, the network collects a given amount of data along the time and space domains and then it takes a decision. In the second case, the number of observations, either in time or in terms of number of involved sensors, is not decided a priori, but it is updated at every new measurement. The network stops collecting information only when some performance criterion is satisfied (typically, false alarm and detection probability) [75], [76], [77].

One of the major difficulties in distributed detection comes from establishing the optimal decision thresholds at local and global level. The main problem is how to optimize the local decisions, taking into account that the final decisions will be only the result of the interaction among the nodes. Taking a local decision can be interpreted as a form of source coding. The simple (binary) hypothesis testing can be seen in fact as a form of binary coding. Whenever the observations are conditionally independent, given each hypothesis, the likelihood ratio test at the sensor nodes is indeed optimal [16]. However, finding the optimal quantization levels is a difficult task. Even when the observations are i.i.d., assuming identical decision rules is very common and apparently well justified. Nevertheless there are counterexamples showing that nonidentical decision rules are optimal [16]. Identical decision rules in the i.i.d. case turns out to be optimal only asymptotically, as the number of nodes tends to infinity [17].

A simple example may be useful to grasp some of the difficulties associated with distributed detection. For this purpose, we briefly recall the seminal work of Tenney and Sandell [23]. Let us consider two sensors, each measuring a real quantity x_i , with $i = 1, 2$. Based on its observation x_i , sensor i decides whether the phenomenon of interest is present or not. In the first case, it sets the decision variable $u_i = 1$, otherwise, it sets $u_i = 0$. The question is how to implement the decision strategy, according to some optimality criterion. The approach proposed in [23] is a Bayesian approach, where the goal of each sensor is to minimize the Bayes risk, which can be made explicit by introducing the cost coefficients and the observation probability model. Let us denote by C_{ijk} the cost of detector 1 deciding on \mathcal{H}_i , detector 2

deciding on \mathcal{H}_j , when the true hypothesis is \mathcal{H}_k . Denoting by P_k the prior probability of event \mathcal{H}_k and by $p(u_1, u_2, x_1, x_2, \mathcal{H}_k)$ the joint pdf of having \mathcal{H}_k , observing the pair (x_1, x_2) and deciding for the pair (u_1, u_2) , the average risk can be written as

$$\begin{aligned}\mathcal{R} &= \sum_{i,j,k} \int C_{ijk} p(u_1, u_2, x_1, x_2, \mathcal{H}_k) dx_1 dx_2 \\ &= \sum_{i,j,k} P_k \int C_{ijk} p(u_1, u_2, x_1, x_2 / \mathcal{H}_k) dx_1 dx_2 \\ &= \sum_{i,j,k} P_k \int C_{ijk} p(u_1, u_2 / x_1, x_2, \mathcal{H}_k) p(x_1, x_2 / \mathcal{H}_k) dx_1 dx_2.\end{aligned}\quad (111)$$

In this case, each node observes only its own variable and takes a decision independently of the other node. Hence, we can set

$$\mathcal{R} = \sum_{i,j,k} P_k \int C_{ijk} p(u_1 / x_1) p(u_2 / x_2) p(x_1, x_2 / \mathcal{H}_k) dx_1 dx_2.\quad (112)$$

Expanding the right hand side by explicitly summing over index i , we get

$$\mathcal{R} = \sum_{j,k} P_k \int p(u_2 / x_2) p(x_1, x_2 / \mathcal{H}_k) [C_{0jk} p(u_1 = 0 / x_1) + C_{1jk} p(u_1 = 1 / x_1)] dx_1 dx_2.\quad (113)$$

Considering that $p(u_1 = 1 / x_1) = 1 - p(u_1 = 0 / x_1)$ and ignoring all terms which do not contain u_1 , we get

$$\mathcal{R} = \int p(u_1 = 0 / x_1) \sum_{j,k} P_k \left\{ \int p(u_2 / x_2) p(x_1, x_2 / \mathcal{H}_k) [C_{0jk} - C_{1jk}] dx_2 \right\} dx_1 + \text{const.}\quad (114)$$

The average risk is minimized if $p(u_1 = 0 / x_1)$ is chosen as follows

$$p(u_1 = 0 / x_1) = \begin{cases} 0, & \text{if } \sum_{j,k} P_k \int p(u_2 / x_2) p(x_1, x_2 / \mathcal{H}_k) [C_{0jk} - C_{1jk}] dx_2 \geq 0 \\ 1, & \text{otherwise.} \end{cases}\quad (115)$$

This expression shows that the optimal local decision rule is a *deterministic* rule. After a few algebraic manipulations, (115) can be rewritten, equivalently, as [12]

$$\Lambda(x_1) := \frac{p(x_1 / \mathcal{H}_1)}{p(x_1 / \mathcal{H}_0)} \underset{\mathcal{H}_0}{\overset{\mathcal{H}_1}{\gtrless}} \frac{P_0 \sum_j \int p(u_2 / x_2) p(x_2 / x_1, \mathcal{H}_0) [C_{1j0} - C_{0j0}] dx_2}{P_1 \sum_j \int p(u_2 / x_2) p(x_2 / x_1, \mathcal{H}_1) [C_{0j1} - C_{1j1}] dx_2},\quad (116)$$

where $\Lambda(x_1)$ is the LR at node 1. Equation (116) has the structure of a LRT. However, note that the threshold on the right hand side of (116) depends on the observation x_1 , through the term $p(x_2 / x_1, \mathcal{H}_1)$, which incorporates the statistical dependency between the observations x_1 and x_2 . Hence, Equation (116) is not a proper LRT.

The situation simplifies if the observations are conditionally independent, i.e. $p(x_2/x_1, \mathcal{H}_k) = p(x_2/\mathcal{H}_k)$.

In such a case, the threshold t_1 can be simplified into

$$t_1 = \frac{P_0 \int p(x_2/\mathcal{H}_0) \{p(u_2 = 0/x_2)[C_{100} - C_{000}] + p(u_2 = 1/x_2)[C_{110} - C_{010}]\} dx_2}{P_1 \int p(x_2/\mathcal{H}_1) \{p(u_2 = 0/x_2)[C_{001} - C_{101}] + p(u_2 = 1/x_2)[C_{011} - C_{111}]\} dx_2}. \quad (117)$$

Since $p(u_2 = 1/x_2) = 1 - p(u_2 = 0/x_2)$, (117) can be rewritten as

$$t_1 = \frac{P_0 \int p(x_2/\mathcal{H}_0) \{[C_{110} - C_{010}] + p(u_2 = 0/x_2)[C_{100} - C_{000} + C_{010} - C_{110}]\} dx_2}{P_1 \int p(x_2/\mathcal{H}_1) \{[C_{011} - C_{111}] + p(u_2 = 0/x_2)[C_{001} - C_{101} + C_{111} - C_{011}]\} dx_2}. \quad (118)$$

Hence, the threshold t_1 to be used at node 1 is a function of $p(u_2 = 0/x_2)$, i.e., on the decision taken by node 2. At the same time, the threshold t_2 to be used by node 2 will depend on the decision rule followed by node 1. This means that, even if the observations are conditionally independent and the decisions are taken autonomously by the two nodes, the decisions are still coupled through the thresholds. This simple example shows how the detection problem can be rather complicated, even under a very simple setting.

In the special case where $C_{000} = C_{111} = 0$, $C_{010} = C_{100} = C_{011} = C_{101} = 1$, and $C_{110} = C_{001} = 2$, i.e., there is no penalty if the decisions are correct, the penalty is 1, when there is one error, and the penalty is 2 when there are two errors, the threshold simplifies into

$$t_1 = \frac{P_0}{P_1}. \quad (119)$$

Hence, in this special case, the two thresholds are independent of each other and the two detectors become independent of each other.

After having pointed out through a simple example some of the problems related to distributed detection, it is now time to consider in more detail the cases where the nodes send their (possibly encoded) data to the FC or they take local decisions first and send them to the FC. In both situations, there are two extreme cases: a) there is only one FC; b) every node is a potential FC, as it is able to take a global decision.

A. Nodes send data to decision center

Let us consider for simplicity the simple (binary) hypothesis testing problem. Given a set of vector observations $\mathbf{x} := [\mathbf{x}_1, \dots, \mathbf{x}_N]$, where \mathbf{x}_i is the vector collected by node i , $i = 1, \dots, N$, the optimal decision rule for the simple hypothesis testing problem, under a variety of optimality criteria, amounts to compute the likelihood ratio (LR) $\Lambda(\mathbf{x})$ and compare it with a threshold. In formulas,

$$\Lambda(\mathbf{x}) := \Lambda(\mathbf{x}_1, \dots, \mathbf{x}_N) = \frac{p(\mathbf{x}_1, \dots, \mathbf{x}_N; \mathcal{H}_1)}{p(\mathbf{x}_1, \dots, \mathbf{x}_N; \mathcal{H}_0)} \underset{\mathcal{H}_0}{\overset{\mathcal{H}_1}{\gtrless}} \gamma. \quad (120)$$

In words, the detector decides for \mathcal{H}_1 if the LR exceeds the threshold, otherwise it decides for \mathcal{H}_0 . In general, what changes the distributed detection problem from the standard centralized detection is that the data are sent to the decision center after source encoding into a discrete alphabet. The simplest form of encoding is quantization. But also taking local decisions can be interpreted as a form of binary coding. Clearly, source coding is going to affect the detection performance. It is then useful to show, through a simple example, how local quantization affects the final detection performance and how we can benefit from the theoretical analysis to optimize the number of bits associated to the quantization step in order to optimize performance of the detection scheme.

1) *Centralized detection of deterministic signal embedded in additive noise:* Let us consider the detection of a deterministic (known) signal embedded in additive noise. In this section, we consider the case where the decision is taken at a FC, after having collected the data sent by the sensors. This case could refer for example to the detection of undesired resonance phenomena in buildings, bridges, etc. The form of the resonance is known. However, the measurements taken by the sensors are affected by noise and then it is of interest to check the performance as a function of the signal to noise ratio.

The measurement vector is $\mathbf{x} = (x_1, \dots, x_N)$, where x_i is the measurement taken by node i . Let us denote as \mathbf{s} the known deterministic signal. The observation can be modeled as

$$\mathbf{x} \sim \begin{cases} \mathbf{v} + \mathbf{w} & \text{under } \mathcal{H}_0 \\ \mathbf{s} + \mathbf{v} + \mathbf{w} & \text{under } \mathcal{H}_1 \end{cases}, \quad (121)$$

where \mathbf{v} is the background noise, whereas \mathbf{w} is the quantization noise. We assume the noise to be Gaussian with zero mean and (spatial) covariance matrix \mathbf{C}_n , i.e. $\mathbf{v} \sim \mathcal{N}(\mathbf{0}, \mathbf{C}_n)$. To simplify the mathematical tractability, we consider a dithered quantization so that the quantization error can be modeled as a random process statistically independent of noise. We may certainly assume that, after dithering, the quantization noise variables over different sensors are statistically independent. Hence, we can state that the quantization noise vector \mathbf{w} has zero mean and a diagonal covariance matrix $\mathbf{C}_q = \text{diag}(\sigma_{q1}^2, \dots, \sigma_{qN}^2)$. If the amplitude of the useful signal spans the dynamic range $[-A, A]$ and the number of bits used by node i is n_i , the quantum range is $q_i = 2A/2^{n_i}$ so that the quantization noise variance at node i is

$$\sigma_{qi}^2 = \frac{(2A)^2}{12 \cdot 2^{2n_i}} = \frac{A^2}{3 \cdot 2^{2n_i}}. \quad (122)$$

The overall noise has then a zero mean and covariance matrix $\mathbf{C} = \mathbf{C}_n + \mathbf{C}_q$.

If the quantization noise is negligible, the Neyman-Pearson criterion applied to this case leads to the following linear detector

$$T(\mathbf{x}) = \mathcal{R}\{\mathbf{s}^H \mathbf{C}^{-1} \mathbf{x}\} \underset{\mathcal{H}_0}{\overset{\mathcal{H}_1}{\gtrless}} \gamma \quad (123)$$

where $\mathcal{R}(x)$ denotes the real part of x and the detection threshold γ is computed in order to guarantee the desired false alarm probability P_{fa} . Unfortunately, since the quantization noise is not Gaussian, the composite noise $\mathbf{v} + \mathbf{w}$ is not Gaussian and then the detection rule in (123) is no longer optimal. Nevertheless, the rule in (123) is still meaningful as it maximizes the signal to noise ratio (SNR). Hence, it is of interest to look at the performance of this detector in the presence of quantization noise. The exact computation of the detection probability is not easy, at least in closed form, because it requires the computation of the pdf of $T(\mathbf{x})$. Nevertheless, when the number of nodes is sufficiently high (an order of a few tens can be sufficient to get a good approximation), we can invoke the central limit theorem to state that $T(\mathbf{x})$ is approximately Gaussian. Using this approximation, the detection probability can be written in closed form for any fixed P_{fa} , following standard derivations (see, e.g. [67]), as

$$P_d = Q \left[Q^{-1}(P_{fa}) - \sqrt{\mathbf{s}^H \mathbf{C}^{-1} \mathbf{s}} \right] = Q \left[Q^{-1}(P_{fa}) - \sqrt{\mathbf{s}^H (\mathbf{C}_n + \mathbf{C}_q)^{-1} \mathbf{s}} \right]. \quad (124)$$

This formula is useful to assess the detection probability as a function of the bits allocated to each transmission. At the same time, we can also use (124) as a way to find out the bit allocation that maximizes the detection probability. This approach establishes an interesting link between the communication and detection aspects. In practice, in fact, encoded data are transmitted over a finite capacity channel. Hence, it is useful to relate the number of quantization bits used by each node and capacity of the channel between that node and the FC. For simplicity, we consider the optimization problem under the assumption of spatially uncorrelated noise, i.e. $\mathbf{C}_n = \text{diag}(\sigma_{n1}^2, \dots, \sigma_{nN}^2)$. The problem we wish to solve is the maximization of the detection probability, for a given false alarm rate and a maximum global transmit power. To guarantee an arbitrarily low transmission error rate, we need to respect Shannon's channel coding theorem, so that the number of bits per symbol must be less than channel capacity. Denoting with p_i the power transmitted by user i and assuming flat fading channel, with channel coefficient h_i^2 , the capacity is given by (103). From (124), maximizing P_d is equivalent to maximizing $\mathbf{s}^H (\mathbf{C}_n + \mathbf{C}_q)^{-1} \mathbf{s}$. Hence, using (122), the maximum P_d , for a given P_{fa} and a given global transmit power P_T , can be

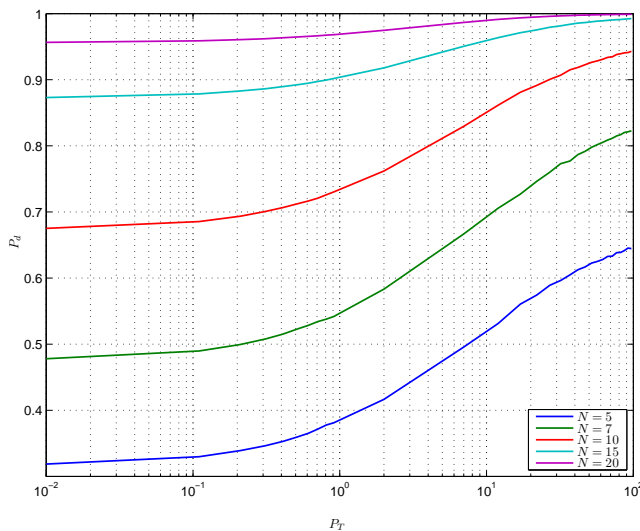


Fig. 16. Detection probability vs. sum transmit power, for different number of sensors.

achieved by finding the power vector $\mathbf{p} = (p_1, \dots, p_N)$ that solves the following constrained problem

$$\max_{\mathbf{p}} \sum_{i=1}^N |s_i|^2 \left(\sigma_{ni}^2 + \frac{A^2}{3(1 + a_i p_i)} \right)^{-1} \quad (125)$$

$$\text{s.t.} \quad \sum_{i=1}^N p_i \leq P_T; \quad p_i \geq 0, i = 1, \dots, N. \quad (126)$$

It is straightforward to check that this is a convex problem. Imposing the Karush-Kuhn-Tucker conditions, the optimal powers can be expressed in closed form as:

$$p_i = \left[\frac{1}{\sqrt{\lambda}} \sqrt{\frac{s_i^2 A^2}{3a_i \sigma_{ni}^4}} - \frac{A^2}{3a_i \sigma_{ni}^2} - \frac{1}{a_i} \right]^+ \quad (127)$$

where the Lagrange multiplier λ associated to the sum-power constraint can be determined as the value that makes $\sum_{i=1}^N p_i = P_T$.

A numerical example is useful to grasp some of the properties of the proposed algorithm. Let us consider a series of sensors placed along a bridge of length L . The purpose of the network is to detect one possible spatial resonance, which we represent as the signal $s(z) = A \cos(\pi z/L)$, where $z \in [-L/2, L/2]$ denotes the spatial coordinate. The sensors are uniformly spaced along the bridge, at positions $z_i = (i-1)L/N$, with $i = 1, \dots, N$. Every sensor measures a shift $x_i = s(z_i) + v_i$, affected by the error v_i . To communicate its own measurement to the FC, every sensor has to quantize the measurement first. The optimal number

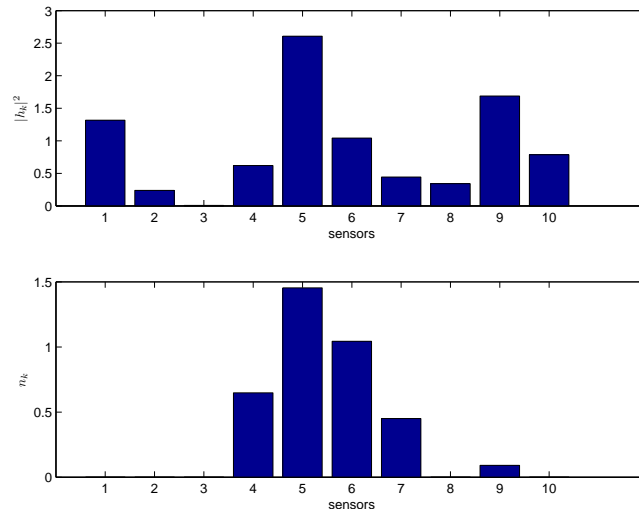


Fig. 17. Optimal bit allocation.

of bits to be used by every sensor can be computed by using the previous theory. In this case, in Fig. 16 we report the detection probability vs. the sum power P_T available to the whole set of sensors, for different numbers N of sensors. As expected, as the total transmit power increases, P_d increases because more bits per symbol can be transmitted and then the quantization errors become negligible. It is also important to notice how, increasing the number of sensors, the detection probability improves, for any given transmit power. Furthermore, in Fig. 17 we can see the optimal per channel bit allocation (bottom), together with the channels profiles $|h_k|^2$ (top). Interestingly, we can see that the method allocates more bits in correspondence with the best channels and the central elements of the array, where the useful signal is expected to have the largest variations.

2) *Decentralized detection under conditionally independent observations*: Let us consider now the case where the globally optimal decision can be taken, in principle, by any node. To enable this possibility, every node must be able to implement the statistical test (120). If the measurements collected by the sensors are conditionally independent, the logarithm of the likelihood ratio can be written as

$$\log \Lambda(\mathbf{x}_1, \dots, \mathbf{x}_N) = \sum_{i=1}^N \log \Lambda_i(\mathbf{x}_i) = \sum_{i=1}^N [\log p_{X_i}(\mathbf{x}_i, \mathcal{H}_1) - \log p_{X_i}(\mathbf{x}_i, \mathcal{H}_0)]. \quad (128)$$

This formula shows that, in the conditionally independent case, running a consensus algorithm is sufficient to enable every node to compute the global LR. It is only required that every sensor initializes its own state with the local log-LR $\log \Lambda_i(\mathbf{x}_i)$ and then runs the consensus iterations. If the network is connected, every node will end up with the average value of the local LR's. In practice, to send the local LR, every node

must quantize it first. Then, we need to refer to the consensus algorithm in the presence of quantization errors. However, we have already seen in Section III-B that the consensus iterations may be properly modified to make the algorithm robust against a series of drawbacks coming from communications through realistic channels, as, eg. random packet drops and quantization. Hence, a consensus algorithm, properly modified, can enable every node to compute the global LR with controllable error.

B. Nodes send local decisions to fusion center

Consider now the case where each node i takes a local decision, according to a locally optimal criterion, and encodes the decision into the binary variable u_i . Then, the node sends the variable u_i to the fusion center, which is asked to take a global decision on the basis of the vector $\mathbf{u} := (u_1, \dots, u_N)$ containing all local decisions. Let us consider for simplicity the binary hypothesis test. This problem was considered in [12] and we will now review the basic results. This problem is distinct from the case studied in the previous section because here the local decision thresholds are optimized according to a detection criterion, whereas in standard quantization the decision thresholds are not optimized.

Under both Bayesian and Neyman-Pearson (NP) formulations, the optimal test amounts to a likelihood ratio test, based on \mathbf{u} , i.e.

$$\frac{p(u_1, \dots, u_N; \mathcal{H}_1)}{p(u_1, \dots, u_N; \mathcal{H}_0)} \geq \eta. \quad (129)$$

In the case of conditionally independent local decisions, the LRT converts into

$$\frac{\prod_{i=1}^N p(u_i; \mathcal{H}_1)}{\prod_{i=1}^N p(u_i; \mathcal{H}_0)} := \prod_{i=1}^N \Lambda_i(u_i) \geq \eta. \quad (130)$$

Since each variable u_i can only assume the values 0 or 1, we can group all the variables into two subsets: the subset S_0 containing all variables $u_i = 0$ and the subset S_1 containing all variables $u_i = 1$, thus yielding

$$\prod_{i \in S_0} \frac{p(u_i = 0; \mathcal{H}_1)}{p(u_i = 0; \mathcal{H}_0)} \prod_{i \in S_1} \frac{p(u_i = 1; \mathcal{H}_1)}{p(u_i = 1; \mathcal{H}_0)} \geq \eta. \quad (131)$$

Denoting with $P_{Mi} = p(u_i = 0; \mathcal{H}_1)$, and $P_{Fi} = p(u_i = 1; \mathcal{H}_0)$, the probabilities of miss and the probability of false alarm of node i , respectively, (131) can be rewritten as

$$\prod_{i \in S_0} \frac{P_{Mi}}{1 - P_{Fi}} \prod_{i \in S_1} \frac{1 - P_{Mi}}{P_{Fi}} \geq \eta. \quad (132)$$

Taking the logarithm of both sides and reintroducing the variables u_i , the fusion rule becomes

$$\sum_{i=1}^N \left[\log \left(\frac{1 - P_{Mi}}{P_{Fi}} \right) u_i + \log \left(\frac{P_{Mi}}{1 - P_{Fi}} \right) (1 - u_i) \right] \geq \log \eta \quad (133)$$

or, equivalently

$$\sum_{i=1}^N \log \left[\frac{(1 - P_{Mi})(1 - P_{Fi})}{P_{Mi}P_{Fi}} \right] u_i \geq \log \left[\eta \prod_{i=1}^N \frac{1 - P_{Fi}}{P_{Mi}} \right]. \quad (134)$$

The optimal fusion rule is then a simple weighted sum of the local decisions, where the weights depend on the reliabilities of the local decisions: Larger weights are assigned to the most reliable nodes.

If instead of having a single FC, we wish to enable every node to implement the decision fusion rule described above, we can see that, again, running a consensus algorithm suffices to reach the goal. In fact, if each local state variable is initialized with a value $x_i[0] = \log \left[\frac{(1 - P_{Mi})(1 - P_{Fi})}{P_{Mi}P_{Fi}} \right] u_i$, running a consensus algorithm allows every node to know the function in (134). The only constraint is, as always, network connectivity. The drawback of this simple approach is that running this sort of consensus algorithm requires the transmission of real variables, rather than the binary variables u_i . In fact, even if the local decision u_i is binary, the coefficient multiplying u_i is a real variable, which needs to be quantized before transmission over a realistic channel. Again, the consensus algorithm can be robustified against quantization errors by using dithered quantization and a decreasing step size, as shown in III-B. However, it is important to clarify that we cannot make any claim of optimality of this kind of distributed decision. In principle, when the nodes exchange their decisions with the neighbors, the decision thresholds should be adjusted in order to accommodate some optimality criterion. This is indeed an interesting, yet still open, research topic.

VI. BEYOND CONSENSUS: DISTRIBUTED PROJECTION ALGORITHMS

In many applications, the field to be reconstructed by a sensor network is typically a smooth function of the spatial coordinates. This happens for example, in the reconstruction of the spatial distribution of the power radiated by a set of transmitters. The problem is that local measurements may be corrupted by local noise or fading effects. An important application of this scenario is given by cognitive networks. In such a case, a secondary node would need to know the channel occupation across space, to find out unoccupied channels, within the area of interest. This requires some sort of spectrum sensing, but in a localized area. The problem of sensing is that wireless propagation is typically affected by fading or shadowing effects, so that a sensor in a shadowed location might indicate that a channel is unoccupied, while this is not true. To avoid this kind of error, which would lead to undue channel occupation from opportunistic users, it is useful to resort to cooperative sensing. In such a case, nearby nodes exchange local measurements to counteract the effect of shadowing.

The problem with local averaging operations is that they should reduce the effect of fading, but without destroying valuable spatial variations. In the following, we recall a distributed algorithm proposed in [87] to recover a spatial map of a field, using local weighted averages where the weights are chosen so as to improve upon local noise or fading effects, but without destroying the spatial variation of the useful signal.

Let us consider a network composed of N sensors located at positions (x_i, y_i) , $i = 1, \dots, N$, and denote the measurement collected by the i -th sensor by $g(x_i, y_i) = z(x_i, y_i) + v_i$, where $z(x_i, y_i)$ represents the useful field while v_i is the observation error. Let us also denote by $u_k(x, y)$, $k = 1, \dots, r$, a set of linearly independent spatial functions defining a basis for the useful signal. The useful signal can then be represented through the basis expansion model

$$z(x_i, y_i) = \sum_{k=1}^r s_k u_k(x_i, y_i). \quad (135)$$

In vector notation, introducing the N -size column vector $\mathbf{g} := [g(x_1, y_1), g(x_2, y_2), \dots, g(x_N, y_N)]^T$ and similarly for the vector \mathbf{z} , we may write

$$\mathbf{g} = \mathbf{z} + \mathbf{v} = \mathbf{U}\mathbf{s} + \mathbf{v}, \quad (136)$$

where \mathbf{U} is the $N \times r$ matrix whose m -th column is $\mathbf{u}_m = (u_m(x_1, y_1), \dots, u_m(x_N, y_N))$, $\mathbf{s} = (s_1, \dots, s_r)$ is an r -size vector of coefficients and $\mathbf{z} = \mathbf{U}\mathbf{s}$ is the useful signal. The spatial smoothness of the useful signal field may be captured by choosing the functions $u_k(x, y)$ to be the low frequency components of the Fourier basis or low-order 2D polynomials. For instance, if the space under monitoring is a square of side L , we may choose the set

$$\{u_{nm}(x, y)\} = \left\{ 1, \cos\left(2\pi\frac{nx+my}{L}\right), \sin\left(2\pi\frac{nx+my}{L}\right) \right\}_{\substack{m=\infty, n=\infty \\ m=0, n=0; m+n \neq 0}} \quad (137)$$

In practice, the dimension r of the useful signal subspace is typically much smaller than the dimension N of the observation space, i.e. of the number of sensors. We can exploit this property to devise a distributed denoising algorithm.

If we use a Minimum Mean Square Error (MMSE) strategy, the goal is to find the useful signal vector $\hat{\mathbf{s}}$ that minimizes the mean square error

$$\mathcal{E} := E\{\|\mathbf{g} - \mathbf{U}\hat{\mathbf{s}}\|^2\}. \quad (138)$$

The solution is well known and is given by [66]:

$$\hat{\mathbf{s}} = (\mathbf{U}^T \mathbf{U})^{-1} \mathbf{U}^T \mathbf{g}. \quad (139)$$

Our goal is actually to recover the vector \mathbf{z} , rather than \mathbf{s} . In such a case, the estimate of \mathbf{z} is

$$\hat{\mathbf{z}} = \mathbf{U}(\mathbf{U}^T \mathbf{U})^{-1} \mathbf{U}^T \mathbf{g}. \quad (140)$$

The operation performed in (140) corresponds to projecting the observation vector onto the subspace spanned by the columns of \mathbf{U} . Assuming, without any loss of generality (w.l.o.g.), the columns of \mathbf{U} to be orthonormal, the projector simplifies into

$$\hat{\mathbf{z}} = \mathbf{U} \mathbf{U}^T \mathbf{g}. \quad (141)$$

The centralized solution to this problem is then very simple: The fusion center collects all the measurements $g(x_i, y_i)$, compute \mathbf{U} and then recovers $\hat{\mathbf{z}}$ from (141).

The previous approach is well known. The interesting point is that the MMSE solution can be achieved with a totally decentralized approach, where every sensor interacts only with its neighbors, with no need to send any data to a fusion center. The proposed approach is based on a very simple iterative procedure, where each node initializes a state variable with the local measurement, let us say $z_i[0] = g(x_i, y_i)$, and then it updates its own state by taking a linear combination of its neighbors' states, similarly with what happens with consensus algorithms, but with coefficients computed in order to solve the new problem.

More specifically, denoting by $\mathbf{z}[k]$, the N -size vector containing the states of all the nodes, at iteration k , and by \mathbf{g} the vector containing the initial measurements collected by all the nodes, the vector $\mathbf{z}[k]$ evolves according to the following linear state equation:

$$\mathbf{z}[k+1] = \mathbf{W} \mathbf{z}[k], \quad \mathbf{z}[0] = \mathbf{g} \in \mathbb{R}^N, \quad (142)$$

where $\mathbf{W} \in \mathbb{R}^{N \times N}$ is typically a *sparse* (not necessarily symmetric) matrix. The network topology is reflected into the sparsity of \mathbf{W} . In particular, the number of nonzero entries of, let us say, the i -th row is equal to the number of neighbors of node i . In a WSN, the neighbors of a node are the nodes falling within the coverage area of that node, i.e. within a circle centered on the location of the node, with radius dictated by the transmit power of the node and by the power attenuation law. Our goal is to find the nonnull coefficients of \mathbf{W} that allow the convergence of $\mathbf{z}[k]$ to the vector $\hat{\mathbf{z}}$ given in (141). In general, not every network topology guarantees the existence of a solution of this problem. In the following, we will show that a solution exists only if each node has a number of neighbors greater than the dimension r of the useful signal subspace.

Let us denote by $\mathbf{P}_{\mathcal{R}(\mathbf{U})} \in \mathbb{R}^{N \times N}$ the orthogonal projector onto the r -dimensional subspace of \mathbb{R}^N spanned by the columns of $\mathcal{R}(\mathbf{U})$, where $\mathcal{R}(\cdot)$ denotes the range space operator and $\mathbf{U} \in \mathbb{R}^{N \times r}$ is a full-column rank matrix, assumed, w.l.o.g., to be semi-unitary. System (142) converges to the desired

orthogonal projection of the initial value vector $\mathbf{z}[0] = \mathbf{g}$ onto $\mathcal{R}(\mathbf{U})$, for *any* given $\mathbf{g} \in \mathbb{R}^N$, if and only if

$$\lim_{k \rightarrow +\infty} \mathbf{z}[k] = \lim_{k \rightarrow +\infty} \mathbf{W}^k \mathbf{g} = \mathbf{P}_{\mathcal{R}(\mathbf{U})} \mathbf{g}, \quad (143)$$

i.e.,

$$\lim_{k \rightarrow +\infty} \mathbf{W}^k = \mathbf{P}_{\mathcal{R}(\mathbf{U})}. \quad (144)$$

Resorting to basic algebraic properties of discrete-time systems, it is possible to derive immediately some basic properties of \mathbf{W} . In particular, denoting with OUD the Open Unit Disk, i.e. the set $\{x \in \mathbb{C} : |x| < 1\}$, a matrix \mathbf{W} is *semistable* if its spectrum $\text{spec}(\mathbf{W})$ satisfies $\text{spec}(\mathbf{W}) \subset \text{OUD} \cup \{1\}$ and, if $1 \in \text{spec}(\mathbf{W})$, then 1 is semisimple, i.e. its algebraic and geometric multiplicities coincide. If \mathbf{W} is semistable, then [86, p. 447]

$$\lim_{k \rightarrow +\infty} \mathbf{W}^k = \mathbf{I} - (\mathbf{I} - \mathbf{W})^\# (\mathbf{I} - \mathbf{W}), \quad (145)$$

where $\#$ denotes group generalized inverse [86, p. 228]. Furthermore, setting, without loss of generality, the matrix \mathbf{W} in the form $\mathbf{W} = \mathbf{I} - \epsilon \mathbf{L}$, (145) can be rewritten as

$$\lim_{k \rightarrow +\infty} \mathbf{W}^k = \mathbf{I} - \mathbf{L}^\# \mathbf{L}. \quad (146)$$

But $\mathbf{I} - \mathbf{L}^\# \mathbf{L}$ is the projector onto the null-space of \mathbf{L} . Hence, we can state the following

Proposition 1: Given the dynamical system in (142) and the projection matrix $\mathbf{P}_{\mathcal{R}(\mathbf{U})}$, the vector $\mathbf{P}_{\mathcal{R}(\mathbf{U})} \mathbf{z}[0]$ is globally asymptotically stable for *any fixed* $\mathbf{z}[0] \in \mathbb{R}^N$, if and only if the following conditions are satisfied:

- i) \mathbf{L} has a nullspace of dimension r , spanned by the columns of \mathbf{U} ;
- ii) \mathbf{L} and ϵ must be chosen so that \mathbf{W} is semistable.

Alternatively, the previous conditions can be rewritten equivalently in the following form

Proposition 2: Given the dynamical system in (142) and the projection matrix $\mathbf{P}_{\mathcal{R}(\mathbf{U})}$, the vector $\mathbf{P}_{\mathcal{R}(\mathbf{U})} \mathbf{z}[0]$ is globally asymptotically stable for *any fixed* $\mathbf{z}[0] \in \mathbb{R}^N$, if and only if the following conditions are satisfied:

$$\mathbf{W} \mathbf{P}_{\mathcal{R}(\mathbf{U})} = \mathbf{P}_{\mathcal{R}(\mathbf{U})} \quad (\text{C.1})$$

$$\mathbf{P}_{\mathcal{R}(\mathbf{U})} \mathbf{W} = \mathbf{P}_{\mathcal{R}(\mathbf{U})} \quad (\text{C.2})$$

$$\rho(\mathbf{W} - \mathbf{P}_{\mathcal{R}(\mathbf{U})}) < 1 \quad (\text{C.3})$$

where $\rho(\cdot)$ denotes the spectral radius operator [81]. □

Remark 1: Conditions C.1-C.3 have an intuitive interpretation. In particular, C.1 and C.2 state that, if system (142) asymptotically converges, then it is guaranteed to converge to the desired value. In fact, C.1 guarantees that the projection of vector $\mathbf{z}[k]$ onto $\mathcal{R}(\mathbf{U})$ is an invariant quantity for the dynamical system, implying that the system in (142), during its evolution, keeps the component $\mathbf{P}_{\mathcal{R}(\mathbf{U})}\mathbf{z}[0]$ of $\mathbf{z}[0]$ unaltered. At the same time, C.2 makes $\mathbf{P}_{\mathcal{R}(\mathbf{U})}\mathbf{z}[0]$ a fixed point of matrix \mathbf{W} and thus a potential accumulation point for the sequence $\{\mathbf{z}[k]\}_k$. Both conditions C.1 and C.2 do not state anything about the convergence of the dynamical system. This is guaranteed by C.3, which imposes that all the modes associated to the eigenvectors orthogonal to $\mathcal{R}(\mathbf{U})$ are asymptotically vanishing.

Remark 2: The conditions C.1-C.3 contain, as a special case, the convergence conditions of average consensus algorithm. In fact, it is sufficient to set in (143), $r = 1$ and $\mathbf{U} = \mathbf{u} = \frac{1}{\sqrt{N}}\mathbf{1}_N$, where $\mathbf{1}_N$ is the N -length vector of all ones. In such a case, C.1-C.3 can be restated as following: the digraph associated to the network described by \mathbf{W} must be strongly connected and balanced.

The previous conditions do not make any explicit reference to the sparsity of matrix \mathbf{W} . However, when we consider a sparse matrix, reflecting the network topology, additional conditions are necessary to make sure that the previous conditions are satisfied. In other words, not every network topology is able to guarantee the asymptotic projection onto a prescribed signal subspace. One basic question is then what network topology is able to guarantee the convergence to a prescribed projector. We provide now the conditions on the sparsity of \mathbf{W} , or equivalently \mathbf{L} , guaranteeing the desired convergence.

From condition *i*) of Proposition 1, given the matrix \mathbf{U} , \mathbf{L} must satisfy the equation $\mathbf{L}\mathbf{U} = \mathbf{0}$. Let us assume that every row of \mathbf{L} has K nonzero entries and let us indicate with $\{i_{j1}, \dots, i_{jK}\}$ the set of the column indices corresponding to the nonzero entries of the j -th row of \mathbf{L} . Hence, every row of \mathbf{L} must satisfy the following equation

$$\begin{pmatrix} u_1(i_{11}), & u_1(i_{12}), & \cdots & u_1(i_{1K}) \\ u_2(i_{21}), & u_2(i_{22}), & \cdots & u_2(i_{2K}) \\ \cdot & \cdot & \cdot & \cdot \\ u_r(i_{r1}), & u_r(i_{r2}), & \cdots & u_r(i_{rK}) \end{pmatrix} \begin{pmatrix} l_{j1} \\ \vdots \\ l_{jK} \end{pmatrix} = \mathbf{0}. \quad (147)$$

To guarantee the existence of a nontrivial solution to (147), the matrix on the left hand side must have a kernel of dimension at least one. This requires K to be strictly greater than r , the dimension of the signal subspace. Since the number of nonzero entries of, let us say the j -th, row of \mathbf{L} is equal to the number of neighbors of node j plus one (the coefficient multiplying the state of node i itself), this implies that the

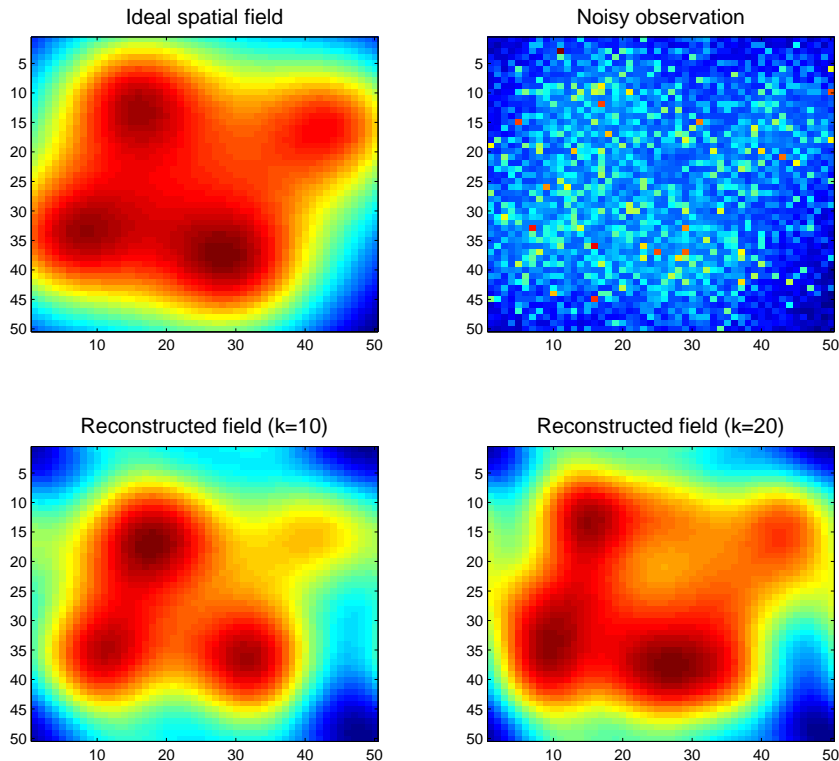


Fig. 18. Example of field reconstruction in the presence of fading: ideal spatial field (top left); measured field (top right); field reconstructed with order $k = 10$ (bottom left) and $k = 20$ (bottom right).

minimum number K of neighbors of each node must be at least equal to the dimension r of the signal subspace. Of course this condition is necessary but not sufficient. It is also necessary to check that the sparse matrix \mathbf{L} built with rows satisfying (147), with $j = 1, \dots, N$, had rank $N - r$. This depends on the location of the nodes and on the specific choice of the orthogonal basis.

An example can be useful to illustrate the benefits achievable with the proposed technique. We consider the case where the observation is corrupted by a multiplicative, spatially uncorrelated, noise, which models, for example a fading effect. Let us denote with $P(x_i, y_i) = A(x_i, y_i) S(x_i, y_i)$ the measurement carried out from node i , located in the point of coordinates (x_i, y_i) , where $S(x_i, y_i)$ denotes the useful field, whereas $A(x_i, y_i)$ represents fading. We consider, for instance, a useful signal composed by $N_s = 4$ transmitters and we assume a polynomial power attenuation, so that the useful signal measured at the point of coordinates (x, y) is

$$S(x, y) = \sum_{i=1}^{N_s} \frac{P_i}{1 + ((x - x_i)^2 + (y - y_i)^2)/\sigma^2}, \quad x \in \left[-\frac{L}{2}, \frac{L}{2}\right], \quad y \in \left[-\frac{L}{2}, \frac{L}{2}\right]. \quad (148)$$

where P_i is the power emitted by source i , located at (x_i, y_i) , and σ specifies the power spatial spread. Furthermore, fading is modeled as a spatially uncorrelated multiplicative noise. The sensor network is composed of 2500 nodes uniformly distributed over a 2D grid. All the transmitters use the same power, i.e. $P_i = P$ in (148), and the noise has zero mean and variance $\sigma_n^2 = P$. In this case, it is useful to apply a homomorphic filtering to the measured field. In particular, we take the log of the measurement, thus getting $\log(P(x_i, y_i)) = \log(S(x_i, y_i)) + \log(A(x_i, y_i))$. To smooth out the undesired effect of fading, we assume a signal model composed by the superposition of 2D sinusoids, so that the columns of the matrix U in (136) are composed of signals of the form $\sin(2\pi(mx + ny)/L)$, and $\cos(2\pi(mx + ny)/L)$, with $m, n = 0, 1, \dots$. We set the initial value of the state of each node equal to $\log(P(x_i, y_i))$ and we run the distributed projection algorithm described above. After convergence, we take the exp of the result.

Fig. 18 shows an example of application. In particular, the spatial behavior of the useful signal power is shown in the top left plot, while the observation corrupted by fading is reported in the top right figure. It is useful to consider that, in the example at hand, the useful signal would require a Fourier series expansion with an infinite number of terms to null the modeling error. Conversely, in our example, we used two different orders, $k = 10$ and $k = 20$. The corresponding reconstructions are shown in the bottom figures. From Fig. 18 it is evident the capability of the proposed distributed approach to provide a significant attenuation of the fading phenomenon, without destroying valuable signal variations.

VII. MINIMUM ENERGY CONSENSUS

Although distributed algorithms to achieve consensus have received a lot of attention because of their capability of reaching optimal decisions without the need of a fusion center, the price paid for this simplicity is that consensus algorithms are inherently iterative. As a consequence the iterated exchange of data among the nodes might cause an excessive energy consumption. Hence, to make consensus algorithms really appealing in practical applications, it is necessary to minimize the energy consumption necessary to reach consensus. The network topology plays a fundamental role in determining the convergence rate [62]. As the network connectivity increases, so does the convergence rate. However, a highly connected network entails a high power consumption to guarantee reliable direct links between the nodes. On the other hand, if the network is minimally connected, with only neighbor nodes connected to each other, a low power is spent to maintain the few short range links, but, at the same time, a large convergence time is required. Since what really matters in a WSN is the overall energy spent to achieve consensus, in [61], [78] it was considered the problem of finding the optimal network topology that minimizes the overall energy consumption, taking into account convergence time and transmit powers *jointly*. More specifically,

in [78] it is proposed a method for optimizing the network topology and the power allocation across every link in order to minimize the energy necessary to achieve consensus. Two different types of networks are considered: a) deterministic topologies, where node positions are arbitrary, but known; b) random geometries, where the unknown node locations are modeled as random variables. We will now review the methodology used in both cases.

A. Optimization criterion

By considering only the power spent to enable wireless communications, the overall energy consumption to reach consensus can be written as the product between the sum of the power P_{tot} necessary to establish the communication links among the nodes and the number of iterations N_{it} necessary to achieve consensus. The exchange of information among the nodes is supposed to take place in the presence of a slotted system, with a medium access control (MAC) mechanism that prevents packet collisions. The number of iterations can be approximated as $N_{it} = T_c/T_s$ where T_s denotes the duration of a time slot unit and

$$T_c = -\frac{\log(\gamma)}{\lambda_2(\mathbf{L})}$$

is the convergence time defined as the time necessary for the slowest mode of the dynamical system (23) to be reduced by a factor $\gamma \ll 1$. The total power spent by the network in each iteration is then $P_{tot} = \sum_{i,j} a_{ij}p_{ij}$ where the coefficient $p_{ij} = p_{ji}$, $i \neq j$ denotes the power transmitted by node i to node j , while the binary coefficients a_{ij} assess the presence ($a_{ij} = 1$) of a link between nodes i and j or not ($a_{ij} = 0$). Our goal is to minimize the energy consumption expressed by the following metric

$$\mathcal{E} = P_{tot}N_{it} = K \frac{\sum_{i=1}^N \sum_{j=1}^N a_{ij}p_{ij}}{\lambda_2(\mathbf{L}(\mathbf{a}))}, \quad (149)$$

where K incorporates all irrelevant constants, N is the number of sensors and $\mathbf{L}(\mathbf{a})$ is the Laplacian matrix depending on the vector $\mathbf{a} = \mathbf{A}(\cdot)$ containing all the coefficients a_{ij} . More specifically, we aim to find the set of active links, i.e., the non-zero coefficients a_{ij} , and the powers p_{ij} that minimize the energy consumption (149), under the constraint of guaranteeing network connectivity, i.e. enforcing $\lambda_2(\mathbf{L}(\mathbf{a})) > 0$. The problem can be formulated as follows [78]:

$$\begin{aligned} \min_{\mathbf{a}, \mathbf{p}} \quad & \frac{\sum_{i=1}^N \sum_{j=1}^N a_{ij}p_{ij}}{\lambda_2(\mathbf{L}(\mathbf{a}))} \\ \text{s.t.} \quad & \epsilon \leq \lambda_2(\mathbf{L}(\mathbf{a})) \quad [\mathbf{P.0}] \\ & a_{ij} \in \{0, 1\} \\ & p_{ij} \geq 0 \quad \forall i, j = 1, \dots, N \end{aligned} \quad (150)$$

where ϵ is an arbitrarily small positive constant used to ensure network connectivity and \mathbf{p} is the vector with entries p_{ij} . Since the topology coefficients are binary variables, [P.0] is a combinatorial problem, with complexity increasing with the size N of the network as $2^{N(N-1)/2}$. In [78] we have modified [P.0] in order to convert it into a convex problem, with negligible performance losses. A first simplification comes from observing that the coefficients a_{ij} and p_{ij} are dependent of each other through the radio propagation model so that the set of unknowns can be reduced to the set of powers p_{ij} . More specifically, by assuming flat fading channel, we can assume that the power p_{Rj} received by node j when node i transmits is given by

$$p_{Rj} = \frac{p_{ij}}{1 + (r_{ij}/r_0)^\eta} \quad (151)$$

where r_{ij} is the distance between nodes i and j , η is the path loss exponent, and the parameter r_0 corresponds to the so called Fraunhofer distance. We have included in the denominator the unitary term to avoid the unrealistic situation in which the received power could be greater than the transmitted one. Given the propagation model (151), the relation between the power coefficients p_{ij} and the topology coefficients a_{ij} is then

$$a_{ij} = \begin{cases} 1 & \text{if } p_{ij} > p_{\min} \left[1 + \left(\frac{r_{ij}}{r_0} \right)^\eta \right] \\ 0 & \text{otherwise} \end{cases} \quad (152)$$

where p_{\min} is the minimum power needed at the receiver side to establish a communication. In [78] we have shown how to relax this relation in order to simplify the solution of the optimal topology control problem considering both the deterministic and random topology.

B. Optimal topology and power allocation for arbitrary networks

In the case where the distances between the nodes are known, to find the optimal solution of problem [P.0] involves a combinatorial strategy that makes the problem numerically very hard to solve. In [78], we have relaxed problem [P.0] so that, instead of requiring a_{ij} to be binary, we assume a_{ij} to be a real variable belonging to the interval $[0, 1]$. This relaxation is the first step to transform the previous problem into a *convex* problem. More specifically, we have introduced the following relationship between the coefficients a_{ij} and the distances r_{ij} :

$$a_{ij} = \frac{1}{1 + (r_{ij}/r_{c_{ij}})^\alpha}, \quad (153)$$

where α is a positive coefficient and $r_{c_{ij}}$ is the coverage radius, which depends on the transmit power. According to (153), a_{ij} is close to one when node j is within the coverage radius of node i , i.e., $r_{ij} \ll r_{c_{ij}}$,

whereas a_{ij} is close to zero, when $r_{ij} \gg r_{c_{ij}}$. The switching from zero to one can be made steeper by increasing the value of α . In [78] we have found the coefficients p_{ij} as a function of a_{ij}

$$p_{ij} = q(a_{ij}) = p_{min} + k_1 \left(\frac{a_{ij}}{1 - a_{ij}} \right)^{\eta/\alpha}, \quad (154)$$

with $k_1 = p_{min} \frac{r_{ij}^\eta}{r_0^\eta}$. Consequently, we can reduce the set of variables to the only power vector \mathbf{p} and problem [P.0] can be relaxed into the following problem:

$$\begin{aligned} \min_{\mathbf{p}} \quad & \frac{\mathbf{p}^T \mathbf{1}}{\lambda_2(\mathbf{L}(\mathbf{p}))} \\ \text{s.t.} \quad & \epsilon \leq \lambda_2(\mathbf{L}(\mathbf{p})) \quad [\mathbf{P.1}] \\ & p_{min} \mathbf{1} \leq \mathbf{p} \end{aligned} \quad (155)$$

The first important result proved in [78] is that the problem [P.1] is a convex-concave fractional problem if $\eta \geq \alpha$, so that we can use one of the methods that solve quasi-convex optimization problems, see e.g., [82], [83]. In [78] we have used the nonlinear parametric formulation proposed in [83]. Hence we have further converted the convex-concave fractional problem [P.1] into the following equivalent parametric problem in terms of vector \mathbf{a} , i.e.

$$\begin{aligned} \min_{\mathbf{a}} \quad & \phi(\mathbf{a}) - \mu \lambda_2(\mathbf{L}(\mathbf{a})) \\ \text{s.t.} \quad & \epsilon \leq \lambda_2(\mathbf{L}(\mathbf{a})) \quad [\mathbf{P.2}] \\ & \mathbf{0} \leq \mathbf{a} < \mathbf{1}. \end{aligned} \quad (156)$$

where $\phi(\mathbf{a}) = \sum_{i=1}^N \sum_{j=1, i \neq j}^N q(a_{ij})$ and μ controls the trade-off between total transmit power and convergence time.

The optimization problem [P.2] is a convex parametric problem [78] and an optimal solution can be found via efficient numerical tools. Furthermore, using Dinkelbach's algorithm [83], we are also able to find the optimal parameter μ in [P.2].

C. Numerical examples

Since our optimization procedure is based on a relaxation technique, we have evaluated the impact of the relaxation on the final topology and performance.

More specifically, the topology coefficients a_{ij} obtained by solving [P.2] are real variables belonging to the interval $[0, 1]$, so that to obtain the network topology, it is necessary a quantization step to convert them into binary values, 1 or 0, by comparing each a_{ij} with a threshold a_{th} . It has been shown that the loss in terms of optimal energy due to the relaxation of the original problem is negligible. To evaluate the

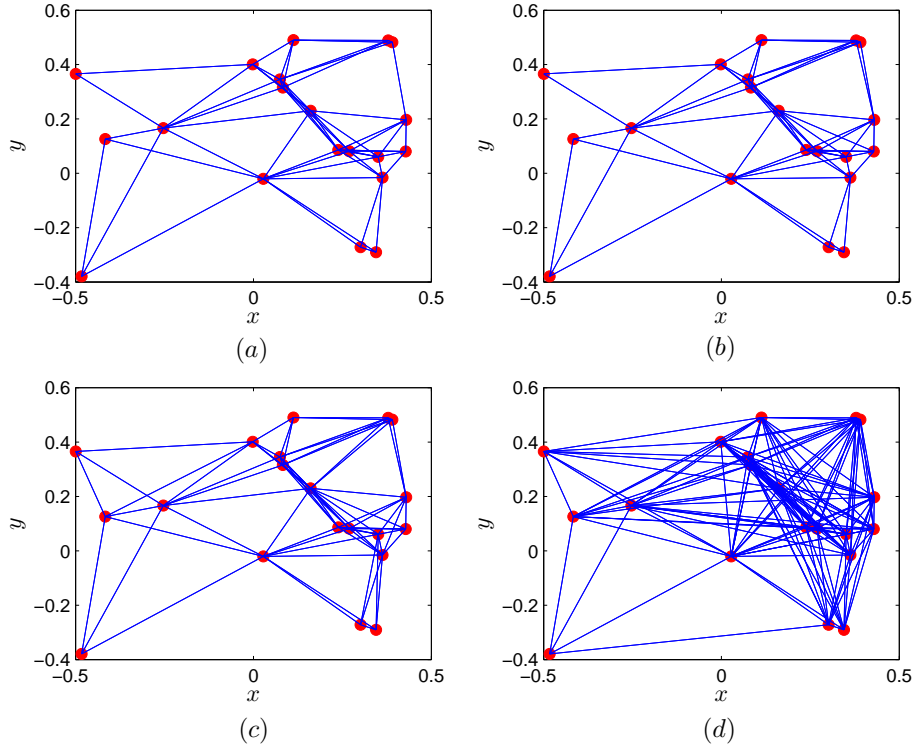


Fig. 19. Optimal topologies, for different threshold values and $\eta = 6$: a) $a_{th} = 0.09$; b) $a_{th} = 0.05$; c) $a_{th} = 10^{-4}$; d) $a_{th} = 10^{-7}$.

impact of thresholding operation in Fig. 19 we show the topologies obtained by solving problem [P.2], for a network composed of $N = 20$ nodes, using different values of a_{th} and assuming $\eta = 6$. Comparing the four cases reported in Fig. 19, we can note that for a large range of values of a_{th} , the final topology is practically the same, while only for very low values of the threshold (i.e., case (d)), we can observe a sensitive change of topology. This means that the relaxation method is robust against the choice of the final threshold.

The previous results pertain to a specific realization of the node locations. To provide results of more general validity, in Fig. 20, we report the average value of a) the energy (\mathcal{E}_r) b) $\lambda_2(\mathbf{L})$, and c) fraction of active links $\frac{\sum_{i=1}^N |\mathcal{N}_i|}{N(N-1)}$, as a function of the path loss exponent η , setting $a_{th} = 0.09$. From Fig. 20, we observe that when the attenuation is high (i.e. η is large), reducing the number of links (making the topology sparser) is more important than reducing convergence time. Conversely, when the attenuation is low (i.e., η is small), increasing network connectivity is more important than reducing power consumption.

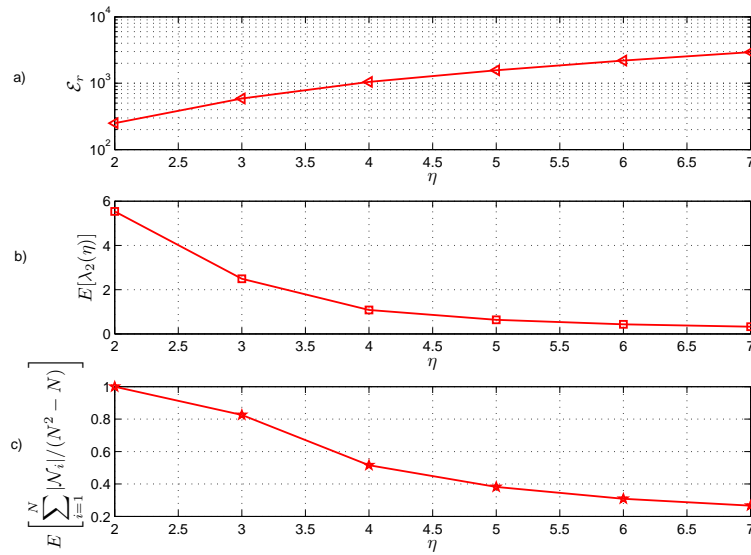


Fig. 20. Average value of a) energy; b) $\lambda_2(\mathbf{L})$; c) fraction of active links vs. path loss η for $a_{th} = 0.09$.

D. Minimization of the energy consumption over random geometric graphs

Let us consider now the problem of minimizing the energy consumption for a sensor network modeled as a random geometric graph. We will use the symbol $G(N, r)$ to indicate an RGG composed of N points, with coverage radius r .

In [62], it has been shown that the degree of an RGG $G(N, r)$ of points uniformly distributed over a two-dimensional unit torus⁷ is equal to

$$d(N) = \pi r^2 N \quad (157)$$

with high probability, i.e., with probability $1 - 1/N^2$, if the radius behaves as $r_0(N)$ in (2). This implies that if the coverage radius is chosen so as to guarantee connectivity with high probability, an RGG tends to behave, asymptotically, as a regular graph. In order to calculate the convergence rate we have to derive the second eigenvalue of the Laplacian, $\mathbf{L} = \mathbf{D} - \mathbf{A}$, where \mathbf{D} is the degree matrix and \mathbf{A} is the adjacency matrix. From (157), $\mathbf{D} = \pi r^2 N \mathbf{I}$, so that we only need to calculate the second *largest* eigenvalue of \mathbf{A} . In Appendix A.2, we study the asymptotic behavior of the spectrum of \mathbf{A} and the result is that the second largest eigenvalue of \mathbf{L} tends asymptotically to

$$\lambda_2(\mathbf{L}) = \pi N r^2 - N r J_1(2\pi r) \quad (158)$$

⁷A torus geometry is typically used to get rid of border effects.

where r is the coverage radius of each node.

1) *An analytic approach for minimizing the energy consumption* : In [78] we studied the energy minimization problem for RGG's, exploiting the previous analytic expressions. In the random topology case, since the distances are unknown, we cannot optimize the power associated with each link. However, we can seek the common transmit power that minimizes energy consumption. Thus, in the random setting we assume a broadcast communication model, where each node broadcasts the value to be shared with its neighbors. In the lack of any information about distances among the nodes, we assume that each node uses the same transmit power. In this case, the network topology can be modeled as a random graph model. In [84],[85] it has been shown that the dynamical system $\dot{\mathbf{x}}(t) = -\mathbf{L}\mathbf{x}(t)$ converges to consensus almost surely, i.e. $\Pr \left\{ \lim_{t \rightarrow \infty} \mathbf{x}(t) = x^* \mathbf{1} \right\} = 1$ assuming that each node has a coverage radius so that the network is asymptotically connected with probability one. Then the rate of convergence to consensus is given [84],[85] by $E[e^{-2T_s \lambda_2(L)}]$. In [78] we proved that the convergence rate can be approximated as

$$E[e^{-2T_s \lambda_2}] \approx e^{-2T_s E[\lambda_2]} \quad (159)$$

so that the energy spent to achieve consensus can now be expressed as

$$\mathcal{E} = K \frac{Np}{2E[\lambda_2(\mathbf{L}(p))]} \quad (160)$$

This is the performance metric we wish to minimize in the random scenario, with respect to the single unknown p .

In particular, using the asymptotic expression (158) for the algebraic connectivity, we can introduce the following metric

$$\mathcal{E}(r) = \frac{N p_{min} [1 + (r/r_0)^\eta]}{N\pi r^2 - rN J_1(2\pi r)} \quad (161)$$

that is a convex function of r , for $r_0(N) \leq r \leq 0.5$, where $r_0(N)$, behaves as in (2) to ensure connectivity. *Numerical examples.* In Fig. 21, we compare the value of $\mathcal{E}(r)$ obtained by our theoretical approach and by simulation, for various values of the path loss exponent η . The results are averaged over 100 independent realizations of random geometric graphs composed of $N = 1000$ nodes. For each η , we indicate the pair of radius and energy providing minimum energy consumption by a circle (simulation) or a star (theory). It can be noted that the theoretical derivations provide a very good prediction of the performance achieved by simulation and, for each η , there is a coverage radius value that minimizes energy consumption.

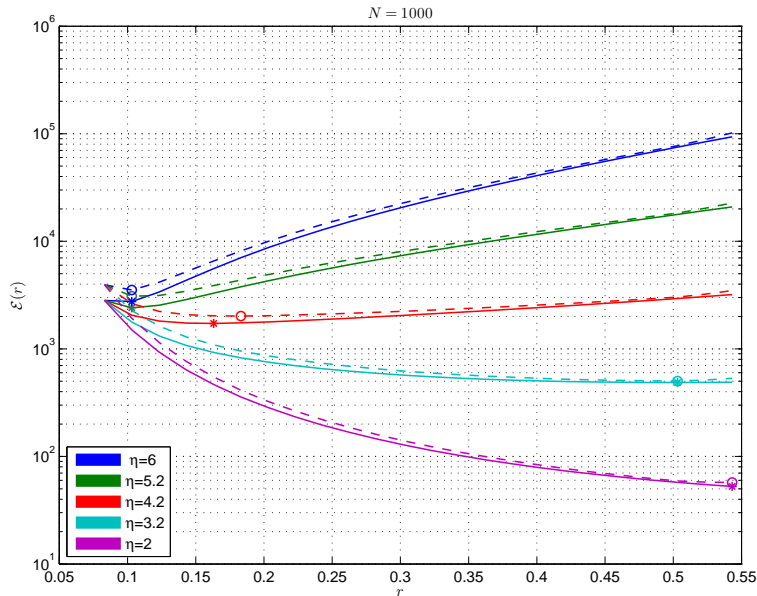


Fig. 21. Global energy consumption versus transmission radius for an RGG; theoretical values (solid) and simulation results (dashed).

VIII. MATCHING COMMUNICATION NETWORK TOPOLOGY TO STATISTICAL DEPENDENCY GRAPH

In Section II-B, we saw that the topology of a sensor network observing a random field should depend on the structure of the graph describing the observed field. In this section, we recall a method proposed in [54], [55] to design the topology of a wireless sensor network observing a Markov random field in order to match the structure of the dependency graph of the observed field, under constraints on the power used to ensure the sensor network connectivity. As in [54], [55], our main task is to recover the sparsity of the dependency graph and to replicate it at the sensor network level, under the constraint of limiting the transmit power necessary to establish the link among the nodes. Also in this case, searching for an optimal topology is a combinatorial problem. To avoid the computational burden of solving the combinatorial problem, we propose an ad hoc relaxation technique that allows us to achieve the solution through efficient algorithms based on difference of convex problems.

Let us assume to have a network composed of N nodes, each one observing a spatial sample of a Gaussian Markov Random Field. We denote by $\mathbf{x} := (x_1, \dots, x_N)$ the vector of the observations collected by the N nodes and we assume that \mathbf{x} has zero mean and covariance matrix \mathbf{C} . The statistical dependency among the random variables x_i is well captured by the structure of the Markov graph, whose vertices correspond to the random variables and whose links denote statistical dependencies among the variables.

As discussed in II-B the main feature of a Markov graph is that it is sparse and there is no link between two nodes if and only if their observations are statistically independent. Moreover, if the random vector \mathbf{x} is also Gaussian, with covariance matrix \mathbf{C} , the sparsity of the Markov graph is completely specified by the sparsity of the precision matrix, which is the inverse of the covariance matrix, i.e. $\mathbf{B} := \mathbf{C}^{-1}$. On the other hand, the topology of the WSN can also be described by a graph, having adjacency matrix \mathbf{A} such that $a_{ij} \neq 0$ only if there is a physical link between nodes i and j . We use a simple propagation model such that there is a link between node i and j if the power received by node j exceeds a minimum power p_{min} . The received power depends on the power $p_T(i, j)$ used by node i to transmit to node j and on the distance r_{ij} between nodes i and j through the equation

$$p_R(i, j) = \frac{p_T(i, j)}{1 + r_{ij}^\eta} \quad (162)$$

where η is the path loss exponent.

As proposed in [54], [55], our goal is to design the topology of the WSN, and hence its adjacency matrix \mathbf{A} , in order to match as well as possible the topology of the dependency graph, compatibly with the power expenditure necessary to establish each link in the network. Without any power constraint, we would choose \mathbf{A} to be equal to $\mathbf{B} = \mathbf{C}^{-1}$, so as to reproduce the same sparsity of the dependency graph. Adding the power constraints, we will end up, in general, with a matrix \mathbf{A} different from \mathbf{B} . We measure the difference between the two matrices \mathbf{A} and \mathbf{B} using the so called Burg divergence, defined as

$$D_B(\mathbf{A}, \mathbf{B}) := \frac{1}{2} \text{trace}(\mathbf{A}\mathbf{B}^{-1} - \mathbf{I}) - \frac{1}{2} \log(\det(\mathbf{A}\mathbf{B}^{-1})) . \quad (163)$$

Even though the Burg divergence does not respect all the prerequisites to be a distance, it holds true that $D_B(\mathbf{A}, \mathbf{B}) = 0$, if and only if $\mathbf{A} = \mathbf{B}$, otherwise, the divergence is strictly positive. If the matrices \mathbf{A} and \mathbf{B} are definite positive, the expression in (163) coincides with the Kullback-Leibler divergence between the probability density function (pdf) of two Gaussian random vectors having zero mean and precision matrices \mathbf{A} and \mathbf{B} or, equivalently, covariance matrices \mathbf{A}^{-1} and \mathbf{C} .

A. Encouraging sparsity by preserving total transmit power

One of the most important tasks in wireless sensor networks is to minimize the energy consumption for reliable data transmission. This need can be accommodated by formulating the search for a sparse topology incorporating a penalization for the presence of links among distant nodes. The first strategy we propose is named Sparsity with Minimum Power (SMP) consumption. We consider both cases where the covariance matrix is perfectly known or estimated from the collected data.

Let us consider a wireless sensor network whose communication graph is a geometric graph, where each node communicates only with the nodes lying within its coverage area of radius r . We assume, initially, that the covariance matrix \mathbf{C} of the GMRF is perfectly known. Our goal is to find the optimal adjacency matrix \mathbf{A} that minimizes the divergence $D_B(\mathbf{A}, \mathbf{B})$ given in (163), under the constraint of limiting the transmit power necessary to maintain the links among the nodes of the WSN. This constraint can be incorporated in our optimization problem by introducing a penalty term given by the sum of the transmit powers over all active links, i.e.

$$P_N(\mathbf{A}) = \sum_{i=1}^N \sum_{\substack{j=1 \\ j \neq i}}^N p_T(i, j) \delta(a_{ij}) \quad (164)$$

where $p_T(i, j)$ denotes the power used by node i to transmit to node j and

$$\delta(a_{ij}) = \begin{cases} 0 & \text{if } a_{ij} = 0 \\ 1 & \text{otherwise} \end{cases}, \quad (165)$$

assuming that a_{ij} is different from zero only if the power $p_R(i, j)$ received by node j when node i transmits, as given in (162), exceeds a suitable minimum level p_{min} , i.e. if

$$p_T(i, j) > (1 + r_{ij}^\eta) p_{min}. \quad (166)$$

The optimization problem can then be formulated as

$$\min_{\mathbf{A} \in \mathbf{S}_{++}^N} D_B(\mathbf{A}, \mathbf{B}) + \rho P_N(\mathbf{A}) \quad (167)$$

where \mathbf{S}_{++}^N is the cone of definite positive symmetric $N \times N$ -dimensional matrices, while $\rho \geq 0$ is the penalty coefficient introduced to control sparsity. In fact, increasing the penalty coefficient, we assign a higher weight to power consumption so that sparse structures are more likely to occur.

Problem (167) is indeed quite hard to solve as the penalty function is a nonconvex discrete function. Optimization problems with a convex penalty have been largely considered in several signal processing applications, for example in compressed sensing [56] where these problems are often formulated as a penalized least-square problem in which sparsity is usually induced by adding a l_1 -norm penalty on the coefficients, as in Lasso algorithm [57].

Indeed, non-convex penalty functions such as l_q -norm, with $q < 1$, are even more effective to recover sparsity than l_1 -norm. Actually, using the so called l_0 norm would be even more effective to measure sparsity, even though the l_0 norm does not respect all requisites to be a norm⁸. Here we adopt the so

⁸The l_0 norm of a vector \mathbf{x} is defined as the number of nonzero entries of \mathbf{x} .

called Zhang penalty function analyzed in [58], i.e.

$$z(a_{ij}) = \min\left(\frac{|a_{ij}|}{\epsilon}, 1\right) = \begin{cases} \frac{|a_{ij}|}{\epsilon} & \text{if } |a_{ij}| \leq \epsilon \\ 1 & \text{otherwise} \end{cases} \quad (168)$$

where ϵ is an infinitesimal positive constant. Hence, by assuming $p_T(i, j) = (1 + r_{ij}^\eta)p_{min}$, the second term in (167) can be written as

$$P_N(\mathbf{A}) = \sum_{i=1}^N \sum_{j=1}^N d_{ij} z(a_{ij}) = \text{trace}[z(\mathbf{A})\mathbf{D}] \quad (169)$$

where \mathbf{D} is a $N \times N$ dimensional symmetric matrix with entries $d_{ij} = (1 + r_{ij}^\eta)p_{min}$, $d_{ii} = 0$, $\forall i, j = 1, \dots, N$, while the matrix mapping $z(\mathbf{A})$ is defined applying the elementwise mapping $z(a_{ij}) : \mathbb{R} \rightarrow \mathbb{R}^+$ given in (168). The combinatorial problem in (167) can then be reformulated as

$$\min_{\mathbf{A} \in \mathbf{S}_{++}^N} D_B(\mathbf{A}, \mathbf{B}) + \rho \text{trace}[z(\mathbf{A})\mathbf{D}]. \quad (170)$$

Unfortunately the second term in (170), is not convex so that the problem we have to solve is a nonconvex, nonsmooth optimization problem. Nevertheless, in [54], [55] we reformulated this problem as a difference of convex (DC) problem. Before proceeding, we simply illustrate how to extend our approach to the case where the covariance matrix of the observed vector is not known but estimated from the data. In such a case, the matrix \mathbf{C} in (170) is substituted by the estimated matrix $\widehat{\mathbf{C}}$, whose entry \widehat{C}_{ij} is

$$\widehat{C}_{ij} = \frac{1}{K} \sum_{k=1}^K x_i(k)x_j(k), \quad (171)$$

where $x_i(k)$ is the observation collected by node i , at time k , with $k = 1, \dots, K$. The practical, relevant, difference is that while the true precision matrix \mathbf{B} is sparse by hypothesis, the inverse of $\widehat{\mathbf{C}}$ in general is not sparse. Also in this case, encouraging sparsity in estimating the inverse of the covariance matrix can be beneficial to improve the quality of the estimation itself⁹.

The problem (170) can be reformulated as a Difference of Convex (DC) functions problem [59], by decomposing the function $z(a_{ij})$ as the difference of two convex functions $z(a_{ij}) = g_v(a_{ij}) - h(a_{ij})$ with $g_v(a_{ij}) = \frac{|a_{ij}|}{\epsilon}$ and

$$h(a_{ij}) = \begin{cases} 0 & \text{if } |a_{ij}| \leq \epsilon \\ \frac{|a_{ij}|}{\epsilon} - 1 & \text{otherwise.} \end{cases} \quad (172)$$

⁹Provided that the observed field is a Markov field.

Hence the optimization problem in (170) can be rewritten as

$$\min_{\mathbf{A} \in \mathbf{S}_{++}^N} D_B(\mathbf{A}, \mathbf{B}) + \rho \text{trace}[(g_v(\mathbf{A}) - h(\mathbf{A}))\mathbf{D}]. \quad (173)$$

To solve this problem, we have used an iterative procedure, known as DC algorithm (DCA), based on the duality of DC programming. The usefulness of using DCA is that its convergence has been proved in [59] and it is simple to implement, as it iteratively solves a convex optimization problem. We refer the reader to [54], [55] for further analytical details.

B. Sparsification and estimation of the precision matrix

In this section we illustrate an alternative sparsification strategy that improves the estimate of the precision matrix with respect to the SMP strategy. In this alternative formulation, the penalty term is the sum of the absolute values of the entries of \mathbf{A} , weighted with the corresponding per-link transmit power consumption. In this way, although the power consumption should not be lower than the SMP method, we expect a sparse topology with a more accurate estimate of the precision matrix. We call this strategy Sparse Estimation Strategy (SES). The new problem is formulated as follows

$$\min_{\mathbf{A} \in \mathbf{S}_{++}^N} D_B(\mathbf{A}, \mathbf{B}) + \rho \text{trace}[|\mathbf{A}|\mathbf{D}] \quad (174)$$

and it can be converted into a convex definite positive problem. In particular, splitting the matrix \mathbf{A} into the difference of two nonnegative matrices representing its positive and negative part, i.e. $\mathbf{A} = \mathbf{A}^+ - \mathbf{A}^-$, we can rewrite (174) as

$$\begin{aligned} \min_{\mathbf{A}^+, \mathbf{A}^- \in \mathbf{S}^N} & D_B(\mathbf{A}^+ - \mathbf{A}^-, \mathbf{B}) + \rho \text{trace}[(\mathbf{A}^+ + \mathbf{A}^-)\mathbf{D}] \\ \text{s.t.} & \quad \mathbf{A}^+ - \mathbf{A}^- \succ \mathbf{0} \\ & \quad \mathbf{A}^+ \geq \mathbf{0} \\ & \quad \mathbf{A}^- \geq \mathbf{0}. \end{aligned} \quad (175)$$

This problem can be solved using standard numerical tools or by applying a projected gradient algorithm [60].

C. Numerical results

In this section we report some simulation results considering a sensors network composed of $N = 20$ nodes, uniformly deployed over a unit area square and observing correlated data from a GMRF. We adopt the Markov model proposed in [7], where the correlation between neighboring nodes is a decreasing function of their distance and the entries of the covariance matrix can be derived in closed form. In

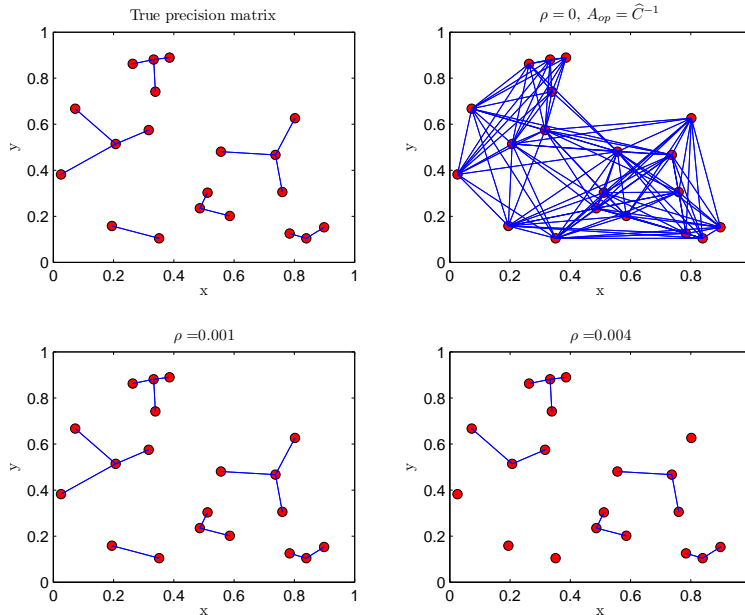


Fig. 22. Optimal links configurations for the SMP strategy using the data estimated covariance matrix \hat{C} .

[54], [55] we have shown that even though the problem is not convex, the numerical results seem to indicate that the method always converges to the same value of the precision matrix entries, irrespective of the initializations. In Fig. 22 we report the final optimal network topology referring to the case of a matrix estimated from the data. In particular, the top left plot of Fig. 22 shows the true dependency graph and all other plots depict the network topologies obtained using the proposed SMP algorithm, with different penalty coefficients. More specifically, the network topologies shown in Fig. 22 are obtained by thresholding the values of the matrix A_{op} obtained through our SMP algorithm, i.e. the coefficients of matrix A_{op} are set to zero if $|a_{op}(i, j)| < 10^{-4}$. In the top right plot of Fig. 22, it can be noted that the precision matrix achieved with a null penalty can be quite dense because of estimation errors. Nevertheless, it is interesting to observe that, as the penalty coefficient increases, the proposed method is not only able to recover the desired topology, but also to correct most of the errors due to estimation. We can say that the introduction of the penalty induces a robustness against estimation errors. Let us now compare the SMP method with the SES strategy, by considering a data estimated covariance matrix in the divergence term and averaging the simulation results over 100 independent realizations of the nodes deployment.

Let us now evaluate the mismatch between the network topology and the dependency graph, as a

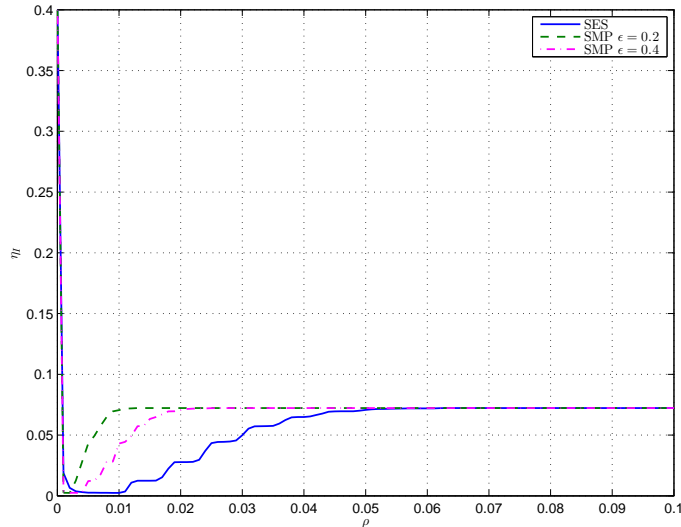


Fig. 23. Fraction of incorrect links versus ρ for the SMP and SES strategies.

function of the penalty coefficient, obtained using the two proposed strategies. We assess the mismatch by counting the number of links appearing in the network topology, which do not appear in the dependency graph. To this end, Fig. 23 shows the fraction of incorrect links η_I , normalized to the total number of links $N_T = N(N-1)/2$, versus ρ . More specifically, considering the true and optimal precision matrices (\mathbf{A}_t and \mathbf{A}_{op} respectively), we can define $\eta_I = \frac{\sum_{i=1}^N \sum_{j=1, j>i}^N q_{ij}}{N_T}$ where $q_{ij} = 1$ if $\delta(a_t(i, j))$ and $\delta(a_{op}(i, j))$ are not equal, assuming $\delta(a_{ij}) = 1$ if $a_{ij} > 0$ and zero otherwise. From Fig. 23, we can deduce that SES provides more correct links than SMP, as it achieves lower values of η_I .

IX. CONCLUSIONS AND FURTHER DEVELOPMENTS

In this article we have provided a general framework to show how an efficient design of a wireless sensor networks requires a joint combination of in-network processing and communication. In particular, we have shown that inferring the structure of the graph describing the statistical dependencies among the observed data can provide important information on how to build the sensor network topology and how to design the flow of information through the network. We have illustrated several possible network architectures where the global decisions, either estimation or hypothesis testing, are taken by a central node or in a totally decentralized way. In particular, various forms of consensus have been shown to be instrumental to achieve globally optimal performance through local interactions only. Consensus algorithms have then been generalized to more sophisticated signal processing techniques able to provide a cartography

of the observed field. In a decentralized framework, the network topology plays an important role in terms of convergence time as well as structure of the final consensus value. Considering that most sensor networks exchange information through a wireless channel, we have addressed the problem of finding the network topology that minimizes the energy consumption required to reach consensus. Finally, we have showed how to match the network topology to the Markov graph describing the observed variables, under constraints imposed by the power consumption necessary to establish direct links among the sensor nodes.

Even though the field of distributed detection and estimation has accumulated an enormous amount of research works, there are still many open problems, both in the theoretical as well as in the application sides. In the following we make a short list of possible topics of future interest.

- 1) The general *multi-terminal source/channel coding* problem is still an open issue. The conventional paradigm established by the source/channel coding separation theorem does not hold for the multi-terminal case. This means that source coding should be studied jointly with channel coding.
- 2) Distributed decision establishes a *strict link between statistical signal processing and graph theory*. In particular, the network topology plays a fundamental role in the design of an efficient sensor network. In this article, we have shown some simple techniques aimed to matching the network topology to the statistical dependency graph of the observed variables, but significant improvements may be expected from cross-fertilization of methods from graph theory and statistical signal processing.
- 3) The design of fully decentralized detection algorithms has already received important contributions. Nevertheless, there are many open issues concerning the refinements of the local decision thresholds as a function of both local observations and the decisions taken from neighbors. In a more general setting, *social learning* is expected to play an important role in future sensor networks.
- 4) An efficient design of wireless sensor networks requires a *strict relation between radio resource allocation and decision aspects*, under physical constraints dictated by energy limitations or channel noise and interference. Some preliminary results have been achieved in the many-to-one setting, but the general many-to-many case needs to be thoroughly studied.
- 5) The application of wireless sensor networks to new fields may be easily expected. The important remark is that, to improve the efficiency of the network at various levels, it is necessary to take the application needs strictly into account in the network design. In other words, a *cross-layer design*

incorporating all layers from the application down to the physical layer is especially required in sensor networks. Clearly, handling the complexity of the network will require some sort of layering, but this layering will not necessarily be the same as in telecommunication networks, because the requirements and constraints in the two fields are completely different.

APPENDIX A

In this appendix we briefly review some important notations and basic concepts of graph theory that have been adopted in the previous sections (for a more detailed introduction to this field see [64]).

A.1 Algebraic graph theory

Given N nodes let us define a directed graph or *digraph* $\mathcal{G} = \{\mathcal{V}, \mathcal{E}\}$ as a set of nodes $\mathcal{V} = \{v_i\}_{i=1}^N$ and a set of edges or links $\mathcal{E} \subseteq \mathcal{V} \times \mathcal{V}$ where the links $e_{ij} \in \mathcal{E}$ connect the ordered pair of nodes (v_i, v_j) , with the convention that the information flows from v_j to v_i . In the case where a positive weight a_{ij} is associated to each edge, the digraph is called *weighted*. Let us assume that there are no loops, i.e. $a_{ii} = 0$.

The graph is called *undirected* if $e_{ij} \in \mathcal{E} \Leftrightarrow e_{ji} \in \mathcal{E}$. The in-degree and out-degree of node v_i are, respectively, defined as $\deg_{in} \triangleq \sum_{j=1}^N a_{ij}$ and $\deg_{out} \triangleq \sum_{j=1}^N a_{ji}$. In the case of undirected graphs $\deg_{in} = \deg_{out}$. Let \mathcal{N}_i denote the set of neighbors of node i , so that $|\mathcal{N}_i| \triangleq \deg_{in}(v_i)$.

The node v_i of a digraph is said to be *balanced* if and only if its in-degree and out-degree coincide, while a digraph is called *balanced* if and only if all its nodes are balanced.

We recall now the basic properties of the matrices associated to a digraph, as they play a fundamental role in the study of the connectivity of the network associated to the graph. Given a digraph \mathcal{G} , we introduce the following matrices associated with \mathcal{G} : 1) The $N \times N$ adjacency matrix \mathbf{A} whose entries a_{ij} are equal to the weight associated to the edge e_{ij} , or equal to zero, otherwise; 2) the degree matrix \mathbf{D} which is the diagonal matrix whose diagonal entries are $d_{ii} = \deg_{in}(v_i) = \sum_{j=1}^N a_{ij}$; 3) the weighted Laplacian matrix \mathbf{L} , defined as $\mathbf{L} = \mathbf{D} - \mathbf{A}$ whose entries are

$$l_{ij} = \begin{cases} \deg_{in}(v_i) & \text{if } j = i \\ -a_{ij} & \text{if } j \neq i \end{cases}. \quad (176)$$

According to this definition \mathbf{L} has the following properties: a) its diagonal elements are positive; b) it has zero row sum; c) it is a diagonally row dominant matrix. It can be easily verified that $\mathbf{L}\mathbf{1} = \mathbf{0}^{10}$, i.e.

¹⁰ We denote by $\mathbf{1}$ and $\mathbf{0}$ the vectors of all ones or zeros, respectively.

zero is an eigenvalue of L corresponding to a right eigenvector $\mathbf{1}$ in the $\text{Null}\{L\} \supseteq \text{span}\{\mathbf{1}\}$, and all the other eigenvalues have positive real parts. Furthermore a digraph is balanced if and only if $\mathbf{1}$ is also a left eigenvector of L associated with the zero eigenvalue or $\mathbf{1}^T L = \mathbf{0}^T$. Note that for undirected graph the Laplacian matrix is a symmetric and then balanced matrix with non negative real eigenvalues.

The algebraic multiplicity of the zero eigenvalue of L is equal to the number of connected components contained in \mathcal{G} . For undirected graphs \mathcal{G} is connected if and only if the algebraic multiplicity of the zero eigenvalue is 1, or, equivalently, $\text{rank}(L) = N - 1$ if and only if \mathcal{G} is connected. Hence if an undirected graph is connected the eigenvector associated with the zero eigenvalue is $\mathbf{1}$, and the second smallest eigenvalue of L , denoted as $\lambda_2(L)$ and called algebraic connectivity [65] of \mathcal{G} , is strictly positive.

A.1.1 Forms of connectivity for digraphs

Before to introduce several forms of graph connectivity [43] we have to define some useful concepts. A *strong path* of a digraph \mathcal{G} is a sequence of distinct nodes $v_1, v_2, \dots, v_p \in \mathcal{V}$ such that $(v_{j-1}, v_j) \in \mathcal{E}$, for $j = 2, \dots, p$. If $v_1 \equiv v_p$, the path is said to be closed. A *weak path* is a sequence of distinct nodes $v_1, v_2, \dots, v_p \in \mathcal{V}$ such that either $(v_{j-1}, v_j) \in \mathcal{E}$ or $(v_j, v_{j-1}) \in \mathcal{E}$, for $j = 2, \dots, p$. A closed strong path is said a *strong cycle*. A digraph with N nodes is a *directed tree* if it has $N - 1$ edges and there exists a node, called the root node, which can reach all the other nodes through an unique strong path. As a consequence a directed tree contains no cycles and every node, except the root, has one and only one incoming edge. A digraph is a *forest* if it consists of one or more directed trees. A subgraph $\mathcal{G}_s = \{\mathcal{V}_s, \mathcal{E}_s\}$ of a digraph \mathcal{G} , with $\mathcal{V}_s \subseteq \mathcal{V}$ and $\mathcal{E}_s \subseteq \mathcal{E}$, is a directed spanning tree (or a spanning forest) if it is a directed tree (or a directed forest) and it has the same node set as \mathcal{G} .

According to this definition we can define many forms of connectivity [43]: a) a digraph is *strongly connected* (SC) if any ordered pair of distinct nodes can be joined by a strong path; b) a digraph is *quasi strongly connected* (QSC) if, for every ordered pair of nodes v_i and v_j , there exists a node r that can reach both v_i and v_j via a strong path; c) a digraph is *weakly connected* (WC) if any ordered pair of distinct nodes can be joined by a weak path; d) a digraph is disconnected if it is not weakly connected. Note that for undirected graphs, the above notions of connectivity are equivalent. Moreover, it is easy to check that the quasi strong connectivity of a digraph is equivalent to the existence of a directed spanning tree in the graph.

A.1.2 Connectivity study from the condensation digraph

When a digraph \mathcal{G} is WC, it may still contain strongly connected subgraphs. A maximal subgraph of \mathcal{G} ,

which is also SC, is called a *strongly connected component* (SCC) of \mathcal{G} [80], [43]. Any digraph \mathcal{G} can be partitioned into SCCs, let us say $\mathcal{G}_k = \{\mathcal{V}_k, \mathcal{E}_k\}$ where $\mathcal{V}_k \subseteq \mathcal{V}$ and $\mathcal{E}_k \subseteq \mathcal{E}$ for $k = 1, \dots, r$. The connectivity properties of a digraph may be better studied by referring to its corresponding *condensation digraph*. We may reduce the original digraph \mathcal{G} to the condensation digraph $\mathcal{G}^* = \{\mathcal{V}^*, \mathcal{E}^*\}$ by associating the node set \mathcal{V}_k of each SCC \mathcal{G}_k of \mathcal{G} to a single distinct node $v_k^* \in \mathcal{V}^*$ of \mathcal{G}^* and introducing an edge in \mathcal{G}^* from v_i^* to v_j^* , if and only if there exists some edges from the SCC \mathcal{G}_i and the SCC \mathcal{G}_j of the original graph. An SCC that is reduced to the root of a directed spanning tree of the condensation digraph is called the *root SCC* (RSCC). Looking at the condensation graph, we may identify the following topologies of the original graph: 1) \mathcal{G} is SC if and only if \mathcal{G}^* is composed by a single node; 2) \mathcal{G} is QSC if and only if \mathcal{G}^* contains a directed spanning tree; 3) if \mathcal{G} is WC, then \mathcal{G}^* contains either a spanning tree or a (weakly) connected forest.

The multiplicity of the zero eigenvalue of \mathbf{L} is equal to the minimum number of directed trees contained in a directed spanning forest of \mathcal{G} . Moreover, the zero eigenvalue of \mathbf{L} is simple if and only if \mathcal{G} contains a spanning directed tree or, equivalently, \mathcal{G} is QSC. If \mathcal{G} is SC then \mathbf{L} has a simple zero eigenvalue and positive left-eigenvector associated to the zero eigenvalue. If \mathcal{G} is QSC with $Q \geq 1$ strongly connected components $\mathcal{G}_i \triangleq \{\mathcal{V}_i, \mathcal{E}_i\}$ with $\mathcal{V}_i \subseteq \mathcal{V}$, $\mathcal{E}_i \subseteq \mathcal{E}$ for $i = 1, \dots, Q$, $|\mathcal{V}_i| = r_i$ and $\sum_i r_i = N$, numbered w.l.o.g. so that \mathcal{G}_1 coincides with the root SCC of \mathcal{G} , then the left-eigenvector $\boldsymbol{\gamma} = [\gamma_1, \dots, \gamma_N]^T$ of \mathbf{L} associated to the zero eigenvalue has entries $\gamma_i > 0$ iff $v_i \in \mathcal{V}_1$ and zero otherwise. If \mathcal{G}_1 is balanced then $\boldsymbol{\gamma}_{r_1} = [\gamma_1, \dots, \gamma_{r_1}]^T \in \text{span}\{\mathbf{1}_{r_1}\}$ where $r_1 \triangleq |\mathcal{V}_1|$.

As a numerical example, in Fig. 24 we report three network topologies: a) a SC digraph; b) a QSC digraph with three SCCs; c) a WC digraph with a two-trees forest. We have also depicted for each digraph its decomposition into SCCs corresponding to the nodes of the associated condensation digraph; RSCC denotes the root SCC. For each network topology, we have also reported the dynamical evolution of the consensus algorithm in (23) versus time. It can be observed that the dynamical system in Fig. 24a) achieves a global consensus since the underlying digraph is SC. For the QSC digraph in Fig. 24b), instead, there is a set of nodes in the RSCC component that is able to reach all other nodes so that the dynamical system can achieve a global consensus. Finally, in Fig. 24c), the system cannot achieve a global consensus since there is no node that can reach all the others. Although we can observe two disjoint clusters corresponding to the two RSCC components, the nodes of the SCC component (middle lines) are affected by the consensus in the two RSCC components but are not able to influence them.

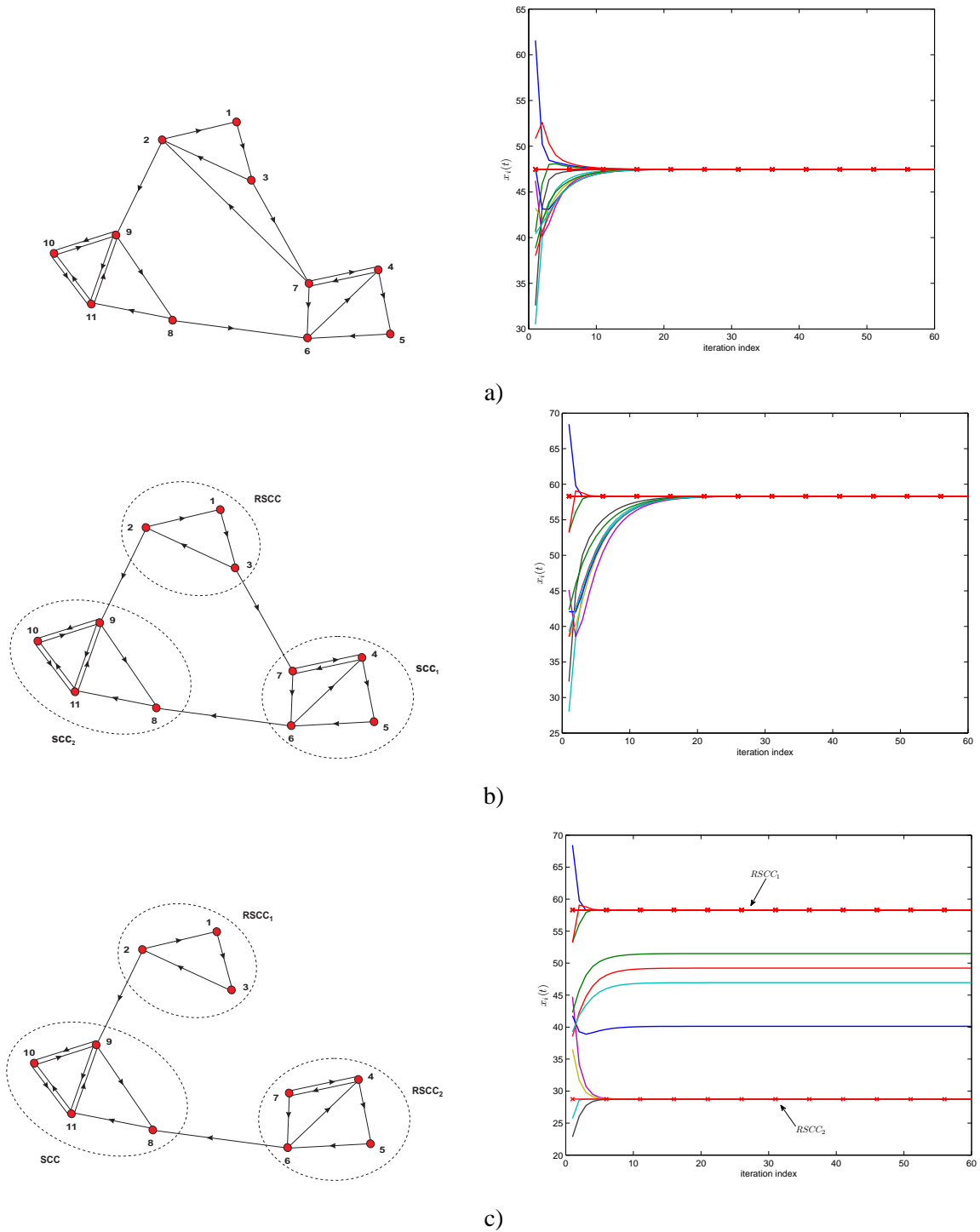


Fig. 24. Consensus for different network topologies: a) SC digraph; b) QSC digraph with three SCCs; c) WC digraph with a forest.

A.2 RGG adjacency matrix

A random graph is obtained by distributing N points randomly over the d -dimensional space \mathbb{R}^d and connecting the nodes according to a given rule. The graph topology is captured by the adjacency matrix \mathbf{A} which, in this case, is a random matrix. An important class of random matrices, is the so called Euclidean Random Matrix (ERM) class, introduced in [79]. Given a set of N points located at positions $\mathbf{x}_i, i = 1, \dots, N$, an $N \times N$ adjacency matrix \mathbf{A} is an ERM if its generic (i, j) entry depends only on the difference $\mathbf{x}_i - \mathbf{x}_j$, i.e., $a_{ij} = F(\mathbf{x}_i - \mathbf{x}_j)$, where F is a measurable mapping from \mathbb{R}^d to \mathbb{R} . An important subclass of ERM is given by the adjacency matrices of the so called Random Geometric Graphs (RGG). In such a case, the entries a_{ij} of the adjacency matrix are either zero or one depending only on the distance between nodes i and j , i.e.,

$$a_{ij} = F(\mathbf{x}_i - \mathbf{x}_j) = \begin{cases} 1 & \text{if } \|\mathbf{x}_i - \mathbf{x}_j\| \leq r \\ 0 & \text{otherwise} \end{cases}, \quad (177)$$

where r is the coverage radius. Next we discuss some important properties of the spectrum of the adjacency matrix of a random geometric graph.

A.2.2 Spectrum of a random geometric graph

Assuming that the RGG $G(N, r)$ is connected with high probability, we have derived in [78] an analytical expression for the algebraic connectivity of the graph, i.e., the second eigenvalue of the symmetric Laplacian, $\mathbf{L} = \mathbf{D} - \mathbf{A}$, where \mathbf{D} is the degree matrix and \mathbf{A} is the adjacency matrix. From (157), $\mathbf{D} = \pi r^2 N \mathbf{I}$, so that we only need to investigate the second *largest* eigenvalue of \mathbf{A} . Hence, let us start by studying the spectrum of \mathbf{A} as discussed in [78]. In [88], [89], it is shown that the eigenvalues of the adjacency matrix tend to be concentrated, as the number of nodes tend to infinity. In particular, in [88] it is shown that the eigenvalues of the normalized adjacency matrix $\mathbf{A}_N = \mathbf{A}/N$ of an RGG $G(N, r)$, composed of points uniformly distributed over a unitary two-dimensional torus, tend to the Fourier series coefficients of the function F defined in (177),

$$\hat{F}(\mathbf{z}) = \int_{\Omega_r} \exp(-2\pi j \mathbf{z}^T \mathbf{x}) d\mathbf{x} \quad (178)$$

almost surely, for all $\mathbf{z} = [z_1, z_2] \in \mathbb{Z}^2$, where $\Omega_r = \{\mathbf{x} = [x_1, x_2]^T \in \mathbb{R}^2 : \|\mathbf{x}\| \leq r\}$. Using polar coordinates, i.e., $x_1 = \rho \sin \theta$ and $x_2 = \rho \cos \theta$, with $0 \leq \rho \leq r$ and $0 \leq \theta \leq 2\pi$, we obtain

$$\hat{F}(\mathbf{z}) = \int_0^r \int_0^{2\pi} \exp(-2\pi j \rho (z_1 \sin \theta + z_2 \cos \theta)) \rho d\rho d\theta.$$

This integral can be computed in closed form. Setting $z_1 = A \sin \phi$ and $z_2 = A \cos \phi$, we have

$$\hat{F}(A, \phi) = \int_0^r \int_{-\phi}^{2\pi-\phi} \exp(-2\pi j \rho A \cos(\xi)) \rho d\rho d\xi$$

with $\xi = \theta - \phi$. Furthermore, using the integral expression for the Bessel function of the first kind of order k , $J_k(x) = \frac{1}{2\pi} \int_{-\pi}^{\pi} \exp(jx \sin(\xi) - jk\xi) d\xi$, we get

$$\hat{F}(A, \phi) = \hat{F}(A) = 2\pi \int_0^r J_0(2\pi\rho A) \rho d\rho .$$

Finally, using the identity $\int_0^u v J_0(v) dv = u J_1(u)$, we can make explicit the dependence of $\hat{F}(A)$ on the index pair $[z_1, z_2]$

$$\hat{F}(z_1, z_2) = \frac{r}{\sqrt{z_1^2 + z_2^2}} J_1 \left(2\pi r \sqrt{z_1^2 + z_2^2} \right) . \quad (179)$$

This formula allows us to rank the eigenvalues of $\mathbf{A}_N = \mathbf{A}/N$. In particular, we are interested in the second largest eigenvalue of \mathbf{A}_N . Considering that the minimum coverage radius ensuring connectivity behaves as $r(N) \sim \sqrt{\frac{\log(N)}{N}}$, i.e., it is a vanishing function of N , we can use the Taylor series expansion of $\hat{F}(z_1, z_2)$, for small r . Recalling that, for small x , $J_1(x) = x/2 - x^3/16 + o(x^5)$, we can approximate the eigenvalues as

$$\hat{F}(z_1, z_2) = \pi r^2 - \frac{\pi^3 (z_1^2 + z_2^2) r^4}{2} + o(r^6) . \quad (180)$$

This expansion shows that, at least for small r , the largest eigenvalue equals πr^2 and occurs at $z_1 = z_2 = 0$, whereas the second largest eigenvalue corresponds to the cases $(z_1 = 1, z_2 = 0)$ and $(z_1 = 0, z_2 = 1)$. More generally, we can check numerically that, for $r \leq 1/2$ and $A \geq 1$, the following inequalities hold true:

$$\pi r^2 \geq r J_1(2\pi r) \geq \frac{r}{A} |J_1(2\pi r A)| . \quad (181)$$

In summary, denoting the spectral radius of \mathbf{A}_N as $\zeta_1(\mathbf{A}_N) = \max_{1 \leq i \leq N} \frac{|\lambda_i(N)|}{N}$, where $\{\lambda_i(N)\}_{i=1}^N$ is the set of eigenvalues of \mathbf{A} , it follows that

$$\lim_{N \rightarrow \infty} \zeta_1(\mathbf{A}_N) = \max_{\mathbf{z} \in \mathbb{Z}^2} |\hat{F}(\mathbf{z})| = \hat{F}(0, 0) = \pi r^2 , \quad (182)$$

while the second largest eigenvalue of \mathbf{A}_N , $\zeta_2(\mathbf{A}_N)$, converges to

$$\lim_{N \rightarrow \infty} \zeta_2(\mathbf{A}_N) = \hat{F}(1, 0) = \hat{F}(0, 1) = r J_1(2\pi r) . \quad (183)$$

We are now able to derive the asymptotic expression for the second largest eigenvalue of the normalized Laplacian $\mathbf{L}_N = \mathbf{D}_N - \mathbf{A}_N$, where $\mathbf{D}_N := \mathbf{D}/N$ is the normalized degree matrix. Because of the

asymptotic property of the degree of an RGG, shown in (157), the second largest eigenvalue of \mathbf{L}_N tends asymptotically to

$$\lambda_2(\mathbf{L}_N) = \pi r^2 - \zeta_2(\mathbf{A}_N) . \quad (184)$$

Thus, the algebraic connectivity of the graph can be approximated, asymptotically, as

$$\lambda_2(\mathbf{L}) = \pi N r^2 - N r J_1(2\pi r) . \quad (185)$$

REFERENCES

- [1] I. F. Akyildiz, W. Su, Y. Sankarasubramaniam, E. Cayirci “Wireless sensor networks: a survey,” *Computer Networks*, pp. 393-422, 2002.
- [2] A. Giridhar and P. R. Kumar, “Computing and Communicating Functions Over Sensor Networks,” *IEEE J. on Selected Areas in Commun.* pp. 755–764, April 2005.
- [3] A. Giridhar and P. R. Kumar, “Toward a Theory of In-Network Computation in Wireless Sensor Networks,” *IEEE Commun. Mag.*, pp. 98–107, April 2006.
- [4] P. Gupta and P. Kumar, “Critical power for asymptotic connectivity in wireless networks,” in *Stochastic Analysis, Control, Optimization and Applications: A Volume in Honor of W. H. Fleming*, W. McEneaney, G. Yin, and Q. Zhang (Eds.), Boston, MA, Birkhauser, 1998.
- [5] J. Whittaker, “Graphical Models in Applied Multivariate Statistics,” John Wiley & Sons, 1990.
- [6] S. L. Lauritzen, *Graphical Models*, Oxford University Press, 1996.
- [7] A. Anandkumar, L. Tong, A. Swami, “Detection of GaussMarkov Random Fields With Nearest-Neighbor Dependency,” *IEEE Trans. on Information Theory*, Vol. 55, pp. 816–827, Feb. 2009.
- [8] A. Anandkumar, J. E. Yukich, L. Tong, A. Swami, “Energy Scaling Laws for Distributed Inference in Random Fusion Networks,” *IEEE Journal of Selected Areas in Commun.*, pp. 1203–1217, Sep. 2009.
- [9] O. P. Kreidl and A. S. Willsky, “An Efficient Message-Passing Algorithm for Optimizing Decentralized Detection Networks,” *IEEE Trans. on Automatic Control.*, pp. 563–578, March 2010.
- [10] A. Anandkumar, L. Tong, A. Swami, “Energy Efficient Routing for Statistical Inference of Markov Random Fields,” *Proc. of CISS 2007*, pp. 643–648, Baltimore, March 2007.
- [11] T. M. Cover, J. A. Thomas, *Elements of Information Theory*, A John-Wiley & Sons, Hoboken, NJ, 2006.
- [12] P. K. Varshney, *Distributed Detection and Data Fusion*, Springer-Verlag, New York, 1997.
- [13] R. Viswanathan, P. K. Varshney, “Distributed Detection with Multiple Sensors: Part I - Fundamentals,” *Proc. of the IEEE*, Vol. 85, pp. 54–63, Jan. 1997.
- [14] R. S. Blum, S. A. Kassam, H. V. Poor, “Distributed Detection with Multiple Sensors: Part II - Advanced Topics,” *Proc. of the IEEE*, Vol. 85, pp. 64–79, Jan. 1997.
- [15] J. F. Chamberland and V. Veeravalli “Wireless Sensors in Distributed Detection Applications,” *IEEE Signal Proc. Magazine*, pp. 16–25, May 2007.
- [16] J. N. Tsitsiklis, “Decentralized Detection,” *Adv. Statistical Signal Processing*, vol. 2, pp. 297–344, 1993.
- [17] J. N. Tsitsiklis, “Decentralized Detection by a Large Number of Sensors,” *Math. Control, Signals, Syst.*, vol. 1, No. 2, pp. 167–182, 1988.

- [18] J. F. Chamberland and V. Veeravalli “Decentralized Detection in Sensor Networks,” *IEEE Trans. on Signal Processing*, pp. 407–416, Feb. 2003.
- [19] J. F. Chamberland and V. Veeravalli “Asymptotic Results for Decentralized Detection in Power Constrained Wireless Sensor Networks,” *IEEE J. Select. Areas Commun.*, pp. 1007–1015, Aug. 2004.
- [20] J. F. Chamberland and V. Veeravalli “How Dense Should a Sensor Network Be for Detection with Correlated Observations ?,” *IEEE Trans. Inform. Theory*, pp. 5099–5106, Nov. 2006.
- [21] J. J. Xiao, S. Cui, Z. Q. Luo, and A. J. Goldsmith, “Power Scheduling of Universal Decentralized Estimation in Sensors Networks,” *IEEE Trans. on Signal Proc.*, vol. 54, no. 2, pp. 413-422, Feb. 2006.
- [22] P. Willett, P. F. Swaszek, R. S. Blum, “The Good, Bad, and Ugly: Distributed Detection of a Known Signal in Dependent Gaussian Noise,” *IEEE Trans. on Signal Proc.*, pp. 3266–3278, Dec. 2000.
- [23] R. R. Tenney, N. R. Sandell, Jr., “Detection with Distributed Sensors,” *IEEE Trans. Aerospace and Electron. Systems*, Vol. AES-17, pp. 98–101, July 1981.
- [24] M. Gastpar, “Information-Theoretic Bounds on Sensor Network Performance,” Chapter 2 in A. Swami, Q. Zhao, Y.-W. Hong, L. Tong (Eds), *Wireless Sensor Networks - Signal Processing and Communications Perspectives*, John Wiley & Sons, 2007.
- [25] S. Barbarossa and G. Scutari, “Bio-inspired sensor network design: distributed decision through self-synchronization,” *IEEE Signal Process. Mag.*, Vol. 24, no. 3, pp. 26-35, May 2007.
- [26] I. D. Schizas, A. Ribeiro and G. B. Giannakis, “Consensus in Ad Hoc WSNs with Noisy Links - Part I: Distributed Estimation of Deterministic Signals,” *IEEE Trans. on Signal Process.*, Vol. 56, pp. 350–364, January 2008.
- [27] I.D. Schizas, G.B. Giannakis, S.I. Roumeliotis, A. Ribeiro, “Consensus in Ad Hoc WSNs With Noisy Links Part II: Distributed Estimation and Smoothing of Random Signals,” *IEEE Trans. Signal Process.*, vol. 56, no. 2, pp. 1650–1666, April 2008.
- [28] F. Cattivelli, C. G. Lopes, and A. H. Sayed, “Diffusion recursive least-squares for distributed estimation over adaptive networks,” *IEEE Trans. Signal Process.*, vol. 56, no. 5, pp. 1865-1877, May 2008.
- [29] P. Braca, S. Marano, V. Matta, “Enforcing Consensus While Monitoring the Environment in Wireless Sensor Networks,” *IEEE Trans. Signal Process.*, vol. 56, no. 7, pp. 3375–3380, July 2008.
- [30] A.G. Dimakis, S. Kar, J.M.F. Moura, M.G. Rabbat, A. Scaglione, “Gossip Algorithms for Distributed Signal Processing,” *Proceedings of the IEEE*, Vol. 98, no. 11, pp. 1847–1864, Nov. 2010.
- [31] A. Bertrand, M. Moonen, “Consensus-Based Distributed Total Least Squares Estimation in Ad Hoc Wireless Sensor Networks,” *IEEE Trans. Signal Process.*, vol. 59, no. 5, pp. 2320–2330, April 2011.
- [32] L. Li, A. Scaglione, J.H. Manton, “Distributed Principal Subspace Estimation in Wireless Sensor Networks,” *IEEE Journal of Selected Topics in Signal Process.*, vol. 5, no. 4, pp. 725–738, Aug. 2011.
- [33] S. Kar, J.M.F. Moura, K. Ramanan, “Distributed Parameter Estimation in Sensor Networks: Nonlinear Observation Models and Imperfect Communication,” *IEEE Trans. Information Theory*, vol. 58, pp. 3575–3605, Feb. 2012.
- [34] G. Mateos, I. D. Schizas, and G. B. Giannakis, “Distributed Recursive Least-Squares for Consensus-Based In-Network Adaptive Estimation,” *IEEE Trans. Signal Process.*, vol. 57, no. 11, pp. 4583-4588, Nov. 2009.
- [35] G. Mateos, J. A. Bazerque, G. B. Giannakis, “Distributed Sparse Linear Regression,” *IEEE Trans. Signal Process.*, Vol. 58, pp. 5262–5276, Oct. 2010.
- [36] D. P. Bertsekas and J. N. Tsitsiklis, *Parallel and Distributed Computation: Numerical Methods*, Belmont, MA: Athena Scientific, 1989.

- [37] S. Boyd, N. Parikh, E. Chu, *Distributed Optimization and Statistical Learning Via the Alternating Direction Method of Multipliers*, Now Publishers, May 2011.
- [38] A. Jadbabaie and S. Morse, "Coordination of groups of mobile autonomous agents using nearest neighbor rules," *IEEE Trans. on Auto. Control*, vol. 48, pp. 988-1001, 2003.
- [39] L. Xiao and S. Boyd, "Fast linear iterations for distributed averaging," *Systems and Control Letters*, vol. 53, pp. 65-78, Sept. 2004.
- [40] W. Ren, R. W. Beard, and E. M. Atkins, "Information consensus in multivehicle cooperative control: collective group behavior through local interaction," *IEEE Control Systems Mag.*, Vol. 27, no. 2, pp. 71-82, April 2007.
- [41] R. Olfati-Saber, J. A. Fax, R. M. Murray, "Consensus and cooperation in networked multi-agent systems," *Proc. of the IEEE*, Vol. 95, pp. 215-233, January 2007.
- [42] S. Barbarossa and G. Scutari, "Decentralized maximum-likelihood estimation for sensor networks composed of nonlinearly coupled dynamical systems," *IEEE Trans. Signal Process.*, vol. 55, no. 7, pp. 3456-3470, Jul. 2007.
- [43] G. Scutari, S. Barbarossa and L. Pescosolido, "Distributed Decision Through Self-Synchronizing Sensor Networks in the Presence of Propagation Delays and Asymmetric Channels," *IEEE Trans. Signal Process.*, vol. 56, no. 4, pp. 1667-1684, April 2008.
- [44] A. Nedić, Asuman Ozdaglar, "Cooperative distributed multi-agent optimization," in D.P.Palomar, Y.C.Eldar, *Convex Optimization in Signal Processing and Communications*, Cambridge Univ. Press, 2010.
- [45] Y. Hatano, A. K. Das, and M. Mesbahi, "Agreement in presence of noise: pseudogradients on random geometric networks," in *Proc. IEEE Conference on Decision and Control (CDC)*, Seville, Spain, pp. 6382-6387, December 2005.
- [46] A. Tahbaz Salehi and A. Jadbabaie, "On consensus over random networks," *Proc. of 44th Allerton Conference*, UIUC, Illinois, USA, Sept. 27-29, 2006.
- [47] A. Tahbaz Salehi and A. Jadbabaie, "Consensus over ergodic stationary graph processes," *IEEE Transactions on Automatic Control*, vol. 55, no. 1, Jan. 2010.
- [48] T. C. Aysal, M. Coates, and M. Rabbat, "Distributed average consensus using probabilistic quantization," in *Proc. IEEE/SP Workshop on Statistical Signal Processing Workshop (SSP)*, Maddison, Wisconsin, USA, August 2007, pp. 640-644.
- [49] M. Huang and J. Manton, "Stochastic approximation for consensus seeking: mean square and almost sure convergence," in *Proc. IEEE Conference on Decision and Control (CDC)*, New Orleans, LA, USA, pp. 306-311, Dec. 2007.
- [50] S. Kar and J. M. F. Moura, "Distributed consensus algorithms in sensor networks with imperfect communication: Link failures and channel noise," *IEEE Transactions on Signal Processing* vol. 57, no. 5, pp. 355-369, January 2009.
- [51] S. P. Lipshitz, R. A. Wannamaker, and J. Vanderkooy, "Quantization and dither: A theoretical survey," *J. Audio Eng. Soc.*, vol. 40, pp. 355-375, May 1992.
- [52] R. Wannamaker, S. Lipshitz, J. Vanderkooy, and J. Wright, "A theory of nonsubtractive dither," *IEEE Transactions on Signal Processing*, vol. 48, no. 2, pp. 499-516, February 2000.
- [53] L. Schuchman, "Dither signals and their effect on quantization noise," *IEEE Trans. Commun. Technol.*, vol. COMM-12, pp. 162-165, December 1964.
- [54] S. Sardellitti, S. Barbarossa, "Energy preserving matching of sensor network topology to the statistical graphical model of the observed field," *17th Intern. Conf. on Digital Signal Process.(DSP)*, Corfu, Greece, July 2011.
- [55] S. Barbarossa, S. Sardellitti, "Energy Preserving Matching of Sensor Network Topology to Dependency Graph of the Observed Field," to be submitted on *IEEE Trans. Signal Process.*, 2012.
- [56] D. Donoho, "Compressive Sensing," *IEEE Trans. on Inform. Theory*, vol. 52, pp. 1289-1306, April 2006.

- [57] R. Tibshirani, "Regression Shrinkage and Selection via the Lasso," *J. Royal Statist. Soc.*, vol. 58, pp. 267–288, 1996.
- [58] G. Gasso, A. Rakotomamonjy and S. Canu, "Recovering Sparse Signals with a Certain Family of Non-Convex Penalties and DC Programming," *IEEE Trans. on Signal Process.*, vol. 57, pp. 4686–4698, December 2009.
- [59] P. D. Tao and L. T. H. An, "A D.C. Optimization Algorithms for Solving the Trust-Region Subproblem," *SIAM J. Optimiz.*, vol. 8, pp. 476–505, May 1998.
- [60] R. Zdunek and A. Cichocki, "Fast Nonnegative Matrix Factorization Algorithms Using Projected Gradient Approaches for Large-Scale Problems," *Computational Intell. and Neuroscience*, 2008.
- [61] S. Sardellitti, S. Barbarossa and A. Swami, "Average Consensus with Minimum Energy Consumption: Optimal Topology and Power Allocation," *Proc. of the European Signal Processing Conference (EUSIPCO 2010)*, pp. 189-193, Aalborg, Denmark, August 2010.
- [62] S. Boyd, A. Ghosh, B. Prabhakar, D. Shah, "Randomized gossip algorithms," *IEEE Trans. on Inform. Theory*, Vol. 52, pp. 2508–2530, June 2006.
- [63] S. Sardellitti, M. Giona and S. Barbarossa, "Fast distributed average consensus algorithms based on advection-diffusion processes," *IEEE Trans. on Signal Process.*, vol. 58, no. 2, pp. 826-842, February 2010.
- [64] C. Godsil and G. Royle, *Algebraic Graph Theory*. New York: Springer, 2001.
- [65] M. Fiedler, "Algebraic connectivity of graphs," *J. Czech. Math.*, Vol. 23, pp. 298-305, 1973.
- [66] S. M. Kay, *Fundamentals of Statistical Signal Processing, Vol I: Estimation Theory*. Englewood Cliffs, NJ: Prentice-Hall PTR, 1993.
- [67] S. M. Kay, *Fundamentals of Statistical Signal Processing, Vol II: Detection Theory*. Englewood Cliffs, NJ: Prentice-Hall PTR, 1998.
- [68] M. Alanyali, V. Saligrama, O. Savas, and S. Aeron, "Distributed Bayesian hypothesis testing in sensor networks, in *Proc. Amer. Control Conf.*, Boston, MA, Jul. 2004, vol. 6, pp. 5369-5374.
- [69] V. Saligrama, M. Alanyali, and O. Savas, "Distributed detection in sensor networks with packet losses and finite capacity links," *IEEE Trans. Signal Process.*, vol. 54, no. 11, pp. 4118-4132, Nov. 2006.
- [70] S. A. Aldosari and J. M. F. Moura, "Topology of sensor networks in distributed detection," in *Proc. IEEE Int. Conf. Acoust., Speech, Signal Process. (ICASSP)*, Toulouse, France, May 2006, pp. 1061-1064.
- [71] L. Xiao, S. Boyd, and S. Lall, "A space-time diffusion scheme for peer-to-peer least-squares estimation," in *Proc. of Intl. Conf. on Info. Proc. in Sensor Networks*, Nashville, TN, 2006, pp. 168-176.
- [72] S. Kar and J. M. F. Moura, "Consensus based detection in sensor networks: Topology optimization under practical constraints," *Workshop Inf. Theory in Sensor Networks*, Santa Fe, NM, Jun. 2007.
- [73] D. Bajovic, D. Jakovetic, J. Xavier, B. Sinopoli, J.M.F. Moura, "Distributed Detection via Gaussian Running Consensus: Large Deviations Asymptotic Analysis" *IEEE Trans. Signal Process.*, vol. 59, pp. 4381-4396, Sept. 2011.
- [74] F. Cattivelli and A. H. Sayed, "Distributed detection over adaptive networks using diffusion adaptation," *IEEE Trans. Signal Process.*, vol. 59, no. 5, pp. 1917–1932, May 2011.
- [75] S. Marano, V. Matta, P. Willett, L. Tong, "Cross-Layer Design of Sequential Detectors in Sensor Networks," *IEEE Trans. Signal Process.*, vol. 54, pp. 4105–4117, Nov. 2006.
- [76] Y. Mei, "Asymptotic Optimality Theory for Decentralized Sequential Hypothesis Testing in Sensor Networks," *IEEE Trans. Information Theory*, vol. 54, pp. 2072–2089, May 2008.
- [77] Sardellitti, S.; Barbarossa, S.; Pezzolo, L. "Distributed Double Threshold Spatial Detection Algorithms in Wireless Sensor

- Networks” in *Proc. of IEEE 10th Workshop on Signal Processing Advances in Wireless Commun. (SPAWC '09)*, Perugia, Italy, pp. 51–55, June 2009.
- [78] S. Sardellitti, S. Barbarossa and A. Swami, “Optimal Topology Control and Power Allocation for Minimum Energy Consumption in Consensus Networks,” *IEEE Trans. on Signal Proc.*, Vol. 60, no. 1, pp. 383-399, January 2012.
- [79] M. Mezard, G. Parisi and A. Zee, “Spectra of Euclidean Random Matrices,” *Nuclear Phys. B*, Vol. 559, pp. 689–701, October 1999.
- [80] R. A. Brualdi and H. J. Ryser, *Combinatorial Matrix Theory*. Cambridge, U.K.: Cambridge Univ. Press, 1991.
- [81] R. Horn and C. R. Johnson, *Matrix Analysis*, Cambridge University Press, 1985.
- [82] A. Jeflea, “A Parametric Study for Solving Nonlinear Fractional Problems,” *An. St. Univ. Ovidius Constanta*, Vol. 11, pp. 87–92, 2003.
- [83] W. Dinkelbach, “On Nonlinear Fractional Programming,” *Management Science*, Vol. 13, pp. 492–498, March 1967.
- [84] Y. Hatano and M. Mesbahi, “Agreement Over Random Networks,” *IEEE Trans. on Automatic Control*, Vol. 50, pp. 1867–1872, November 2005.
- [85] T. C. Aysal and K. E. Barner, “Convergence of Consensus Models with Stochastic Disturbances,” *IEEE Trans. on Information Theory*, Vol. 56, pp. 4101–4113, August 2010.
- [86] D. S. Bernstein, *Matrix Mathematics*, Princeton Univ. Press, 2005.
- [87] S. Barbarossa, G. Scutari, T. Battisti, “Distributed signal subspace projection algorithms with maximum convergence rate for sensor networks with topological constraints”, *ICASSP 2009*, April 2009.
- [88] C. Bordenave, “Eigenvalues of Euclidean Random Matrices,” *Random Structures & Algorithms*, John Wiley & Sons, NY, USA, Vol. 33, pp. 515–532, December 2008.
- [89] S. Rai, “The Spectrum of a Random Geometric Graph is Concentrated,” *Journal of Theoretical Probability*, Vol. 20, pp. 119–132, June 2007.
- [90] B. Polyak, *Introduction to Optimization*, Optimization Software Inc., New York, 1987.
- [91] A. Jadbabaie and S. Morse, “Coordination of groups of mobile autonomous agents using nearest neighbor rules,” *IEEE Trans. on Auto. Control*, vol. 48, pp. 988-1001, 2003.
- [92] A. Nedic, A. Ozdaglar, “Cooperative distributed multi-agent optimization,” in D.P.Palomar, Y.C.Eldar, *Convex Optimization in Signal Processing and Communications*, Cambridge Univ. Press, 2010.
- [93] S. Barbarossa, G. Scutari, T. Battisti, “Cooperative sensing for cognitive radio using decentralized projection algorithms,” in *IEEE 10th Workshop on Signal Process. in Wireless Commun.*, Perugia, Italy, pp. 116-120, 2009.